

**KARADENİZ TECHNICAL UNIVERSITY
THE GRADUATE SCHOOL OF NATURAL AND APPLIED SCIENCES**

CIVIL ENGINEERING DEPARTMENT

**SPAN-SKEWED EFFECT ON THE RESPONSE OF
I- GIRDER PRESTRESSED CONCRETE BRIDGES**



MASTER THESIS

Osama GHZAYEL

**June 2016
TRABZON**

**KARADENİZ TECHNICAL UNIVERSITY
THE GRADUATE SCHOOL OF NATURAL AND APPLIED SCIENCES**

CIVIL ENGINEERING DEPARTMENT

**SPAN-SKEWED EFFECT ON THE RESPONSE OF
I- GIRDER PRESTRESSED CONCRETE BRIDGES**

Osama GHZAYEL

**This thesis is accepted to give the degree of
"MASTER OF SCIENCE"**

By

**The Graduate School of Natural and Applied Sciences at
Karadeniz Technical University**

The Date of Submission : 26.05.2016

The Date of Examination : 21.06.2016

Supervisor : Assoc. Prof. Süleyman ADANUR

Trabzon 2016

**KARADENİZ TECHNICAL UNIVERSITY
THE GRADUATE SCHOOL OF NATURAL AND APPLIED SCIENCES**

**CIVIL ENGINEERING DEPARTMENT
Osama GHZAYEL**

**SPAN-SKEWED EFFECT ON THE RESPONSE OF
I- GIRDER PRESTRESSED CONCRETE BRIDGES**

**Has been accepted as a thesis of
MASTER OF SCIENCE**

**After the Examination by the Jury Assigned by the Administrative Board of
the Graduation School of Natural and Applied Sciences with the Decision Number 1638 dated
02/02/2016**

Approved By

Chairman : Assoc. Prof. Süleyman ADANUR

Member : Assoc. Prof. Ahmet Can ALTUNIŞIK

Member : Assoc. Prof. Barış SEVİM

**Prof. Sadettin KORKMAZ
Director, Graduate School of Natural and Applied Sciences**

ACKNOWLEDGEMENTS

It is a pleasure to thank the many people who made this thesis possible. I would never have been able to finish my thesis without the guidance of my committee members, help from friends, and support from my family.

I would like to express my deepest gratitude to my advisor Assoc.Prof. Süleyman ADANUR, for his excellent guidance, caring, patience, and providing me with an excellent atmosphere for doing research.

I offer my regards and blessings to all my teachers in civil engineering department in Karadeniz Technical University who supported me with any information about bridges during the completion of the thesis.

T.C. Başbakanlık, Yurtdışı Türkler ve Akraba Topluluklar Başkanlığı (YTB) is also gratefully acknowledged due to the financial support provided during my M.Sc. research.

I would like to thank all my classmate friends, who were good friends, were always willing to help and give their best suggestions. I would have been a lonely without them, my research would not have been possible without their helps.

Lastly, and most importantly, I wish to thank my parents. They bore me, raised me, supported me, taught me, and loved me. To them I dedicate this thesis.

Osama GHZAYEL

Trabzon 2016

THESIS STATEMENT

The skewness angle of span affects on the responses of I-girder prestressed concrete bridges due to the magnitude of this of skewness degree, in this thesis these responses we will be studied very well generally for five different angles. The importance of this studying came from knowing the different between more than one design with different skewness angles when is wanted to take a decision which design for a bridge will be more appropriate between others, but before studying these responses we have to know generally information about bridges like the concept of prestressed concrete bridges and it was written it in the theoretical part of this thesis and i hereby declare that this part was written from bridge engineering references and the names of these references was written under the title "REFERENCES" at the end of this thesis. I hereby declare that all information in this thesis titled as “Span-Skewed Effect on the Response of the I-Girder Prestressed Concrete Bridges” has been completed under the responsibility of my supervisor Assoc.Prof. Süleyman ADANUR and presented in accordance with academic rules and ethical conduct. 21/06/2016

Osama GHZAYEL

TABLE OF CONTENTS

	<u>Page</u>
ACKNOWLEDGEMENTS.....	III
THESIS STATEMENT.....	IV
TABLE OF CONTENTS.....	V
SUMMARY.....	VIII
ÖZET.....	IX
LIST OF FIGURES.....	X
LIST OF TABLES.....	XIII
NOTATIONS.....	XV
1. GENERAL INFORMATION ABOUT BRIDGES.....	1
1.1. Introduction	1
1.2. Literature Review	2
1.3. Definition of Bridge.....	11
1.4. Bridge Construction Materials.....	11
1.4.1 Stone.....	11
1.4.2. Iron.....	12
1.4.3. Reinforced and Pre-stressed Concrete.....	12
1.4.4. Steel.....	13
1.5. Main Types of Bridges in the World.....	15
1.5.1 Girder Bridges.....	15
1.5.2. Arch Bridges.....	16
1.5.3. Cable Stayed Bridges.....	17
1.5.4. Rigid Frame Bridges.....	18
1.5.5. Truss Bridges.....	18
1.5.6. Reinforced Concrete Bridges.....	20
1.5.7. Prestressed Concrete Bridges.....	20
1.5.8. Steel - Concrete Composite Box Girder Bridges.....	20
1.5.9. Horizontally Curved Bridges.....	21

1.5.10.	Suspension Bridges.....	21
1.5.11.	Timber Bridges.....	21
2.	PRESTRESSED CONCRETE BRIDGES.....	23
2.1.	Introduction.....	23
2.1.1.	Materials.....	23
2.1.1.1	Concrete.....	23
2.1.1.2	Steel for Prestressing.....	25
2.1.1.3.	Advanced Composites for Prestressing.....	27
2.1.1.4.	Grout.....	27
2.1.2.	Prestressing Systems.....	28
2.2.	Section Types.....	29
2.2.1.	Void Slabs.....	29
2.2.2.	I-Girders.....	29
2.2.3.	Box Girders.....	29
2.3.	Losses of Prestress.....	31
2.3.1.	Instantaneous Losses.....	34
2.3.1.1.	Anchorage Set Loss.....	34
2.3.1.2.	Friction Loss.....	35
2.3.1.3.	Elastic Shortening Loss Δf_{pES}	35
2.3.2.	Time-Dependent Losses.....	37
2.3.2.1.	Lump Sum Estimation.....	37
2.3.2.2.	Refined Estimation.....	37
2.4.	Design Considerations.....	38
2.4.1.	Basic Theory.....	38
2.4.2.	Stress Limits.....	40
2.4.3.	Cable Layout.....	41
2.4.4.	Secondary Moments.....	43
2.4.5.	Flexural Strength.....	44
2.4.6.	Shear Strength.....	47
2.4.7.	Camber and Deflections.....	50
2.4.8.	Anchorage Zones.....	51

3.	NUMERICAL APPLICATION.....	52
3.1.	Assumptions of the Numerical Application.....	52
3.2.	Model Bridge Description.....	52
3.3.	Dimensions of the Bridge Components.....	54
3.3.1.	First Model (angle 0°).....	54
3.3.2.	Second Model (angle 21°).....	57
3.3.3.	Third Model (angle 37.6°).....	59
3.3.4.	Fourth Model (angle 57°).....	61
3.3.5.	Fifth Model (angle 66.6°).....	63
3.4.	Strands Properties.....	65
3.5.	Applied Loads.....	66
3.6.	Model Analysis Type Selection.....	67
3.7.	Construction Stages.....	67
3.8.	Analysis of Models.....	67
3.9.	Results and Diagrams.....	68
3.9.1.	The Moment of I-girders.....	68
3.9.2.	The Shear Forces of I-girders.....	72
3.9.3.	The Torsion of I-girders.....	76
3.9.4.	The Axial Forces of I-girders.....	80
3.9.5.	The Displacement of I-girders.....	84
3.9.6.	The Losses in Strands of I-girders.....	88
3.9.7.	The Axial Stresses in I-girders.....	91
4.	CONCLUSION AND RECOMMENDATIONS.....	94
5.	REFERENCES.....	97
6.	APPENDIX.....	101

CURRICULUM VITAE

Master Thesis

SUMMARY

**SPAN-SKEWED EFFECT ON THE RESPONSE OF
I-GIRDER PRESTRESSED CONCRETE BRIDGES**

Osama GHZAYEL

Karadeniz Technical University
The Graduate School of Natural and Applied Sciences
Civil Engineering Department

Supervisor: Assoc.Prof. Süleyman ADANUR
2016, 100 Pages, 28 Pages Appendix

Span-skewed bridges nowadays are constructed widely in the world and also in Turkey. This thesis is about the span-skewed effects on the responses of I-girder prestressed concrete bridges. The thesis prepared with this scope includes the following chapters.

In the beginning, the general information about the bridges, the importance of the matter, previous studies about the subject are given. The formulations are also presented in this chapter. After that, simply supported I-girder pretension prestressed concrete bridge with five different models of 0° , 21° , 37.6° , 57° , 66.6° degrees of skewness angle, respectively are analyzed using Midas Civil computer program. This program is made especially for analyze and design all the components and all types of bridges by using the finite element method using the most common codes in the world. Response values like displacements and internal forces in the internal and external I-girders of the bridges, which obtained from analysis of different types of span-skewed bridges, are discussed. Then, the results and recommendations obtained from the analysis are given. The references are presented in the last chapter.

Keywords: Skewed bridge, Skewness angle, I-girder, Prestress concrete, Finite element method, Displacement, Internal forces.

Yüksek Lisans Tezi

ÖZET

**I KESİTLİ ÖNGERMELİ BETON KİRİŞ TABLİYEYE SAHİP KÖPRÜLERİN
DAVRANIŞINA AÇIKLIK VEREVLİĞİNİN ETKİSİ**

Osama GHZAYEL

Karadeniz Teknik Üniversitesi
Fen Bilimleri Enstitüsü
İnşaat Mühendisliği Anabilim Dalı

Danışman: Doç. Süleyman ADANUR
2016,.100 Sayfa, 28 Ek Sayfa

Verev köprüler dünyada ve Türkiye’de yaygın olarak inşa edilmektedirler. Bu tez, I kesitli öngermeli beton kiriş tabliyeye sahip köprülerin davranışına açıklık verevliğinin etkisi ile ilgilidir. Bu amaçla hazırlanan tez aşağıdaki bölümlerden oluşmaktadır.

İlk olarak köprüler hakkında genel bilgilerden, konunun öneminden ve bu konuda daha önce yapılmış çalışmalardan bahsedilmekte ve formülasyon verilmektedir. Daha sonra sonlu elemanlar yöntemi ile her tür köprünün analiz ve tasarımı yapan ve dünyada yaygın olarak kullanılan Midas Civil bilgisayar programı kullanılarak, bir açıklıklı öngermeli beton kirişli bir köprünün 0° ; 21° ; 37.6° , 57° ; 66.6° gibi beş farklı verevlik açısı dikkate alınarak analizleri gerçekleştirilmiştir. Analizler sonucunda beş farklı verevlik açısı için köprünün tabliye kirişlerindeki yerdeğiştirme ile burulma momenti, eğilme momenti, kesme kuvveti ve normal kuvvet gibi iç kuvvetler ve tendonlardaki eksenel kuvvetler elde edilmiştir. Analizlerden elde edilen tepki değerleri birbirleriyle karşılaştırılmıştır. Sonrada çalışmadan elde edilen sonuçlar ve öneriler sunulmuştur. Referanslar ise son bölümde verilmiştir.

Anahtar Kelimeler: Verev köprü, Verevlik açısı, I kesitli kiriş, Öngermeli beton, Sonlu eleman yöntemi, Yerdeğiştirme, İç kuvvetler.

LIST OF FIGURES

	<u>Page</u>
Figure 2.1.	Typical stress–strain curves for prestressing steel.....25
Figure 2.2.	A post–tensioned box–girder bridge under construction.....28
Figure 2.3.	Typical cross sections of prestressed concrete bridge superstructures.....30
Figure 2.4.	Prestressed box–girder bridge (I-280/110 Interchange, CA).....33
Figure 2.5.	Anchorage set loss model.....34
Figure 2.6.	Prestressed concrete member section at service limit state.....37
Figure 2.7.	Cable layout for bridge superstructures.....42
Figure 2.8.	Cable layout envelopes.....42
Figure 2.9.	Secondary moments43
Figure 2.10.	A flanged section at nominal moment capacity state44
Figure 2.11.	Illustration of A_c for shear strength calculation47
Figure 3.3.1.1.	Elevation of first model (angle 0°).....54
Figure 3.3.1.2.	Plan of first model (angle 0°).....54
Figure 3.3.1.3.	Number of elements for first model (angle 0°).....55
Figure 3.3.1.4.	Number of nodes for first model (angle 0°).....55
Figure 3.3.1.5.	Dimensions of pier and pier cap for first model (angle 0°).....55
Figure 3.3.1.6.	Dimensions of slab for first model (angle 0°).....56
Figure 3.3.1.7.	Dimensions of I-girder according to AASHTO LRFD (type III) for all models.....56
Figure 3.3.2.1.	Elevation of second model (angle 21°).....57
Figure 3.3.2.2.	Plan of second model (angle 21°).....57
Figure 3.3.2.3.	Dimensions of slab for second model (angle 21°).....57
Figure 3.3.2.4.	Number of elements for second model (angle 21°).....58
Figure 3.3.2.5.	Number of nodes for second model (angle 21°).....58
Figure 3.3.2.6.	Dimensions of pier and pier cap for second model (angle 21°).....58
Figure 3.3.3.1.	Elevation of third model (angle 37.6°).....59
Figure 3.3.3.2.	Plan of third model (angle 37.6°).....59

Figure 3.3.3.3.	Dimensions of slab for third model (angle 37.6°).....	59
Figure 3.3.3.4.	Number of elements for third model (angle 37.6°).....	60
Figure 3.3.3.5.	Number of nodes for third model (angle 37.6°).....	60
Figure 3.3.3.6.	Dimensions of pier and pier cap for third model (angle 37.6°).....	60
Figure 3.3.4.1.	Elevation of fourth model (angle 57°).....	61
Figure 3.3.4.2.	Plan of fourth model (angle 57°).....	61
Figure 3.3.4.3.	Dimensions of slab for fourth model (angle 57°).....	61
Figure 3.3.4.4.	Number of elements for fourth model (angle 57°).....	62
Figure 3.3.4.5.	Number of nodes for fourth model (angle 57°).....	62
Figure 3.3.4.6.	Dimensions of pier and pier cap for fourth model (angle 57°).....	62
Figure 3.3.5.1.	Elevation of fifth model (angle 66.6°).....	63
Figure 3.3.5.2.	Plan of fifth model (angle 66.6°).....	63
Figure 3.3.5.3.	Dimensions of slab for fifth model (angle 66.6°).....	63
Figure 3.3.5.4.	Number of elements for fifth model (angle 66.6°).....	64
Figure 3.3.5.5.	Number of nodes for fifth model (angle 66.6°).....	64
Figure 3.3.5.6.	Dimensions of pier and pier cap for fifth model (angle 66.6°).....	64
Figure 3.5.	Moving load HL-93 vehicle and lane loading.....	66
Figure 3.9.1.1.	Moment diagram of the first I-girder.....	68
Figure 3.9.1.2.	Moment diagram of the second I-girder.....	69
Figure 3.9.1.3.	Moment diagram of the third I-girder.....	70
Figure 3.9.1.4.	Moment diagram of the fourth I-girder.....	71
Figure 3.9.2.1.	Shear force diagram of the first I-girder.....	72
Figure 3.9.2.2.	Shear force diagram of the second I-girder.....	73
Figure 3.9.2.3.	Shear force diagram of the third I-girder.....	74
Figure 3.9.2.4.	Shear force diagram of the fourth I-girder.....	75
Figure 3.9.3.1.	Torsion diagram of the first I-girder.....	76
Figure 3.9.3.2.	Torsion diagram of the second I-girder.....	77
Figure 3.9.3.3.	Torsion diagram of the third I-girder.....	78
Figure 3.9.3.4.	Torsion diagram of the fourth I-girder.....	79
Figure 3.9.4.1.	Axial forces diagram of the first I-girder.....	80
Figure 3.9.4.2.	Axial forces diagram of the second I-girder.....	81

Figure 3.9.4.3.	Axial forces diagram of the third I-girder.....	82
Figure 3.9.4.4.	Axial forces diagram of the fourth I-girder.....	83
Figure 3.9.5.1.	Displacement diagram of the first I-girder.....	84
Figure 3.9.5.2.	Displacement diagram of the second I-girder.....	85
Figure 3.9.5.3.	Displacement diagram of the third I-girder.....	86
Figure 3.9.5.4.	Displacement diagram of the fourth I-girder.....	87
Figure 3.9.6.1.	Diagram of final forces in strands after losses in the first I-girder.....	88
Figure 3.9.6.2.	Diagram of final forces in strands after losses in the second I-girder.....	88
Figure 3.9.6.3.	Diagram of final forces in strands after losses in the third I-girder.....	89
Figure 3.9.6.4.	Diagram of final forces in strands after losses in the fourth I-girder.....	89
Figure 3.9.7.1.	Axial stresses diagram of the first I-girder.....	91
Figure 3.9.7.2.	Axial stresses diagram of the second I-girder.....	91
Figure 3.9.7.3.	Axial stresses diagram of the third I-girder.....	92
Figure 3.9.7.4.	Axial stresses diagram of the fourth I-girder.....	92

LIST OF TABLES

		<u>Page</u>
Table 2.1.	Properties of prestressing strand and bars.....	26
Table 2.2.	Precast prestressed voided slabs section properties (figure. 2.3a).....	31
Table 2.3.	Precast prestressed I-beam section properties (figures. 2.3b and c).....	32
Table 2.4.	Precast prestressed box section properties (figure. 2.3d).....	33
Table 2.5.	Friction coefficients for post-tensioning tendons	34
Table 2.6.	Lump sum estimation of time-dependent prestress losses.....	36
Table 2.7.	Stress limits for prestressing tendons.....	39
Table 2.8.	Temporary concrete stress limits at jacking state before losses due to creep and shrinkage - fully prestressed components.....	39
Table 2.9.	Concrete stress limits at service limit state after all losses-fully prestressed components.....	40
Table 2.10.	Values of θ and β for sections with transverse reinforcement	48
Table 3.4.	Strand profile 3-D coordinates.....	65
Table 6.1.	Bending moment in longitudinal direction of the bridge in the first I-girder for all models.....	101
Table 6.2.	Torsion moment of the bridge in the first I-girder for all models.....	102
Table 6.3.	Shear forces in z-direction of the bridge in the first I-girder for all models.....	103
Table 6.4.	Axial forces of the bridge in the first I-girder for all models.....	104
Table 6.5.	Axial stresses of the bridge in the first I-girder for all models.....	105
Table 6.6.	Displacement in z-direction of the bridge in the first I-girder for all models.....	106
Table 6.7.	Final forces in pre-tentioned steel of the bridge in the first I-girder for all models.....	107
Table 6.8.	Bending moment in longitudinal direction of the bridge in the first I-girder for all models.....	108
Table 6.9.	Torsion moment of the bridge in the first I-girder for all models.....	109
Table 6.10.	Shear forces in z-direction of the bridge in the first I-girder for all models.....	110
Table 6.11.	Axial forces of the bridge in the first I-girder for all models.....	111
Table 6.12.	Axial stresses of the bridge in the first I-girder for all models.....	112

Table 6.13.	Displacement in z-direction of the bridge in the first I-girder for all models.....	113
Table 6.14.	Final forces in pre-tentioned steel of the bridge in the first I-girder for all models.....	114
Table 6.15.	Bending moment in longitudinal direction of the bridge in the first I-girder for all models.....	115
Table 6.16.	Torsion moment of the bridge in the first I-girder for all models.....	116
Table 6.17.	Shear forces in z-direction of the bridge in the first I-girder for all models.....	117
Table 6.18.	Axial forces of the bridge in the first I-girder for all models.....	118
Table 6.19.	Axial stresses of the bridge in the first I-girder for all models.....	119
Table 6.20.	Displacement in z-direction of the bridge in the first I-girder for all models.....	120
Table 6.21.	Final forces in pre-tentioned steel of the bridge in the first I-girder for all models.....	121
Table 6.22.	Bending moment in longitudinal direction of the bridge in the first I-girder for all models.....	122
Table 6.23.	Torsion moment of the bridge in the first I-girder for all models.....	123
Table 6.24.	Shear forces in z-direction of the bridge in the first I-girder for all models.....	124
Table 6.25.	Axial forces of the bridge in the first I-girder for all models.....	125
Table 6.26.	Axial stresses of the bridge in the first I-girder for all models.....	126
Table 6.27.	Displacement in z-direction of the bridge in the first I-girder for all models.....	127
Table 6.28.	Final forces in pre-tentioned steel of the bridge in the first I-girder for all models.....	128

NOTATIONS

I	Impact factor
w_c	The density of concrete
E_C	The modulus of elasticity of concrete
E_s	The modulus of elasticity for reinforcement
E_p	The modulus of elasticity for prestressing
E_{ci}	Modulus of elasticity of concrete at transfer (for pre-tensioned members) or after jacking (for post-tensioned members)
<i>AASHTO</i>	American Association of State Highway and Transportation Officials
f_c'	Compressive strength of concrete at 28 days
f_r	The modulus of rupture of concrete
ε_{sh}	The strain due to shrinkage
k_s	Size factor
k_h	Humidity factors
V/S	Volume to surface area ratio
Ψ	The creep coefficient
H	Relative humidity (%)
t_i	Age of concrete when load is initially applied (days)
K_c	The effect factor of the volume-to-surface ratio
K_f	The effect factor of concrete strength
f_{pu}	Tensile Strength of prestressing steel
f_{py}	Yield Strength of prestressing steel
f_{ps}	Stress of prestressing steel
ε_{ps}	Strain of prestressing steel
Δf_{pT}	The total prestress loss
Δf_{pSR}	Losses due to shrinkage
Δf_{pTM}	Time-dependent losses
Δf_{pCR}	Losses due to creep
Δf_{pR}	Losses due to relaxation of the steel during the service life

Δf_{pA}	Losses due to anchorage set
Δf_{pF}	Losses due to friction between tendons and surrounding materials
Δf_{pES}	Losses due to elastic shortening of concrete during the construction stage
α	Curvature coefficient (1/rad)
K	Wobble coefficient
Δf_{pA}	The change in stress due to the effect of anchorage set on the cable stress
ΔL	The thickness of anchorage set
E	The modulus of elasticity of anchorage set
Δf	The change in stress due to anchor set
L_{pA}	The length influenced by anchor set
L_{pF}	The length to a point where loss is known
μ	The curvature friction coefficient
α	The sum of the absolute values of angle change in the prestressing steel path from the jacking end
PPR	Partial prestress ratio $= (A_{ps}f_{py}) / (A_{ps}f_{py} + A_s f_y)$.
$FHWA$	The Federal Highway Administration
N	The number of identical prestressing tendons
f_{cgp}	Concrete stress at center of gravity of prestressing steel at transfer
Δf_{cdp}	Concrete stress change at center of gravity of prestressing steel due to permanent loads, except the load acting at the time the prestressing force is applied
P_j	The prestress force
I	The moment of inertia
e	The distance from the center of gravity to the centroid of the prestressing cable
y	The distance from the centroidal axis
f_t	Limited tension stress
e'	Additional eccentricities for limited tension stress ft
e_{limit}	The limiting eccentricity
b_w	The web width of a section
h_f	The compression flange depth of the cross section

d_p	Distances from extreme compression fiber to the centroid of prestressing tendons
d_s	Distances from extreme compression fiber to centroid of tension reinforcement
L_1	Length of loaded span or spans affected by the same tendons
L_2	Total length of tendon between anchorage
Ω_u	The bond reduction coefficient
ϕ	Flexural resistance factor 1.0 for prestressed concrete and 0.9 for reinforced concrete
M_{cr}	The cracking moment strength
f_{pe}	Compressive stress in concrete due to effective prestresses
f_d	Stress due to unfactored self-weight
b_v	The effective web width
d_v	The effective depth between the resultants of the tensile and compressive forces due to flexure
A_v	The area of transverse reinforcement
β	A factor indicating ability of diagonally cracked concrete to transmit tension
θ	The angle of inclination of diagonal compressive stresses
A_c	Area of concrete on the flexural tension side of the member
$A_{v\ min}$	Minimum transverse reinforcement

1. GENERAL INFORMATION ABOUT BRIDGES

1.1. Introduction

Bridges are needed for a variety of reasons. Generally, they ‘bridge’ a gap between the banks of a river or they span the distance between two sides of a valley. They are made from materials including stone and steel. Bridges can carry people, cars, lorries, railways and even rivers. The first bridges made by humans were probably spans of wooden logs or planks and eventually stones, using a simple support and crossbeam arrangement. The first writer in science of bridge engineering was Hubert Gautier in 1716. (URL-1)

By the time, when the new industrial technology came, a lot of new systems helped the scientists to develop a new types from bridges like the truss systems of wrought iron which were developed for larger bridges, but iron did not have the tensile strength to support large loads. With the advent of steel, which has a high tensile strength, much larger bridges were built. (URL-1)

Bridges are classified on the basis that how the four forces namely shear, compression, tension, and moment are distributed in the bridge structure. One from the most commonly types is the prestressed concrete bridges. This type from bridges was classified to two types. First one is the pre-tension prestressed concrete bridges and other one is post-tension prestressed concrete bridges. In this thesis the first one will be discussed in numerical application.

Nowadays, skewed-span prestressed concrete bridges are used widely around the world and are used in Turkey too. There are a lot of researchers wrote a lot of researches about analysis and design of this type of bridges but i want to complete in same way but this time by making a comparison between the responses of these bridges when different skewness angles were applied to know the effect of magnitude of the skewness angle on the responses of bridges in general.

1.2. Literature Review

Many researchers have worked to find the effect of skewness angle of span on responses of concrete bridges. Some of these studies can be summarized as follows:

Bakiit (1988), presented analysis of some skew bridges as right bridges. Those methods of bridge analysis that are developed basically for right bridges are also sometimes used for analyzing skew bridges provided that the angle of skew is less than 20° . A critical review of this practice was presented in this research. It was concluded from the results which presented that the ratio $(S \tan \theta/L)$, rather than θ , should be taken as an appropriate measure of skewness. It is shown that the errors in analyzing skew slab-on-girder bridges as right are not characterized by the angle of skew but by two dimensionless parameters, which depend upon the angle of skew, the spacing and span of girders, and their flexural rigidities relative to the flexural rigidity of the deck slab. Recommendations are given for the use of the simplified methods of analysis for skew slab-on-girder bridges. It is proposed that bridges having $(S \tan \theta/L)$, less than 0.05 can be analyzed as equivalent right bridges, where S , L , and θ are the girder spacing, bridge span, and angle of skew, respectively.

Khaleel and Itani (1990), presented a method for determining moments in continuous normal and skew slab-and-girder bridges due to live loads. Using the finite element method, 112 continuous bridges are analyzed, each having five pretensioned I girders. The spans vary between 24.4 and 36.6 m (80 and 120 ft), and are spaced between 1.8 and 2.7 m (6 and 9 ft) on center. The angle of skew, α varies between 0 and 60° . From the results, For a skew angle of 60° , maximum moment in the interior girder is approximately 71% of that in a normal bridge; and reduction in maximum bending moment is 20% in the exterior girders, which control the design for a bridge with long span, small girder spacing, and small relative stiffness of girders to slab. It is concluded that the AASHTO distribution of wheel loads for exterior girders in normal bridges underestimates the bending moments by as much as 28%.

Helba and Kennedy (1994), performed a parametric study on collapse loads of skew composite bridges. The influence of the various parameters, such as skew angle, aspect ratio, span, loading conditions, moments of resistance on the failure patterns and minimum collapse loads of simply supported and continuous two-span skew composite bridges have been examined. Both eccentric and concentric critical loadings were considered. For eccentric

loading it was shown that the critical crack length is significantly affected by the bridge aspect ratio and to a much lesser extent, by skew, while the critical location of the load is influenced significantly by both skew and aspect ratio. For concentric loading, the inclination of the positive transverse failure line is shown to be a function of the number of loaded lanes as well as of skew.

Kankam and Dagher (1995), described a nonlinear finite-element analysis of skewed slab bridges (Kankam 1993) to obtain the effects of steel redistribution near the obtuse corners on the serviceability and ultimate strength of these bridges. Comparison of results obtained for the two models of skewed slab bridges confirms that a skewed slab bridge whose design is based on linear finite-element analysis in which more reinforcement is placed near the obtuse corner than near the acute corner has a higher crack initiation load than a corresponding bridge designed with uniform reinforcement, even though the total amount of steel in the two bridges may be practically the same. A skewed slab bridge with more reinforcement near the obtuse corner than near the acute corner has a higher ultimate strength than a corresponding bridge designed with uniform reinforcement.

Ebeido et al. (1996a), made a research about girder moments in continuous skew composite bridges. test results from three continuous composite steel-concrete bridge models with two unequal span are used to verify a finite-element analysis for such bridges. From the results they conclude that in the design of continuous skew composite bridges the exterior girder is the controlling girder in terms of both span and support moments. Both the span and the support girder moments decrease significantly with increase in the skew angle. Skew has a greater influence on the design of interior girders than exterior girders. The effect of skew becomes more significant for skew greater than 30° . For bridges with skew angles greater than 30° , both span and support girder moments decrease significantly with increase in the spans ratio, S (= long span length/short span length).

Ebeido et al. (1996b), investigated the influence of skew, as well as other design parameters, on the shear and reaction distribution factors of continuous two-span composite steel-concrete bridges. They found that the reactions and shear forces at the simply supported ends of a two-span continuous skew composite bridge can be estimated accurately using the shear distribution factors for simply supported skew bridges presented by Ebeido and Kennedy (1995). The distribution of the reactions at the pier support of a two-equal-span continuous

composite bridge is almost uniform and is not sensibly affected by skew. However, it is significantly affected by skew in a two-unequal-span continuous composite bridge. Increasing the skew increases significantly the reaction of the exterior girder and decreases it for the interior girder. The distribution of shear forces at the pier support is critical for two-equal-span as well as for two-unequal span continuous skew bridges. The shear forces increase at the exterior girders and decrease at the interior girders with increasing skew. Both the reaction and the shear distribution factors at the pier support are very sensitive to changes in the girder spacing. These factors decrease significantly with increase in the ratio, N (=number of lanes/number of girders), which is a measure of the girder spacing. An increase in the spans ratio (=long-span length/short span length) reduces the shear forces and reactions at the pier support.

Khaloo and Mirzabozorg (2003), performed a research about load distribution factors in simply supported skew bridges. Simply supported bridges consisting of five I-section concrete girders are analyzed using the finite element method. The main parameters of this study are: girder spacing (1.8–2.7) m, span length (25–35) m, skew angle (0–60°), and different arrangements of internal transverse diaphragms. The results of the research showed that the arrangement of internal transverse diaphragms has a great effect on the load distribution pattern. This effect varies for different skew angles such that, in low skew angles, the difference between the first and second systems is high while, in high skew angles, this difference decreases and the difference between the second and third or (fourth) Systems increases. The decks with internal transverse diaphragms perpendicular to the longitudinal girders are the best arrangement for load distribution in skew bridges. It has been shown that, even in right bridges without internal transverse diaphragms, the load distribution factors of the AASHTO code are very conservative.

Huang et al. (2004), presented in this research, a two-span, continuous, slab-on-steel girder highway bridge with a skew angle of 60° was field tested. A finite element model was developed and verified by the test results. The AASHTO LRFD specifications were compared with the field test results. Based on the test results and analyses, the following conclusions can be drawn. The recently published AASHTO LRFD formulas for transverse load distribution appear to be conservative for positive bending (based on detailed testing and analysis of this one bridge), for slab-on-steel girder bridges with skews as large as 60° and can be used with

confidence. The recently published AASHTO LRFD formulas for transverse load distribution appear to be accurate but not conservative for negative bending (based on detailed testing and analysis of this one bridge), for slab-on-steel girder bridges with skews as large as 60° and should be applied in design with this in mind.

Qaqish (2006), started a research about effect of skew angle on distribution of bending moments in bridge slabs by a finite element model was carried out for prestressed precast beams and cast in situation slab bridge. The results of his research for transverse and longitudinal moments were compared with the results obtained from AASHTO specifications. This comparison shows that applying AASHTO specifications for slab bridge deck is safe and economical.

Saber et al. (2007), investigated the effect of full-depth continuity diaphragms on the deflection of, and stress in, skewed precast, prestressed concrete girders. This study investigated the load transfer mechanism through full-depth continuity diaphragms. The effect of continuity diaphragms on the maximum stress in the girders and maximum deflection of the girders was negligible. This indicated that continuity diaphragms could be eliminated from skewed, continuous, precast prestressed concrete girder bridges. Thus, continuity diaphragms are ineffective and full-depth diaphragms are not needed to control deflections or reduce member stresses but may be needed for construction, lateral stability during erection, or resisting/transferring earthquake or other transverse loads. The theoretical results of this investigation were based on finite element analysis to determine the effects of full-depth continuity diaphragms for skewed, continuous, precast prestressed concrete girder bridges.

Menassa et al. (2007), studied influence of skew angle on reinforced concrete slab bridges. The longitudinal bending moment, edge beam moment, transverse moment, and live-load deflection were compared with AASHTO Standard Specifications and LRFD procedures. The AASHTO Standard Specifications gave similar results to the finite element analysis maximum longitudinal bending moment when the skew angle is less than or equal to 20° . The ratio between the finite element analysis longitudinal moments for skewed and straight bridges was almost one for bridges with skew angle less than 20° . In general, this research supports the AASHTO standard specifications as well as the LRFD procedure in recommending that bridges with skew angles less than or equal to 20° be designed as straight (non skewed) bridges.

Huo and Sharon (2008), studied effect of skewness on the distribution of live load reaction at piers of skewed continuous bridges and it was found that the reaction distribution factors at the piers of continuous skewed bridges increase with increased skew angles. The distribution factors of reactions at the piers are higher than those for shear near the same piers. The increase in reaction distribution factor at the piers in the interior beam lines is more significant than that in shear distribution factor when the skew angle is greater than 30° .

Kalantari and Amjadian (2010), using a three degree of freedom analytical model an approximate hand-method was presented for dynamic analysis of skewed highway bridges with continuous rigid deck. In modeling the structure it is assumed that the deck of the bridge is rigid in-plane. They generalized a hand-method and this was proposed for dynamic analysis of skewed highway bridges with continuous rigid deck. A computational procedure was presented to determine the natural frequencies, mode shapes and internal forces of this kind of bridge. The method was comprehensively verified using a finite element model subjected to earthquake excitation. It was shown that the results from the proposed method as an approximate method in the preliminary analysis are in good agreement with the finite element method as a reliable method in the final stage of analysis.

Fu et al. (2011), studied behavior of reinforced concrete bridge decks on skewed steel superstructure under truck wheel loads and it was reached in this study that a numerical modeling of complex structures such as skewed highway bridges requires measurement data for verification and/or calibration. Truck wheel loads induce relatively low strains/stresses in RC highway bridge decks on steel superstructure in Michigan as an example. These strains/stresses are not significant enough to initiate concrete deck cracking. Thermal strains/stresses can be much higher, and merit attention in investigating the cause of concrete deck cracking.

Harba (2011), studied effect of skew angle on behavior of simply supported reinforcement concrete T-beam bridge decks. It found that the max. Live load bending moment in T-beams Bridge decks decrease for skewed bridges. The max. Live load deflections in T-beams bridge decks decrease for skewed bridges. The max. Live load shear in T- beams bridge decks increase for exterior beams and decreases for interior beams for skewed bridges. The maximum Live load torsions in T-beams bridge decks increases for skewed bridges for all considered span lengths (12, 16, 20 and 24m).

Kaliyaperumal et al. (2011), presented dynamic analysis of a case-study bridge in Sweden and comparison with available field measurements as well as eigenvalue analyses. The eigenvalue analyses were carried out on a number of different FE models to investigate the effect of modeling assumptions on dynamic behavior. It was found that secondary elements such as bracings may have a significant effect on the frequency of the bridge and it is suggested that they are modeled during an FE analysis. It was also found that in order to capture the out-of-plane and torsional behavior of the main girders, which led to the development of fatigue cracks on the case-study bridge, shell elements should be used in the finite element models, as beams are unable to capture such type of behavior. The comparison of the results obtained from dynamic FE analyses with available field measurements showed that implicit dynamic analysis is a reasonable and computationally efficient method of capturing the dynamic behavior of a bridge and obtaining dynamic stress histories. The results were found to be in good agreement in terms of strain histories, maximum strains/stresses as well in terms of mean stress ranges, the latter for the purposes of fatigue assessment.

Vayas et al. (2011), the research was made about three dimensional modeling for steel-concrete composite bridges using systems of bar elements-modeling of skewed bridges. The results of their research showed that the three dimensional modeling can be as accurate as a relatively fine mesh finite element model both for orthogonal and skewed bridges, while it has the advantages of being quicker and easier to set up. In contrast to grillage models, the three dimensional models are able to predict the real 3D behavior of a skewed bridge and the out of plane rotation of the steel girders during the concreting. In addition, they can also be used for the stability analysis during erection stages, providing the modal shapes of the structure as together with the corresponding critical load factors.

Theoret et al. (2012), studied analysis and design of straight and skewed slab bridges and modeled them using grillage and finite-element models to characterize their behavior under uniform and moving loads with the objective of determining the most appropriate modeling approach for design. Comparison of finite-element analyses with grillage models suggested that nonorthogonal grid arrangements are preferred over orthogonal grillages. Not only are nonorthogonal arrangements simpler to realize than orthogonal grid models for skewed geometries, but their accuracy was found comparable to finite-element plate model values for determining the longitudinal bending moments in skewed slab bridges. In

orthogonal-grillage and finite element analysis, concomitant flexural and torsional moments for moving loads must be combined for determining the bending moments required for designing reinforcements which was found unnecessary with skewed grillage models in the longitudinal direction. Finally, all grillage and finite-element models require post processing to correctly predict the transverse bending moments using concomitant flexural and torsional moments. The results of a parametric study carried out on 390 slab bridges indicated that the shear forces and the secondary bending moments increase with increasing skew angle while longitudinal bending moments diminish. The study also showed that the moment reduction factor in AASHTO is accurate for skew angles of up to 30°, but becomes very conservative for larger skew angles.

Khatri et al. (2012), studied the analysis of skew bridges using computational methods and it was found that variation of grid sizes analysis results predicts that, variation in reaction value is same in finite element method and grillage method but variation of bending and torsion moment in finite element method is lower than grillage results. So, finite element method may be preferred for analysis of skew bridges efficiently with certain limitation.

Nouri and Ahmadi (2012), studied influence of skew angle on continuous composite girder bridge. The results showed that an increase of skew angle causes a reduction in both the exterior and interior support moment girders. The effect of the skew angle on the moment and shear was considerable on interior girders compared with exterior girders; thus, in the design of continuous skewed two-lane bridges, the moment and shear of exterior girders control the design. With an increase of skew angle, the shear decreased significantly in the interior girders. It increased in the exterior girders at the pier support of continuous composite two-lane bridges.

Sheng et al. (2012), studied the skewed concrete box girder bridge static and dynamic testing and analysis. It was found For box girder bridges having similar spans and bearing conditions, a higher width to span ratio (B/L) reduces the vertical displacement and torsional deformations but increases the torsional stresses in the structure. Vertical bending moments are slightly affected. In addition, increasing or decreasing box girder width can result in impractical structures even if the effects are beneficial. It appeared that the selected B/L value for the prototype was a good compromise between practicality and structural efficiency. As box girder bridge skew angles increase, vertical bending moments and deformations decrease.

However, torsional stresses and deformations increase as well as differential reaction levels. Consequently, large skew angles (above 45°) were not recommended for skewed bridges on the high speed railway.

Ansuman kar et al. (2012), perform their study about effect of skew angle in skew bridges. Simple supported single span bridge was considered in that study. The analysis results shows that as skew angle increases, reaction increases, bending moment decreases but torsion and transverse moment increases up to a certain angle, after which it decreases. The effect of skewness on the behavior of bridge deck is studied for skew angle 00, 300, 450, and 600 and presented graphically using finite element method and grillage analogy method. Results are presented for both analysis method for dead load and combined dead and live load.

Sindhu et al. (2013), studied effect of skew angle on static behavior of reinforced concrete slab bridge decks. It was found that the maximum deflection for skewed deck slabs decreases with the increase in skew angle for all aspect ratios for dead load. Longitudinal bending moment shows similar pattern of reduction with increase in skew angle and maximum reduction due to dead load. For right bridge deck slab (0° skew), maximum longitudinal sagging moments are orthogonal to abutments in central region. As the skew angle increases maximum longitudinal moments gradually shifts towards obtuse angle. The peak value of torsional moment is at 45° and is two times more than corresponding value for a right bridge deck.

Dhar et al. (2013), studied effect of skew angle on longitudinal girder (support shear, moment, torsion) and deck slab of an I section reinforcement concrete skew bridge and the results showed that the skew angle increase results in increasing the support shear of the obtuse longitudinal girder and decreasing that of the acute longitudinal girder. Similarly, the mid-span longitudinal moment steadily increases with increasing skew angle for obtuse angled girder and decreases for the acute angled one. Also, the mid-span lateral moments of the longitudinal girders, both obtuse and acute, register a reduction with increasing skew angle. With the increasing skew angle, torsional moments rise rapidly in obtuse angled girders.

Aravindan and ameerutheen (2014), made a research about the effect of skew angle in composite bridge. it was found that for skew angle up to 15 values and its direction is very small. The analysis considering the slab as if it is right deck with skew span as one side and right width as another side is adequate for design purposes. When skew angle increases

beyond 15°, more accurate analysis is required since change in the behavior of slab is considerable. It may be understood that behavior is not only dependent on skew angle but also on aspect ratio, namely skew span to right width ratio.

Abozaid et al. (2014), studied nonlinear behavior of a skew slab bridge under traffic loads. Based on the results of the finite element analysis and the comparisons of skew bridges with straight bridges, the following points can be concluded. Skew bridges exhibit greater displacements for the same loadings and boundary conditions compared to those of straight bridges. As the skew angle increased, the deflection increased and the failure load decreased. The results of this study agree well with the AASHTO standard specifications in recommending that bridges with skew angles less than or equal to 20° should be designed as straight bridges. With an increase in the skew angle, the stresses in the skewed bridge deck differ significantly compared to those in a straight bridge deck.

Deepak and Sabeena (2015), studied effect of skew angle on uplift and deflection of reinforcement concrete skew slab. It was found that the maximum deflection for skew slabs decreases with the increase in skew angle. This indicates that the load carrying capacity of skew slab increases with increase in skew angle. The uplift at acute corners of skew slab increases with increase in skew angle.

Deshmukh, and Waghe (2015), the main aim in this study was to observe and conclude bending moment, torsional moment and shear force with respect to change in skew angle by modeling and analyzing continuous I section reinforcement concrete bridge. The increase in shear force for low skew angle (<15°) the shear force increases linearly. There is about 20% increase in shear force when span increases from 4m to 6m. As the skew angle is increase, shear force is decreased about 30% when span change to 6m from 4m from thereon, shear force for each span increase. The bending moment increases with increase of skew angle and spans of bridges. For each span and skew angle, the change of about 20% is observed in bending moment nature. In case of torsional moment, the pattern of increment in torsional moment is similar to pattern of bending moment. There is about 10% of linear variation increase in torsional moment comparing to bending moment can be noticed broadly.

1.3. Definition of Bridge

A structure built to span and provide passage over a river, chasm, road, or any other physical hurdle. The function required from the bridge and the area where it is constructed decides the design of the bridge. (URL-1)

1.4. Bridge Construction Materials

The traditional building materials for bridges are stones, timber and steel, and more recently reinforced and pre-stressed concrete. For special elements aluminum and its alloys and some types of plastics are used. These materials have different qualities of strength, workability, durability and resistance against corrosion. They differ also in their structure, texture and color or in the possibilities of surface treatment with differing texture and color. For bridges one should use that material which results in the best bridge regarding shape, technical quality, economics and compatibility with the environment. (URL-1)

1.4.1. Stone

The great old bridges of the Etruscans, the Romans, the Fratres Pontifices of the middle ages (since about 1100) and of later master builders were built with stone masonry. The arches and piers have lasted for thousands of years when hard stone was used and the foundations constructed on firm ground. With stone one can build bridges which are both beautiful, durable and of large span (up to 150 m). (URL-1)

Unfortunately, stone bridges have become very expensive. Over a long period, however, stone bridges, which are well designed and well built, might perhaps turn out be the cheapest, because they are long-lasting and need almost no maintenance over centuries unless attacked by extreme air pollution. (URL-1)

Stone is nowadays usually confined to the surfaces, the stones being preset or fixed as facing for abutments, piers or arches. of course, sound weather-resisting stone must be chosen, and fundamental rock like granite, gneiss, porphyry, diabas or crystallized limestone are especially

suitable. Caution is necessary with sandstones, as only siliceous sandstone is durable. The choice of colors of the stone is also relevant. Granite of a uniform grey color and sawn surface can look as dull as simple plain concrete. A harmonious mixture of different colors and slightly embossed surfaces can look very lively, even when the masonry areas are extensive. Surfaces can also be enlivened by bright or dark joint-filling. The sizes of the stone blocks and the roughness of their surfaces must be harmonized with the size of the structure, the abutments, the piers etc. Coarse embossing does not suit a small pier only 1 m thick and 5 m high, but large sized ashlar masonry is suitable for large arch bridges such as the Saalebrücke Jena or the Lahntalbrücke Limburg. Granite masonry was preferred for piers of bridges across the River Rhine, because it resists erosion by sandy water much better than the hardest concrete. (URL-1)

1.4.2. Iron

1.4.3. Reinforced and Pre-stressed Concrete

Concrete is a construction material used in almost all construction works. Having a dull grey color, usually concrete is not preferred in construction like bridges but some of concrete bridges have turned out to be beauties, if someone knows the art. Good concrete attains high compressive strength and resistance against most natural attacks though not against de-icing saltwater, or CO₂ and SO₂ in polluted air. However, its tensile strength is low, so is not preferred in areas of tensile stresses. For tensile reinforcement of concrete steel bars are embedded into it. Steel bars start functioning when concrete cracks i.e. when concrete can no longer resist further tensile stresses. The cracks remain harmless called "hair cracks", if bars are designed and placed correctly. A second method of resisting tensile forces in concrete structures is by pre-stressing. (URL-1)

1.4.4. Steel

Amongst bridge materials steel has the highest and most favorable strength qualities, and it is therefore suitable for the most daring bridges with the longest spans. Normal building steel has compressive and tensile strengths of 370 N/mm², about ten times the compressive strength of a medium concrete and a hundred times its tensile strength. A special merit of steel is its ductility due to which it deforms considerably before it breaks, because it begins to yield above a certain stress level. This yield strength is used as the first term in standard quality terms. (URL-1)

For bridges high strength steel is often preferred. The higher the strength, the smaller the proportional difference between the yield strength and the tensile strength, and this means that high strength steels are not as ductile as those with normal strength. Nor does fatigue strength rise in proportion to the tensile strength. It is therefore necessary to have a profound knowledge of the behavior of these special steels before using them. For building purposes, steel is fabricated in the form of plates (6 to 80mm thick) by means of rolling when red hot. For bearings and some other items, cast steel is used. For members under tension only, like ropes or cables, there are special steels, processed in different ways which allow us to build bold suspension or cable-stayed bridges. (URL-1)

The high strengths of steel allow small cross-sections of beams or girders and therefore a low dead load of the structure. It was thus possible to develop the light-weight "orthotropic plate" steel decks for roadways, which have now become common with an asphalt wearing course, 60 to 80 mm thick. (URL-1)

The pioneers of this orthotropic plate construction called it by the less mysterious and less scientific name "stiffened steel slabs". Plain steel plate, stiffened by cells or ribs, forms the chord of both the transverse cross girders and the longitudinal main-girders. Simultaneously it acts as a wind girder. This bridge deck owes its successful application mainly to mechanized welding, which is now in general use and which has greatly influenced the design of steel bridges. (URL-1)

So plate girder construction now prevails, in which large thin steel plates must be stiffened against buckling. Previously, vertical stiffeners were placed by preference on the outer faces; longitudinal stiffeners were then arranged on the inside. (URL-1)

Today all stiffeners are placed on this inside so as to achieve a smooth outer surface allowing no accumulation of dust or dirt deposits that retain humidity and promote corrosion - the "Achilles heel" of steel structures. Modern steel girder bridges now hardly differ from prestressed concrete bridges in their external appearance - except perhaps in their color. This is perhaps regrettable, because stiffeners on the outside enliven the plate-faces, give scale and make the girder look less heavy. In addition to plate girders, trusses also take full advantage of the material properties of steel. Very delicate looking bridges can be built by joining slender steel sections together to form a truss. Again welding has improved the potential for good form, because hollow sections can be fabricated and joined without the use of big gusset plates. In this way smooth looking trusses arise without the "unrest" which occurs by joining two or four profiles of rolled section with lattice or plates. Steel must be protected against corrosion and this is usually done by applying a protective paint to the bare steel surface. Painting of normal steels is technically necessary and can be used for color design of the bridge. (URL-1)

The choice of colors is an important feature for achieving good appearance. There are steels which do not corrode in a normal environment (the stainless steels V2A and V4A to DIN 17440), but are so expensive that they are used only for components that are either particularly susceptible to the attacks of corrosion or that are very inaccessible. (URL-1)

From the USA came Tentor steel, alloyed with copper, its 'first corrosion layer being said to protect it against further corrosion. This protective rust has a warm sepia-toned color which looks fine in open country. This type of protection, however, does not last in polluted air and the corrosion continues. For steel bridges, good use should be made of the technical necessity of protecting the steel with paint to improve appearance and to achieve harmonious integration of the structure within the landscape. (URL-1)

Aluminum was occasionally used for bridges and the same form was used as for steel girders. Aluminum profiles are fabricated by the extrusion process which allows many varied hollow shapes to be formed, so that aluminum structures can be more elegant than those of steel. Aluminum profiles are popular for bridge parapets because they need no protective paint. (URL-1)

1.5. Main Types of Bridges in the World

Below is the list of main types of bridges:

- 1- Girder bridges.
- 2- Arch bridges.
- 3- Cable-stayed bridges.
- 4- Rigid frame bridges.
- 5- Truss bridges.
- 6- Reinforced concrete bridges.
- 7- Prestressed concrete bridges.
- 8- Steel-concrete composite box-girder bridges.
- 9- Horizontally curved bridges.
- 10- Suspension bridges.
- 11- Timber bridges.

1.5.1. Girder Bridges

It is the most common and most basic bridge type. In its simplest form, a log across a creek is an example of a girder bridge; the two most common girders are I-beam girders and box-girders used in steel girder bridges. Examining the cross section of the I-Beam speaks for its so name. The vertical plate in the middle is known as the *web*, and the top and bottom plates are referred to as flanges. (URL-1)

A box girder takes the shape of a box. The typical box girder has two webs and two flanges. However, in some cases there are more than two webs, creating a multiple chamber box girder. Other examples of simple girders include pi girders, named for their likeness to the mathematical symbol for pi, and T shaped girders. Since the majority of girder bridges these days are built with box or I-beam girders we will skip these rarer cases. (URL-1)

An I-beam is very simple to design and build and works very well in most cases. However, if the bridge contains any curves, the beams become subject to twisting forces, also known as torque. The added second web in a box girder adds stability and increases resistance

to twisting forces. This makes the box girder the ideal choice for bridges with any significant curve in them. Box girders, being more stable are also able to span greater distances and are often used for longer spans, where I-beams would not be sufficiently strong or stable. However, the design and fabrication of box girders is more difficult than that of I beam. For example, in order to weld the inside seams of a box girder, a human or welding robot must be able to operate inside the box girder. (URL-1)

1.5.2. Arch Bridges

Arch bridges pose a classic architecture and the oldest after the girder bridges. Unlike simple girder bridges, arches are well suited to the use of stone. Since the arch doesn't require piers in the center so arches are good choices for crossing valleys and rivers. Arches can be one of the most beautiful bridge types. Arches use a curved structure which provides a high resistance to bending forces. Arches can only be used where the ground or foundation is solid and stable because unlike girder and truss bridges, both ends of an arch are fixed in the horizontal direction (i.e. no horizontal movement is allowed in the bearing). Thus when a load is placed on the bridge (e.g. a car passes over it) horizontal forces occur in the bearings of the arch. Like the truss, the roadway may pass over or through an arch or in some cases. (URL-1)

Structurally there are four basic arch types:

- 1- Hinge-less
- 2- Two-hinged
- 3- Three hinged
- 4- Tied arches

The hinge-less arch uses no hinges and allows no rotation at the foundations. As a result a great deal of force is generated at the foundation (horizontal, vertical, and bending forces) and the hinge-less arch can only be built where the ground is very stable. However, the hinge-less arch is a very stiff structure and suffers less deflection than other arches. The two hinged arch uses hinged bearings which allow rotation. (URL-1)

The only forces generated at the bearings are horizontal and vertical forces. This is perhaps the most commonly used variation for steel arches and is generally a very economical

design. The three-hinged arch adds an additional hinge at the top or crown of the arch. The three-hinged arch suffers very little if there is movement in either foundation (due to earthquakes, sinking, etc.). (URL-1)

However, the three-hinged arch experiences much more deflection and the hinges are complex and can be difficult to fabricate. The three-hinged arch is rarely used anymore. The tied arch is a variation on the arch which allows construction even if the ground is not solid enough to deal with the horizontal forces. Rather than relying on the foundation to restrain the horizontal forces, the girder itself "ties" both ends of the arch together, thus the name "tied arch." (URL-1)

1.5.3. Cable Stayed Bridges

A typical cable stayed bridge is a continuous girder with one or more towers erected above piers in the middle of the span. From these towers, cables stretch down diagonally (usually to both sides) and support the girder. Steel cables are extremely strong but very flexible. Cables are very economical as they allow a slender and lighter structure which is still able to span great distances. Though only a few cables are strong enough to support the entire bridge, their flexibility makes them weak to a force we rarely consider: the wind. (URL-1)

For longer span cable-stayed bridges, careful studies must be made to guarantee the stability of the cables and the bridge in the wind. The lighter weight of the bridge, though a disadvantage in a heavy wind, is an advantage during an earthquake. However, should uneven settling of the foundations occur during an earthquake or over time, the cable-stayed bridge can suffer damage so care must be taken in planning the foundations. The modern yet simple appearance of the cable-stayed bridge makes it an attractive and distinct landmark. (URL-1)

The unique properties of cables, and the structure as a whole, make the design of the bridge a very complex task. For longer spans where winds and temperatures must be considered, the calculations are extremely complex and would be virtually impossible without the aid of computers and computer analysis. The fabrication of cable stay bridges is also relatively difficult. The cable routing and attachments for the girders and towers are complex structures requiring precision fabrication. There are no distinct classifications for cable-stayed

bridges. However, they can distinguish by the number of spans, number of towers, girder type, number of cables, etc. There are many variations in the number and type of towers, as well as the number and arrangement of cables. Typical towers used are single, double, portal, or even A-shaped towers. Cable arrangements also vary greatly. Some typical varieties are mono, harp, fan, and star arrangements. In some cases, only the cables on one side of the tower are attached to the girder, the other side being anchored to a foundation or other counterweight. (URL-1)

1.5.4. Rigid Frame Bridges

Rigid frame bridges are sometimes also known as Rahmen bridges. In a standard girder bridge type, the girder and the piers are separate structures. However, a rigid frame bridge is one in which the piers and girder are one solid structure. The cross sections of the beams in a rigid frame bridge are usually I shaped or box shaped. Design calculations for rigid frame bridges are more difficult than those of simple girder bridges. The junction of the pier and the girder can be difficult to fabricate and requires accuracy and attention to detail. (URL-1)

Though there are many possible shapes, the styles used almost exclusively these days are the pi-shaped frame, the batter post frame, and the V shaped frame. The batter post rigid frame bridge is particularly well suited for river and valley crossings because piers tilted at an angle can straddle the crossing more effectively without requiring the construction of foundations in the middle of the river or piers in deep parts of a valley. V shaped frames make effective use of foundations. Each V-shaped pier provides two supports to the girder, reducing the number of foundations and creating a less cluttered profile. Pi shaped rigid frame structures are used frequently as the piers and supports for inner city highways. The frame supports the raised highway and at the same time allows traffic to run directly under the bridge. (URL-1)

1.5.5. Truss Bridges

Thus, for the most part, all beams in a truss bridge are straight. Trusses are comprised of many small beams that together can support a large amount of weight and span great distances. In most cases the design, fabrication, and erection of trusses is relatively simple. However, once assembled trusses take up a greater amount of space and, in more complex structures, can serve as a distraction to drivers. Like the girder bridges, there are both simple and continuous trusses. (URL-1)

The small size of individual parts of a truss make it the ideal bridge for places where large parts or sections cannot be shipped or where large cranes and heavy equipment cannot be used during erection. Because the truss is a hollow skeletal structure, the roadway may pass over or even through the structure allowing for clearance below the bridge often not possible with other bridge types. Trusses are also classified by the basic design used. The most representative trusses are the Warren truss, the Pratt truss, and the Howe truss. The Warren truss is perhaps the most common truss for both simple and continuous trusses. For smaller spans, no vertical members are used lending the structure a simple look. (URL-1)

For longer spans vertical members are added providing extra strength. Warren trusses are typically used in spans of between 50-100m. The Pratt truss is identified by its diagonal members which, except for the very end ones, all slant down and in toward the center of the span. Except for those diagonal members near the center, all the diagonal members are subject to tension forces only while the shorter vertical members handle the compressive forces. This allows for thinner diagonal members resulting in a more economic design. The Howe truss is the opposite of the Pratt truss. The diagonal members face in the opposite direction and handle compressive forces. This makes it very uneconomic design for steel bridges and its use is rarely seen. (URL-1)

The designer should have first seen and studied many bridges in the course of a long learning process. He should know what type of beam may be suitable in the available conditions, either a beam bridge an arch bridge or a suspended one. He should also know the influence of foundation conditions on the choice of spans and structural systems etc. hence, the designer of the bridge should not only be a learned person but also an experienced one. At auspicious moments an intuitive flash may provide a new solution, which fulfills the task

better than known conventional solutions (intuition, creativity leading to innovations). (URL-1)

1.5.6. Reinforced Concrete Bridges.

The raw materials of concrete, consisting of water, fine aggregate, coarse aggregate, and cement, can be found in most areas of the world and can be mixed to form a variety of structural shapes. The great availability and flexibility of concrete material and reinforcing bars have made the reinforced concrete bridge a very competitive alternative. Reinforced concrete bridges may consist of precast concrete elements, which are fabricated at a production plant and then transported for erection at the job site, or cast-in-place concrete, which is formed and cast directly in its setting location. Cast-in-place concrete structures are often constructed monolithically and continuously. They usually provide a relatively low maintenance cost and better earthquake-resistance performance. Cast-in-place concrete structures, however, may not be a good choice when the project is on a fast-track construction schedule or when the available false work opening clearance is limited. (Chen and Duan, 2000)

1.5.7. Prestressed Concrete Bridges

This type will be discussed in the next part.

1.5.8. Steel - Concrete Composite Box Girder Bridges

Box girders are used extensively in the construction of urban highway, horizontally curved, and long-span bridges. Box girders have higher flexural capacity and torsional rigidity, and the closed shape reduces the exposed surface, making them less susceptible to corrosion. Box girders also provide smooth, aesthetically pleasing structures. There are two types of steel box girders: steel-concrete composite box girders (i.e., steel box composite with concrete deck) and steel box girders with orthotropic decks. Composite box girders are

generally used in moderate- to medium-span (30 to 60 m) bridges, and steel box girders with orthotropic decks are often used for longer-span bridges. (Chen and Duan, 2000)

1.5.9. Horizontally Curved Bridges

As a result of complicated geometrics, limited rights of way, and traffic mitigation, horizontally curved bridges are becoming the norm of highway interchanges and urban expressways. This type of superstructure has gained popularity since the early 1960s because it addresses the needs of transportation engineering. (Chen and Duan, 2000)

1.5.10. Suspension Bridges

The origins of the suspension bridge go back a long way in history. Primitive suspension bridges, or simple crossing devices, were the forebears to today's modern suspension bridge structures. Suspension bridges were constructed with iron chain cables over 2000 years ago in China and a similar record has been left in India. The iron suspension bridge, assumed to have originated in the Orient, appeared in Europe in the 16th century and was developed in the 18th century. Although wrought iron chain was used as the main cables in the middle of the 18th century, a rapid expansion of the center span length took place in the latter half of the 19th century triggered by the invention of steel. Today, the suspension bridge is most suitable type for very long-span bridge and actually represents 20 or more of all the longest span bridges in the world. (Chen and Duan, 2000)

1.5.11. Timber Bridges

Wood is one of the earliest building materials, and as such often its use has been based more on tradition than on principles of engineering. However, the structural use of wood and wood-based materials has increased steadily in recent times, including a renewed interest in the use of timber as a bridge material. Supporting this renewed interest has been an evolution of our understanding of wood as a structural material and our ability to analyze and design

safe, durable, and functional timber bridge structures. An accurate and complete understanding of any material is key to its proper use in structural applications, and structural timber and other wood-based materials are no exception to this requirement. (Chen and Duan, 2000)



2. PRESTRESSED CONCRETE BRIDGES

2.1. Introduction

Prestressed concrete structures, using high-strength materials to improve serviceability and durability, are an attractive alternative for long-span bridges, and have been used worldwide since the 1950s. This part focuses only on conventional prestressed concrete bridges. For more detailed discussion on prestressed concrete, references are made to textbooks by Lin and Burns 1981, Nawy 1996, Collins and Mitchell 1991. (Chen and Duan, 2000)

2.1.1. Materials

2.1.1.1. Concrete

A 28-day cylinder compressive strength (f'_c) of concrete 28 to 56 MPa is used most commonly in United States. A higher early strength is often needed, however, either for the fast precast method used in the production plant or for the fast removal of formwork in the cast-in-place method. The modulus of elasticity of concrete with density between 1440 and 2500 kg/m³ may be taken as (Chen and Duan, 2000)

$$E_c = 0.043 w_c \sqrt{f'_c} \quad (1)$$

Where w_c is the density of concrete (kg/m³). Poisson's ratio ranges from 0.11 to 0.27, but 0.2 is often assumed.

The modulus of rupture of concrete may be taken as (AASHTO LRFD, 1994)

$$f_r = \begin{cases} 0.63 \sqrt{f'_c} & \text{for normal weight concrete - flexural} \\ 0.52 \sqrt{f'_c} & \text{for sand - light weight concrete - flexural} \\ 0.44 \sqrt{f'_c} & \text{for all - light weight concrete - flexural} \\ 0.1 f'_c & \text{for direct tension} \end{cases} \quad (2)$$

Concrete shrinkage is a time-dependent material behavior and mainly depends on the mixture of concrete, moisture conditions, and the curing method. Total shrinkage strains range from 0.0004 to 0.0008 over the life of concrete and about 80% of this occurs in the first year.

For moist-cured concrete devoid of shrinkage-prone aggregates, the strain due to shrinkage ε_{sh} may be estimated by (AASHTO LRFD, 1994; Chen and Duan, 2000)

$$\varepsilon_{sh} = -k_s k_h \left(\frac{t}{t+35} \right) 0.51 \times 10^{-3} \quad (3)$$

$$k_s = \left[\frac{\frac{t}{26e^{0.0142(V/S)} + t}}{\frac{t}{45+t}} \right] \left[\frac{1064 - 3.7(V/S)}{923} \right] \quad (4)$$

where t is drying time (days); k_s is size factor and k_h is humidity factors may be approximated by $K_n = (140-H)/70$ for $H < 80\%$; $K_n = 3(100-H)/70$ for $H \geq 80\%$; and V/S is volume to surface area ratio. If the moist-cured concrete is exposed to drying before 5 days of curing, the shrinkage determined by eq. (3) should be increased by 20%. (Chen and Duan, 2000)

For stem-cured concrete devoid of shrinkage-prone aggregates:

$$\varepsilon_{sh} = -k_s k_h \left(\frac{t}{t+55} \right) 0.56 \times 10^{-3} \quad (5)$$

Creep of concrete is a time-dependent inelastic deformation under sustained load and depends primarily on the maturity of the concrete at the time of loading. Total creep strain generally ranges from about 1.5 to 4 times that of the “instantaneous” deformation. The creep coefficient may be estimated as (AASHTO LRFD, 1994; Chen and Duan, 2000)

$$\psi(t, t_1) = 3.5 K_C K_f \left(1.58 - \frac{H}{120} \right) t_i^{-0.118} \frac{(t-t_i)^{0.6}}{10 + (t-t_i)^{0.6}} \quad (6)$$

$$K_f = \frac{62}{42 + f_c'} \quad (7)$$

$$k_s = \left[\frac{\frac{t}{26e^{0.0142(V/S)} + t}}{\frac{t}{45 + t}} \right] \left[\frac{1.8 + 1.77e^{-0.0213(V/S)}}{2.587} \right] \quad (8)$$

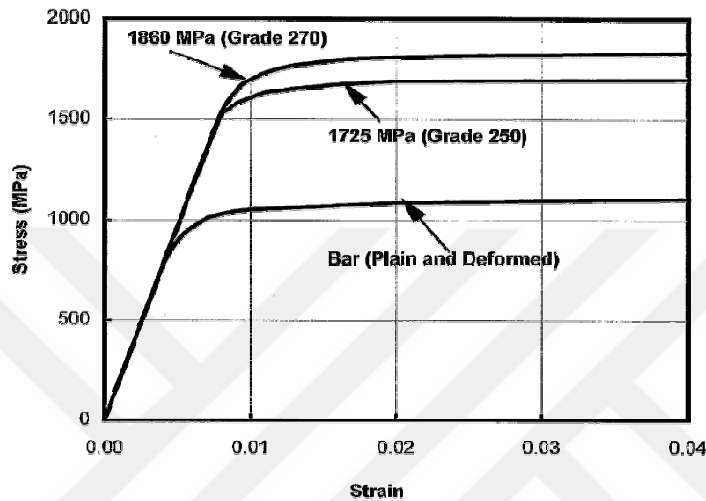


Figure 2.1. Typical stress–strain curves for prestressing steel

Where H is relative humidity (%); t is maturity of concrete (days); t_i is age of concrete when load is initially applied (days); K_c is the effect factor of the volume-to-surface ratio; and K_f is the effect factor of concrete strength. (Chen and Duan, 2000)

Creep, shrinkage, and modulus of elasticity may also be estimated in accordance with (CEB-FIP Mode Code, 1993; Chen and Duan, 2000)

2.1.1.2. Steel for Prestressing

Uncoated, seven-wire stress-relieved strands (AASHTO M203 or ASTM A416), or low-relaxation seven-wire strands and uncoated high-strength bars (AASHTO M275 or ASTM A722) are commonly used in prestressed concrete bridges. Prestressing reinforcement, whether wires, strands, or bars, are also called tendons. The properties for prestressing steel are shown in table 2.1. (Chen and Duan, 2000)

Table 2.1. Properties of prestressing strand and bars

Material	Grade and Type	Diameter (mm)	Tensile Strength f_{pu} (MPa)	Yield Strength f_{py} (MPa)	Modulus of Elasticity E_p (MPa)
Strand	1725 MPa (Grade 250)	6.35–15.24	1725	80% of f_{pu} except 90% of f_{pu}	197,000
	1860 MPa (Grade 270)	10.53–15.24	1860	for low relaxation strand	
Bar	Type 1, Plain	19 to 25	1035	85% of f_{pu}	207,000
	Type 2, Deformed	15 to 36	1035	80% of f_{pu}	

Typical stress–strain curves for prestressing steel are shown in figure 2.1. These curves can be approximated by the following equations: (Chen and Duan, 2000)

For Grade 250: (PCI,1985)

$$f_{ps} = \begin{cases} 197,000\varepsilon_{ps} & \text{for } \varepsilon_{ps} \leq 0.008 \\ 1710 - \frac{0.4}{\varepsilon_{ps} - 0.006} < 0.98f_{pu} & \text{for } \varepsilon_{ps} > 0.008 \end{cases} \quad (9)$$

For Grade 270: (PCI, 1985)

$$f_{ps} = \begin{cases} 197,000\varepsilon_{ps} & \text{for } \varepsilon_{ps} \leq 0.008 \\ 1848 - \frac{0.517}{\varepsilon_{ps} - 0.0065} < 0.98f_{pu} & \text{for } \varepsilon_{ps} > 0.008 \end{cases} \quad (10)$$

For Bars:

$$f_{ps} = \begin{cases} 207,000\varepsilon_{ps} & \text{for } \varepsilon_{ps} \leq 0.004 \\ 1020 - \frac{0.192}{\varepsilon_{ps} - 0.003} < 0.98f_{pu} & \text{for } \varepsilon_{ps} > 0.004 \end{cases} \quad (11)$$

2.1.1.3. Advanced Composites for Prestressing

Advanced composites-fiber-reinforced plastics (FPR) with their high tensile strength and good corrosion resistance work well in prestressed concrete structures. Application of advanced composites to prestressing have been investigated since the 1950s. (Wines et al, 1966; Eubunsky and Rubinsky, 1954)

Extensive research has also been conducted in Germany and Japan (Iyer and Anigol, 1991). The Ulenbergstrasse bridge, a two-span (21.3 and 25.6 m) solid slab using 59 fiberglass tendons, was built in 1986 in Germany. It was the first prestressed concrete bridge to use advanced composite tendons in the world. (Miesslerer and Wolff, 1991; Chen and Duan, 2000)

FPR cables and rods made of aramid, glass, and carbon fibers embedded in a synthetic resin have an ultimate tensile strength of 1500 to 2000 MPa, with the modulus of elasticity ranging from 62,055 MPa to 165,480 MPa (Iyer and Anigol, 1991). The main advantages of FPR are (1) a high specific strength (ratio of strength to mass density) of about 10 to 15 times greater than steel; (2) a low modulus of elasticity making the prestress loss small; (3) good performance in fatigue; tests show (Kim and Meier, 1991) that for CFRP, at least three times the higher stress amplitudes and higher mean stresses than steel are achieved without damage to the cable over 2 million cycles. (Chen and Duan, 2000)

Although much effort has been given to exploring the use of advanced composites in civil engineering structures and the cost of advanced composites has come down significantly, the design and construction specifications have not yet been developed. Time is still needed for engineers and bridge owners to realize the cost-effectiveness and extended life expectancy gained by using advanced composites in civil engineering structures. (Chen and Duan, 2000)

2.1.1.4. Grout

For post-tensioning construction, when the tendons are to be bound, grout is needed to transfer loads and to protect the tendons from corrosion. Grout is made of water, sand, and cements or epoxy resins.(AASHTO LRFD, 1994) requires that details of the protection

method be indicated in the contract documents. Readers are referred to the post-tensioning manual. (PTI, 1981; Chen and Duan, 2000)

2.1.2. Prestressing Systems

There are two types of prestressing systems: pre-tensioning and post-tensioning systems. Pre-tensioning systems are methods in which the strands are tensioned before the concrete is placed. This method is generally used for mass production of pre-tensioned members. Post-tensioning systems are methods in which the tendons are tensioned after concrete has reached a specified strength. This technique is often used in projects with very large elements figure 2.2. The main advantage of post-tensioning is its ability to post-tension both precast and cast-in-place members. Mechanical prestressing-jacking is the most common method used in bridge structures. (Chen and Duan, 2000)



Figure 2.2. A post-tensioned box-girder bridge under construction

2.2. Section Types

2.2.1. Void Slabs

Figure 2.3a shows (FHWA, 1990) standard precast prestressed voided slabs. Sectional properties are listed in table 2.2. Although the cast-in-place prestressed slab is more expensive than a reinforced concrete slab, the precast prestressed slab is economical when many spans are involved. Common spans range from 6 to 15 m. Ratios of structural depth to span are 0.03 for both simple and continuous spans. (Chen and Duan, 2000)

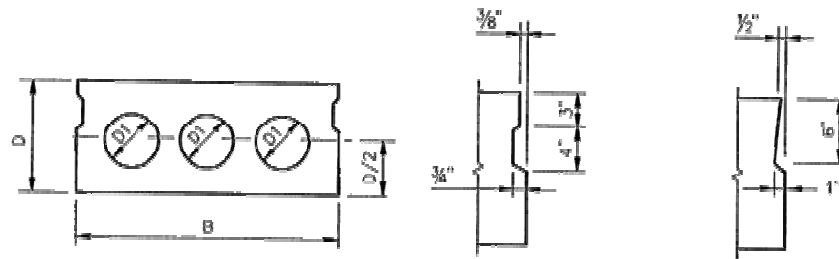
2.2.2. I-Girders

Figures 2.3b and c show AASHTO standard I-beams (FHWA, 1990). The section properties are given in table 2.3. This bridge type competes well with steel girder bridges. The formwork is complicated, particularly for skewed structures. These sections are applicable to spans 9 to 36 m. Structural depth-to-span ratios are 0.055 for simple spans and 0.05 for continuous spans. (Chen and Duan, 2000)

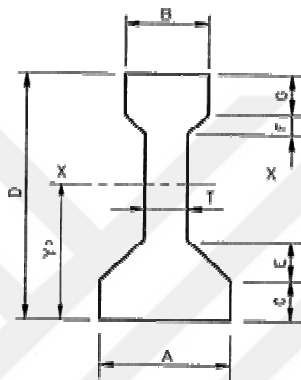
2.2.3. Box Girders

Figure 2.3d shows (FHWA, 1990) standard precast box sections. Section properties are given in table 2.4. These sections are used frequently for simple spans of over 30 m and are particularly suitable for widening bridges to control deflections. (Chen and Duan, 2000)

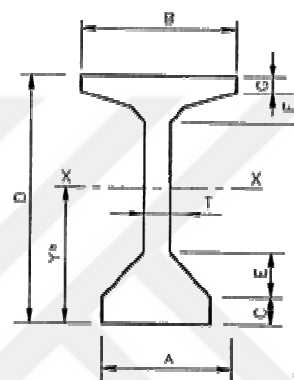
The box-girder shape shown in figure 2.3e is often used in cast-in-place prestressed concrete bridges. The spacing of the girders can be taken as twice the depth. . This type is used mostly for spans of 30 to 180 m. Structural depth-to-span ratios are 0.045 for simple spans, and 0.04 for continuous spans. The high torsional resistance of the box girder makes it particularly suitable for curved alignment (figure 2.4) such as those needed on freeway ramps. (Chen and Duan, 2000)



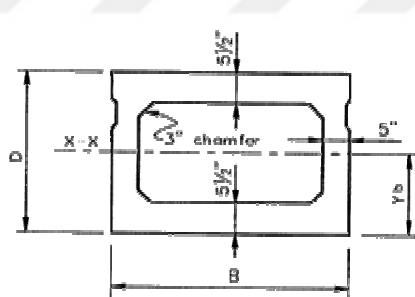
(a) Precast voided slab section and shear key



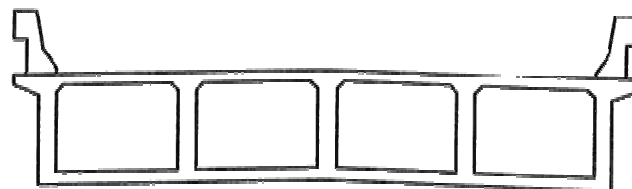
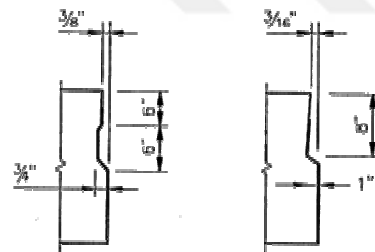
(b) AASHTO Beam Types II, III and IV



(c) AASHTO Beam Types V and IV



(d) Precast Box Section and Shear Key



(e) Cast-in-Place Box Section

Figure 2.3. Typical cross sections of prestressed concrete bridge superstructures

2.3. Losses of Prestress

Loss of prestress refers to the reduced tensile stress in the tendons. Although this loss does affect the service performance (such as camber, deflections, and cracking), it has no effect on the ultimate strength of a flexural member unless the tendons are unbounded or the final stress is less than $0.5f_{pu}$ (PCI, 1985). It should be noted, however, that an accurate estimate of prestress loss is more pertinent in some pre-stressed concrete members than in others. Prestress losses can be divided into two categories: (Chen and Duan, 2000)

Table 2.2. Precast prestressed voided slabs section properties (figure. 2.3a)

Span Range, ft (m)	Section Dimensions				Section Properties		
	Width B in. (mm)	Depth D in. (mm)	D1 in. (mm)	D2 in. (mm)	A in ² (mm ² 106)	I _x in ⁴ (mm ⁴ 109)	S _x in ³ (mm ³ 106)
25 (7.6)	48 (1,219)	12 (305)	0 (0)	0 (0)	576 (0.372)	6,912 (2.877)	1,152 (18.878)
30~35 (10.1~10.70)	48 (1,219)	15 (381)	8 (203)	8 (203)	569 (0.362)	12,897 (5.368)	1,720 (28.185)
40~45 (12.2~13.7)	48 (1,219)	18 (457)	10 (254)	10 (254)	628 (0.405)	21,855 (10.097)	2,428 (310.788)
50 (15.2)	48 (1,219)	21 (533)	12 (305)	10 (254)	703 (0.454)	34,517 (1.437)	3,287 (53.864)

Table 2.3. Precast prestressed I-beam section properties (figures. 2.3b and c)

AASHTO Beam Type	Section Dimensions, in. (mm)							
	Depth D	Bottom Width A	Web Width T	Top Width B	C	E	F	G
II	36 (914)	18 (457)	6 (152)	12 (305)	6 (152)	6 (152)	3 (76)	6 (152)
III	45(1143)	22 (559)	7 (178)	16(406)	7 (178)	7.5(191)	4.5 (114)	7 (178)
IV	54(1372)	26 (660)	8 (203)	20(508)	8 (203)	9(229)	6(152)	8 (203)
V	65(1651)	28 (711)	8 (203)	42(1067)	8 (203)	10(254)	3(76)	5 (127)
VI	72(1829)	28(711)	8(203)	42(1067)	8 (203)	10(254)	3(76)	5 (127)
	Section Properties							
	A in ² (mm ² 10b)	Y _b in (mm)	I _x in ⁴ (mm ⁴ 109)	S _b in ³ (mm ⁴ 106)	S _t in ³ (mm ⁴ 106)	Span Ranges, ft (m)		
II	369 (0.2381)	15.83 (402.1)	50,980 (21.22)	3220 (52.77)	2528 (41.43)	40~ 45 (12.2~ 13.7)		
III	560 (0.3613)	20.27 (514.9)	125,390 (52.19)	6186 (101.38)	5070 (83.08)	50~ 65 (15.2 ~ 110.8)		
IV	789 (0.5090)	24.73 (628.1)	260,730 (108.52)	10543 (172.77)	8908 (145.98)	70~ 80 (21.4~ 24.4)		
V	1013 (0.6535)	31.96 (811.8)	521,180 (216.93)	16307 (267.22)	16791 (275.16)	90 ~ 100 (27.4~ 30.5)		
VI	1085 (0.7000)	36.38 (924.1)	733,340 (305.24)	20158 (330.33)	20588 (337.38)	110~ 120 (33.5~ 36.6)		

Instantaneous losses including losses due to anchorage set (Δf_{pA}), friction between tendons and surrounding materials (Δf_{pF}), and elastic shortening of concrete (Δf_{pES}) during the construction stage;

Time-dependent losses including losses due to shrinkage (Δf_{pSR}), creep (Δf_{pCR}), and relaxation of the steel (Δf_{pR}) during the service life. (Chen and Duan,2000)

The total prestress loss (Δf_{pT}) is dependent on the prestressing methods.

For pre-tensioned members:

$$\Delta f_{pT} = \Delta f_{pES} + \Delta f_{pSR} + \Delta f_{pCR} + \Delta f_{pR} \quad (12)$$

For post-tensioned members:

$$\Delta f_{pT} = \Delta f_{pA} + \Delta f_{pF} + \Delta f_{pES} + \Delta f_{pSR} + \Delta f_{pCR} + \Delta f_{pR} \quad (13)$$



Figure 2.4. Prestressed box-girder bridge (I-280/110 Interchange, CA)

Table 2.4. Precast prestressed box section properties (figure. 2.3d)

Span ft.(m)	Section Dimensions		Section Properties				
	Width B in. (mm)	Depth D in (mm)	A in ² (mm ² 10 ⁶)	Y _b in (mm)	I _x in ⁴ (mm ⁴ 10 ⁹)	S _b in ³ (mm ³ 10 ⁶)	S _t in ³ (mm ³ 10 ⁶)
50 (15.2)	48 (1,219)	27 (686)	693 (0.4471)	13.37 (3310.6)	65,941 (27.447)	4,932 (80.821)	4,838 (710.281)
60 (18.3)	48 (1,219)	33 (838)	753 (0.4858)	16.33 (414.8)	110,499 (45.993)	6,767 (110.891)	6,629 (108.630)
70 (21.4)	48 (1,219)	39 (991)	813 (0.5245)	110.29 (490.0)	168,367 (70.080)	8,728 (143.026)	8,524 (1310.683)
80 (24.4)	48 (1,219)	42 (1,067)	843 (0.5439)	20.78 (527.8)	203,088 (84.532)	9,773 (160.151)	9,571 (156.841)

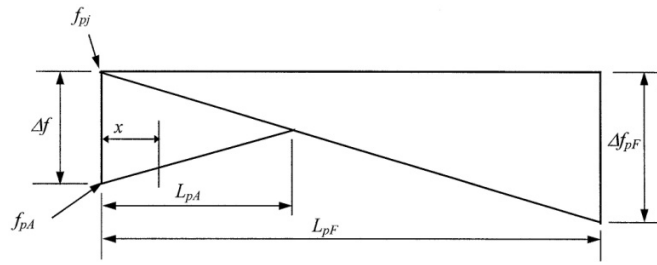


Figure 2.5. Anchorage set loss model

Table 2.5. Friction coefficients for post-tensioning tendons (AASHTO LRFD, 1994)

Type of Tendons and Sheathing	Wobble Coefficient K (1/mm).(10 ⁻⁶)	Curvature Coefficient α (1/rad)
Tendons in rigid and semi rigid galvanized ducts, seven-wire strands	0.66	0.05 ~ 0.15
Pregreased tendons, wires and seven-wire strands	0.98 ~ 6.6	0.05 ~ 0.15
Mastic-coated tendons, wires and seven-wire strands	3.3 ~ 6.6	0.05 ~ 0.15
Rigid steel pipe deviations	66	0.25, lubrication required

2.3.1. Instantaneous Losses

2.3.1.1. Anchorage Set Loss

As shown in figure 2.5, assuming that the anchorage set loss changes linearly within the length (L_{pA}), the effect of anchorage set on the cable stress can be estimated by the following formula: (Chen and Duan, 2000)

$$\Delta f_{pA} = \Delta f \left(1 - \frac{\chi}{L_{pA}} \right) \quad (14)$$

$$L_{pA} = \sqrt{\frac{E (\Delta L) L_{pF}}{\Delta f_{pF}}} \quad (15)$$

$$\Delta f = \frac{2\Delta f_{pF} L_{pA}}{L_{pF}} \quad (16)$$

where ΔL is the thickness of anchorage set; E is the modulus of elasticity of anchorage set; Δf is the change in stress due to anchor set; L_{pA} is the length influenced by anchor set; L_{pF} is the length to a point where loss is known; and X is the horizontal distance from the jacking end to the point considered. (Chen and Duan, 2000)

2.3.1.2. Friction Loss

For a post-tensioned member, friction losses are caused by the tendon profile curvature effect and the local deviation in tendon profile wobble effects. AASHTO LRFD specifies the following formula:

$$\Delta f_{pF} = f_{pj} (1 - e^{-(Kx + \alpha\mu)}) \quad (17)$$

Where K is the wobble friction coefficient and μ is the curvature friction coefficient (see table 2.5); x is the length of a prestressing tendon from the jacking end to the point considered; and α is the sum of the absolute values of angle change in the prestressing steel path from the jacking end. (Chen and Duan, 2000)

2.3.1.3. Elastic Shortening Loss Δf_{pES}

The loss due to elastic shortening can be calculated using the following formula (AASHTO LRFD, 1994):

$$\Delta f_{pES} = \begin{cases} \frac{E_p}{E_{ci}} f_{cgp} & \text{for pretensioned members} \\ \frac{N-1}{2N} \frac{E_p}{E_{ci}} f_{cgp} & \text{for post tensioned members} \end{cases} \quad (18)$$

Table 2.6. Lump sum estimation of time-dependent prestress losses (AASHTO LRFD, 1994)

Type of Beam Section	Level	For Wires and Strands with $f_{pu} = 1620, 1725, \text{ or } 1860 \text{ MPa}$	For Bars with $f_{pu} = 1000 \text{ or } 1100 \text{ MPa}$
Rectangular beams and solid slab	Upper bound Average	200 + 28 PPR 180 + 28 PPR	130 + 41 PPR
Box girder	Upper bound Average	145 + 28 PPR 130 + 28 PPR	100
I-girder	Average	$230 \left[1.0 - 0.15 \frac{f_{c'} - 41}{41} \right] + 41\text{PPR}$	130 + 41 PPR
Single-T, double-T hollow core and voided slab	Upper bound	$230 \left[1.0 - 0.15 \frac{f_{c'} - 41}{41} \right] + 41\text{PPR}$	$230 \left[1.0 - 0.15 \frac{f_{c'} - 41}{41} \right] + 41\text{PPR}$
	Average	$230 \left[1.0 - 0.15 \frac{f_{c'} - 41}{41} \right] + 41\text{PPR}$	

Note:

- 1- PPR is partial prestress ratio = $(A_{ps}f_{py}) / (A_{ps}f_{py} + A_s f_y)$.
- 2- For low-relaxation strands, the above values may be reduced by
 - 28 MPa for box girders
 - 41 MPa for rectangular beams, solid slab and I-girders, and
 - 55 MPa for single-T, double-T, hollow-core and voided slabs.

Where E_{ci} is modulus of elasticity of concrete at transfer (for pre-tensioned members) or after jacking (for post-tensioned members); N is the number of identical prestressing tendons; and f_{cgp} is sum of the concrete stress at the center of gravity of the prestressing tendons due to the prestressing force at transfer (for pre-tensioned members) or after jacking (for post-tensioned members) and the self-weight of members at the section with the maximum moment. For post-tensioned structures with bonded tendons, f_{cgp} may be calculated at the center section of the span for simply supported structures, at the section with the maximum moment for continuous structures. (Chen and Duan, 2000)

2.3.2. Time-Dependent Losses

2.3.2.1. Lump Sum Estimation

AASHTO LRFD provides the approximate lump sum estimation (table 2.6) of time-dependent losses Δf_{pTM} resulting from shrinkage and creep of concrete, and relaxation of the prestressing steel. While the use of lump sum losses is acceptable for “average exposure conditions,” for unusual conditions, more-refined estimates are required. (Chen and Duan, 2000)

2.3.2.2. Refined Estimation

A. Shrinkage Loss: Shrinkage loss can be determined by formulas (AASHTO LRFD, 1994):

$$\Delta f_{pSR} = \begin{cases} 93 - 0.85H & \text{for pre-tensioned members} \\ 11 - 1.03H & \text{for post-tensioned members} \end{cases} \quad (19)$$

Where H is average annual ambient relative humidity (%).

B. Creep Loss: Creep loss can be predicted by: (AASHTO LRFD, 1994)

$$\Delta f_{pCR} = 12f_{cgp} - 7\Delta f_{cdp} \geq 0 \quad (20)$$

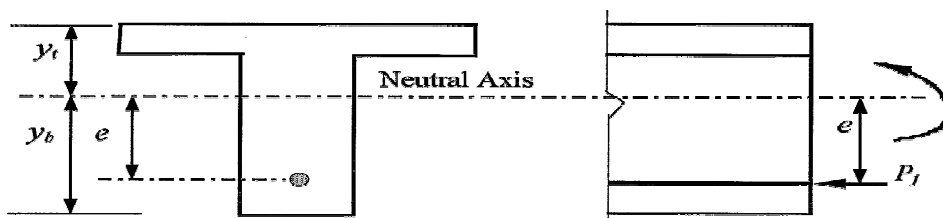


Figure 2.6. Prestressed concrete member section at service limit state

Where f_{cgp} is concrete stress at center of gravity of prestressing steel at transfer, and Δf_{cdp} is concrete stress change at center of gravity of prestressing steel due to permanent loads, except the load acting at the time the prestressing force is applied. (Chen and Duan, 2000)

C. Relaxation Loss: The total relaxation loss (Δf_{pR}) includes two parts: relaxation at time of transfer Δf_{pR1} and after transfer Δf_{pR2} . For a pre-tensioned member initially stressed beyond $0.5f_{pu}$, AASHTO LRFD specifies

$$\Delta f_{pR1} = \begin{cases} \frac{\log 24t}{10} \left[\frac{f_{pi}}{f_{py}} - 0.55 \right] f_{pi} & \text{for stress - relieved strand} \\ \frac{\log 24t}{40} \left[\frac{f_{pi}}{f_{py}} - 0.55 \right] f_{pi} & \text{for low - relaxation strand} \end{cases} \quad (21)$$

For stress-relieved strands

$$\Delta f_{pR2} = \begin{cases} 138 - 0.4\Delta f_{pES} - 0.2(\Delta f_{pSR} + \Delta f_{pCR}) & \text{for pre - tensioning} \\ 138 - 0.3\Delta f_{pF} - 0.4\Delta f_{pES} - 0.2(\Delta f_{pSR} + \Delta f_{pCR}) & \text{for post - tensioning} \end{cases} \quad (22)$$

Where t is time estimated in days from testing to transfer. For low-relaxation strands, Δf_{pR2} is 30% of those values obtained from eq. (22). (Chen and Duan, 2000)

2.4. Design Considerations

2.4.1. Basic Theory

The main distinguishing characteristics of prestressed concrete are that: (Chen and Duan, 2000)

- The stresses for concrete and prestressing steel and deformation of structures at each stage, i.e., during prestressing, handling, transportation, erection, and the service life, as well as stress concentrations, need to be investigated on the basis of elastic theory.
- The prestressing force is determined by concrete stress limits under service load.

- Flexure and shear capacities are determined based on the ultimate strength theory.

For the prestressed concrete member section shown in figure 2.6, the stress at various load stages can be expressed by the following formula:

$$f = \frac{P_j}{A} \pm \frac{P_j ey}{I} \pm \frac{My}{I} \quad (23)$$

Table 2.7. Stress limits for prestressing tendons (AASHTO LRFD, 1994)

Stress Type	Prestressing Method	Prestressing Tendon Type		
		Stress Relieved Strand and Plain High-Strength Bars	Low Relaxation Strand	Deformed High-Strength Bars
At jacking, f_{pj}	Pre-tensioning	$0.72f_{pu}$	$0.78f_{pu}$	—
	Post-tensioning	$0.76f_{pu}$	$0.80f_{pu}$	$0.75f_{pu}$
After transfer, f_{pt}	Pre-tensioning	$0.70f_{pu}$	$0.74f_{pu}$	—
	Post-tensioning - at anchorages and couplers immediately after anchor set	$0.70f_{pu}$	$0.70f_{pu}$	$0.66f_{pu}$
	Post-tensioning - general	$0.70f_{pu}$	$0.74f_{pu}$	$0.66f_{pu}$
At Service Limit State, f_{pc}	After all losses	$0.80f_{py}$	$0.80f_{py}$	$0.80f_{py}$

Table 2.8. Temporary concrete stress limits at jacking state before losses due to creep and shrinkage - fully prestressed components (AASHTO LRFD, 1994)

Stress Type	Area and Condition	Stress (MPa)
Compressive	Pre-tensioned.	$0.60 f_{ci}'$
	Post-tensioned.	$0.55 f_{ci}'$
Tensile	Pre-compressed tensile zone without bonded reinforcement.	N/A
	Area other than the pre-compressed tensile zones and without bonded auxiliary reinforcement.	$0.25\sqrt{f_{ci}'} \leq 1.38$
	Area with bonded reinforcement which is sufficient to resist 120% of the tension force in the cracked concrete computed on the basis of uncracked section.	$0.58\sqrt{f_{ci}'}$
	Handling stresses in prestressed piles.	$0.415\sqrt{f_{ci}'}$

Note: Tensile stress limits are for non segmental bridges only.

Where P_j is the prestress force; A is the cross-sectional area; I is the moment of inertia; e is the distance from the center of gravity to the centroid of the prestressing cable; y is the distance from the centroidal axis; and M is the externally applied moment. (Chen and Duan, 2000)

Section properties are dependent on the prestressing method and the load stage. In the analysis, the following guidelines may be useful: (Chen and Duan, 2000)

- Before bounding of the tendons, for a post-tensioned member, the net section should be used theoretically, but the gross section properties can be used with a negligible tolerance.
- After bounding of tendons, the transformed section should be used, but gross section properties may be used approximately.
- At the service load stage, transformed section properties should be used.

2.4.2. Stress Limits

The stress limits are the basic requirements for designing a prestressed concrete member. The purpose for stress limits on the prestressing tendons is to mitigate tendon fracture, to avoid inelastic tendon deformation, and to allow for prestress losses. Tables 2.7 lists the AASHTO LRFD stress limits for prestressing tendons. (Chen and Duan, 2000)

Table 2.9. Concrete stress limits at service limit state after all losses-fully prestressed components (AASHTO LRFD, 1994)

Stress Type	Area and Condition		Stress (MPa)
Compressive	Nonsegmental bridge at service stage		$0.45f_c'$
	Nonsegmental bridge during shipping and handling		$0.60f_c'$
	Segmental bridge during shipping and handling		$0.45f_c'$
Tensile	Precompressed tensile zone assuming uncracked section	With bonded prestressing tendons other than piles	$0.50\sqrt{f_c'}$
		Subjected to severe corrosive conditions	$0.25\sqrt{f_c'}$
		With unbonded prestressing tendon	No tension

Note: Tensile stress limits are for nonsegmental bridges only.

The purpose for stress limits on the concrete is to ensure no overstressing at jacking and after transfer stages and to avoid cracking (fully prestressed) or to control cracking (partially prestressed) at the service load stage. Tables 2.8 and 2.9 list the AASHTO LRFD stress limits for concrete. (Chen and Duan, 2000)

A prestressed member that does not allow cracking at service loads is called a fully prestressed member, whereas one that does is called a partially prestressed member. Compared with full prestress, partial prestress can minimize camber, especially when the dead load is relatively small, as well as provide savings in prestressing steel, in the work required to tension, and in the size of end anchorages and utilizing cheaper mild steel. On the other hand, engineers must be aware that partial prestress may cause earlier cracks and greater deflection under overloads and higher principal tensile stresses under service loads. Nonprestressed reinforcement is often needed to provide higher flexural strength and to control cracking in a partially prestressed member. (Chen and Duan, 2000)

2.4.3. Cable Layout

A cable is a group of prestressing tendons and the center of gravity of all prestressing reinforcement. It is a general design principle that the maximum eccentricity of prestressing tendons should occur at locations of maximum moments. Although straight tendons (figure 2.7a) and harped multi-straight tendons (figure 2.7b and c) are common in the precast members, curved tendons are more popular for cast-in-place post-tensioned members. Typical cable layouts for bridge super-structures are shown in figure 2.7. (Chen and Duan,2000)

To ensure that the tensile stress in extreme concrete fibers under service does not exceed code stress limits ACI code (AASHTO LRFD, 1994), cable layout envelopes are delimited. Figure 2.8 shows limiting envelopes for simply supported members. From eq. (23), the stress at extreme fiber can be obtained.

$$f = \frac{P_j}{A} \pm \frac{P_j e C}{I} \pm \frac{MC}{I} \quad (24)$$

Where C is the distance of the top or bottom extreme fibers from the center gravity of the section (y_b or y_t as shown in figure 2.6). (Chen and Duan, 2000)

When no tensile stress is allowed, the limiting eccentricity envelope can be solved from eq. (24) with

$$e_{\text{limit}} = \frac{I}{AC} \pm \frac{M}{IP_j} \quad (25)$$

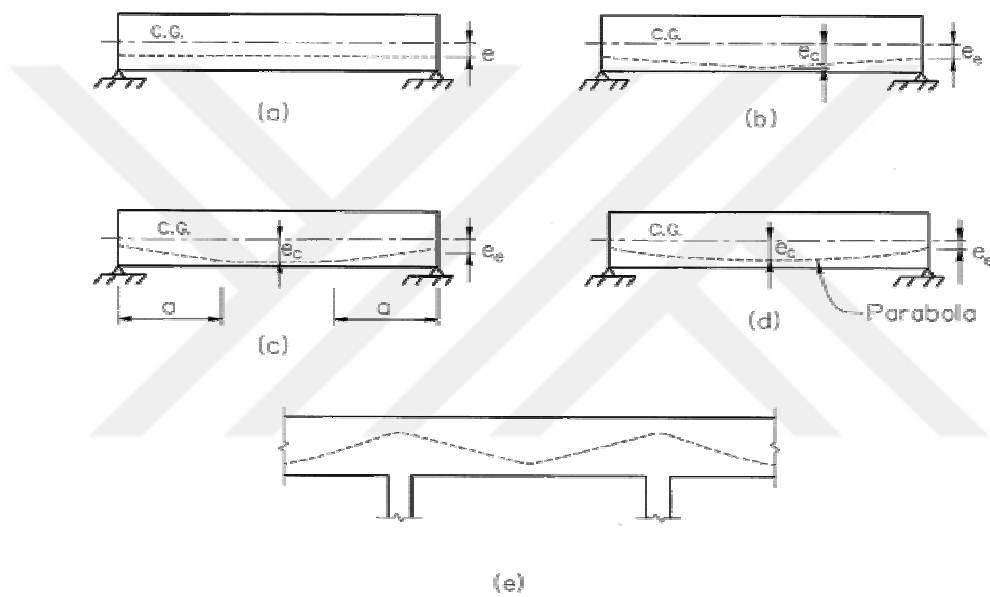


Figure 2.7. Cable layout for bridge superstructures

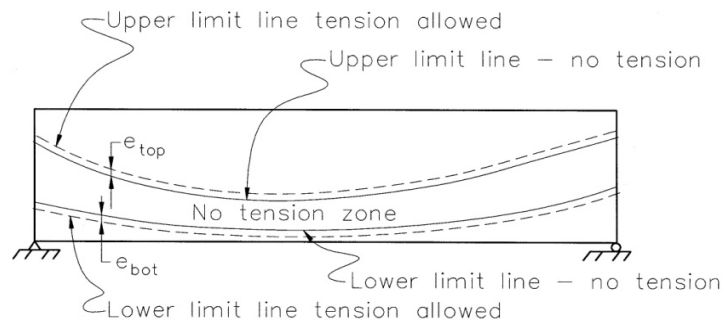


Figure 2.8. Cable layout envelopes

For limited tension stress f_t , additional eccentricities can be obtained:

$$e' = \frac{f_t I}{p_j C} \quad (26)$$

2.4.4. Secondary Moments

The primary moment ($M_1 = P_j e$) is defined as the moment in the concrete section caused by the eccentricity of the prestress for a statically determinate member. The secondary moment M_s (figure 2.9d) is defined as moment induced by prestress and structural continuity in an indeterminate member. Secondary moments can be obtained by various methods. The resulting moment is simply the sum of the primary and secondary moments. (Chen and Duan, 2000)

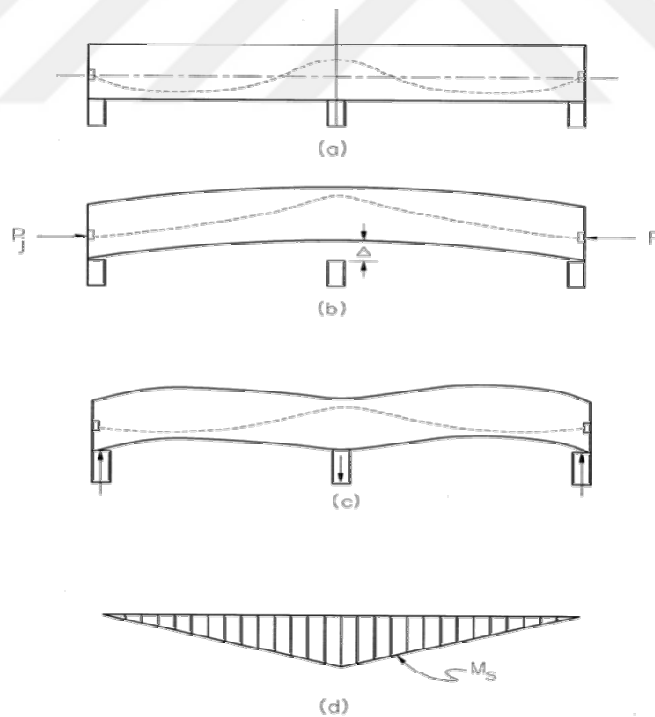


Figure 2.9. Secondary moments

2.4.5. Flexural Strength

Flexural strength is based on the following assumptions (AASHTO LRFD, 1994):

- For members with bonded tendons, strain is linearly distributed across a section; for members with unbonded tendons, the total change in tendon length is equal to the total change in member length over the distance between two anchorage points.
 - The maximum usable strain at extreme compressive fiber is 0.003.
 - The tensile strength of concrete is neglected.
 - A concrete stress of $0.85f_c'$ is uniformly distributed over an equivalent compression zone.
 - Nonprestressed reinforcement reaches the yield strength, and the corresponding stresses in the prestressing tendons are compatible based on plane section assumptions.
- For a member with a flanged section (figure 2.10) subjected to uniaxial bending, the equations of equilibrium are used to give a nominal moment resistance of

$$M_n = A_{ps}f_{ps}\left(d_p - \frac{a}{2}\right) + A_s f_y \left(d_s - \frac{a}{2}\right) - A'_s f'_y \left(d'_s - \frac{a}{2}\right) + 0.85f'_c(b - b_w)\beta_1 h_f \left(\frac{a}{2} - \frac{h_f}{2}\right) \quad (27)$$

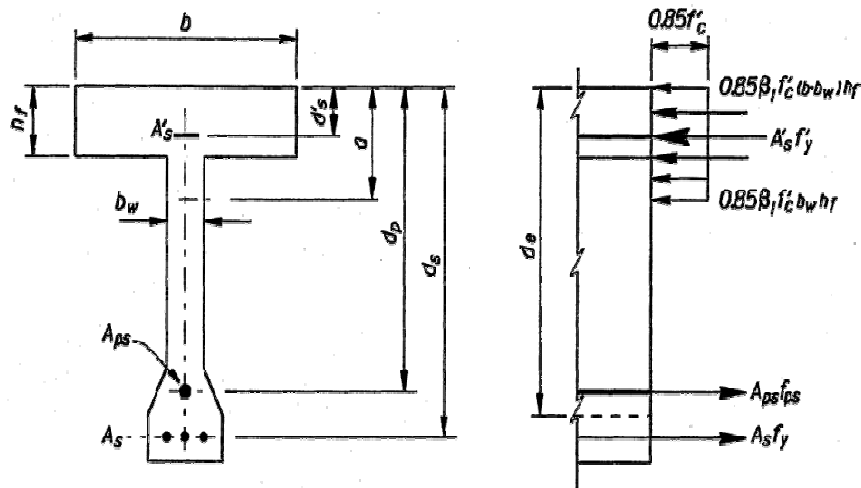


Figure 2.10. A flanged section at nominal moment capacity state

$$\alpha = \beta_1 c \quad (28)$$

For bonded tendons

$$c = \frac{A_{ps} f_{pu} + A_s f_y - A'_s f'_y - 0.85 \beta_1 f'_c (b - b_w) h_f}{0.85 \beta_1 f'_c b_w + k A_{ps} \frac{f_{pu}}{d_p}} \geq h_f \quad (29)$$

$$f_{ps} = f_{pu} \left(1 - k \frac{c}{d_p} \right) \quad (30)$$

$$k = 2 \left(1.04 - \frac{f_{py}}{f_{pu}} \right) \quad (31)$$

$$0.85 \geq \beta_1 = 0.85 - \frac{(f'_c - 28)(0.05)}{7} \geq 0.65 \quad (32)$$

Where A represents area; f is stress; b is the width of the compression face of member; b_w is the web width of a section; h_f is the compression flange depth of the cross section; d_p and d_s are distances from extreme compression fiber to the centroid of prestressing tendons and to centroid of tension reinforcement, respectively; subscripts c and y indicate specified strength for concrete and steel, respectively; subscripts p and s mean prestressing steel and reinforcement steel, respectively; sub-scripts ps, py, and pu correspond to states of nominal moment capacity, yield, and specified tensile strength of prestressing steel, respectively; superscript ' represents compression. The above equations also can be used for rectangular section in which $b_w = b$ is taken. (Chen and Duan, 2000)

For unbound tendons:

$$c = \frac{A_{ps} f_{pu} + A_s f_y - A'_s f'_y - 0.85 \beta_1 f'_c (b - b_w) h_f}{0.85 \beta_1 f'_c b_w} \geq h_f \quad (33)$$

$$f_{ps} = f_{pe} + \Omega_u E_p \varepsilon_{cu} \left(\frac{d_p}{c} - 1.0 \right) \frac{L_1}{L_2} \leq 0.94 f_{py} \quad (34)$$

Where L_1 is length of loaded span or spans affected by the same tendons; L_2 is total length of tendon between anchorage; Ω_u is the bond reduction coefficient given by (Chen and Duan, 2000)

$$\Omega_u = \begin{cases} \frac{3}{L/d_p} & \text{for uniform and near third point loading} \\ \frac{1.5}{L/d_p} & \text{for near midspan loading} \end{cases} \quad (35)$$

In which L is span length.

Maximum reinforcement limit:

$$\frac{c}{d_e} \leq 0.42 \quad (36)$$

$$d_e = \frac{A_{ps} f_{ps} d_p + A_s f_y d_s}{A_{ps} f_{ps} + A_s f_y} \quad (37)$$

Minimum reinforcement limit:

$$\phi M_n \geq 1.2 M_{cr} \quad (38)$$

In which ϕ is flexural resistance factor 1.0 for prestressed concrete and 0.9 for reinforced concrete; M_{cr} is the cracking moment strength given by the elastic stress distribution and the modulus of rupture of concrete. (Chen and Duan, 2000)

$$M_{cr} = \frac{I}{y_t} (f_r + f_{pe} - f_d) \quad (39)$$

Where f_{pe} is compressive stress in concrete due to effective prestresses; and f_d is stress due to unfactored self-weight; both f_{pe} and f_d are stresses at extreme fiber where tensile stresses are produced by externally applied loads. (Chen and Duan, 2000)

2.4.6. Shear Strength

The shear resistance is contributed by the concrete, the transverse reinforcement and vertical component of prestressing force. The modified compression field theory-based shear design strength (Collins and Mitchell, 1991) was adopted by the AASHTO LRFD and has the formula: (Chen and Duan, 2000)

$$V_n = \text{the lesser of } \begin{cases} V_c + V_s + V_p \\ 0.25 f_c' b_v d_v + V_p \end{cases} \quad (40)$$

Where:

$$V_c = 0.083 \beta \sqrt{f_c'} b_v d_v \quad (41)$$

$$V_s = \frac{A_v f_y d_v (\cos \Theta + \cot \alpha) \sin \alpha}{s} \quad (42)$$

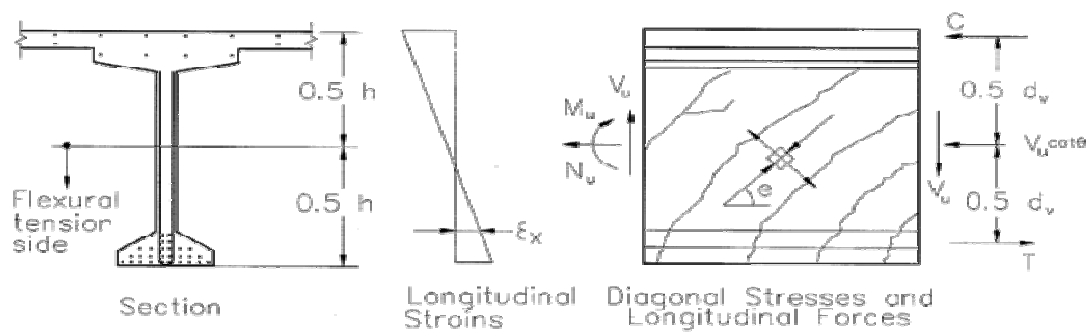


Figure 2.11. Illustration of A_c for shear strength calculation (AASHTO LRFD, 1994)

Table 2.10. Values of θ and β for sections with transverse reinforcement (AASHTO LRFD, 1994)

v/f_c'	Angle (degree)	$\epsilon_x \times 1000$										
		-0.02	-0.15	-0.1	0	0.125	0.25	0.50	0.75	1.00	1.50	2.00
≤ 0.05	θ	27.0	27.0	27.0	27.0	27.0	28.5	29.0	33.0	36.0	41.0	43.0
	β	6.78	6.17	5.63	4.88	3.99	3.49	2.51	2.37	2.23	1.95	1.72
0.075	θ	27.0	27.0	27.0	27.0	27.0	27.5	30.0	33.5	36.0	40.0	42.0
	β	6.78	6.17	5.63	4.88	3.65	3.01	2.47	2.33	2.16	1.90	1.65
0.100	θ	23.5	23.5	23.5	23.5	24.0	26.5	30.5	34.0	36.0	38.0	39.0
	β	6.50	5.87	5.31	3.26	2.61	2.54	2.41	2.28	2.09	1.72	1.45
0.127	θ	20.0	21.0	22.0	23.5	26.0	28.0	31.5	34.0	36.0	37.0	38.0
	β	2.71	2.71	2.71	2.60	2.57	2.50	2.37	2.18	2.01	1.60	1.35
0.150	θ	22.0	22.5	23.5	25.0	27.0	29.0	32.0	34.0	36.0	36.5	37.0
	β	2.66	2.61	2.61	2.55	2.50	2.45	2.28	2.06	1.93	1.50	1.24
0.175	θ	23.5	24.0	25.0	26.5	28.0	30.0	32.5	34.0	35.0	35.5	36.0
	β	2.59	2.58	2.54	2.50	2.41	2.39	2.20	1.95	1.74	1.35	1.11
0.200	θ	25.0	25.5	26.5	27.5	29.0	31.0	33.0	34.0	34.5	35.0	36.0
	β	2.55	2.49	2.48	2.45	2.37	2.33	2.10	1.82	1.58	1.21	1.00
0.225	θ	26.5	27.0	27.5	29.0	30.5	32.0	33.0	34.0	34.5	36.5	39.0
	β	2.45	2.38	2.43	2.37	2.33	2.27	1.92	1.67	1.43	1.18	1.14
0.250	θ	28.0	28.5	29.0	30.0	31.0	32.0	33.0	34.0	35.5	38.5	41.5
	β	2.36	2.32	2.36	2.30	2.28	2.01	1.64	1.52	1.40	1.30	1.25

Where b_v is the effective web width determined by subtracting the diameters of ungrouted ducts or one half the diameters of grouted ducts; d_v is the effective depth between the resultants of the tensile and compressive forces due to flexure, but not to be taken less than the greater of $0.9d_c$ or $0.72h$; A_v is the area of transverse reinforcement within distance s ; s is the spacing of stirrups; α is the angle of inclination of transverse reinforcement to longitudinal axis; β is a factor indicating ability of diagonally cracked concrete to transmit tension; θ is the angle of inclination of diagonal compressive stresses (figure 2.11). The values of β and θ for sections with transverse reinforcement are given in table 2.10. (Chen and Duan, 2000)

In using this table, the shear stress v and strain ϵ_x in the reinforcement on the flexural tension side of the member are determined by

$$v = \frac{V_u - \phi V_p}{\phi b_v d_v} \quad (43)$$

$$\varepsilon_x = \frac{\frac{M_u}{d_v} + 0.5N_u + 0.5V_u \cot \Theta - A_{ps}f_{po}}{E_s A_s + E_p A_{ps}} \leq 0.002 \quad (44)$$

Where M_u and N_u are factored moment and axial force (taken as positive if compressive) associated with V_u and f_{po} is stress in prestressing steel when the stress in the surrounding concrete is zero and can be conservatively taken as the effective stress after losses f_{pe} . When the value of ε_x calculated from the above equation is negative, its absolute value shall be reduced by multiplying by the factor F_ε taken as (Chen and Duan, 2000)

$$F_\varepsilon = \frac{E_s A_s + E_p A_{ps}}{E_c A_c + E_s A_s + E_p A_{ps}} \quad (45)$$

where E_s , E_p , and E_c are modulus of elasticity for reinforcement, prestressing steel, and concrete, respectively; A_c is area of concrete on the flexural tension side of the member as shown in figure 2.11. (Chen and Duan, 2000)

Minimum transverse reinforcement:

$$A_{v \min} = 0.083 \sqrt{f'_c} \frac{b_v s}{f_y} \quad (46)$$

Maximum spacing of transverse reinforcement:

$$\text{For } V_u < 0.1f'_c b_v d_v \quad s_{\max} = \text{the smaller of } \begin{cases} 0.8d_v \\ 600 \text{ mm} \end{cases} \quad (47)$$

$$\text{For } V_u \geq 0.1f'_c b_v d_v \quad s_{\max} = \text{the smaller of } \begin{cases} 0.4d_v \\ 300 \text{ mm} \end{cases} \quad (48)$$

2.4.7. Camber and Deflections

As opposed to load deflection, camber is usually referred to as reversed deflection and is caused by prestressing. A careful evaluation of camber and deflection for a prestressed concrete member is necessary to meet serviceability requirements. The following formulas developed by the moment–area method can be used to estimate mid span immediate camber for simply supported members as shown in figure 2.7. (Chen and Duan, 2000)

For straight tendon (figure 2.7a):

$$\Delta = \frac{L^2}{8E_c I} (M_e) \quad (49)$$

For one-point harping tendon (figure 2.7b):

$$\Delta = \frac{L^2}{8E_c I} \left(M_c + \frac{2}{3} M_e \right) \quad (50)$$

For two-point harping tendon (figure 2.7c):

$$\Delta = \frac{L^2}{8E_c I} \left(M_c + M_e - \frac{M_e}{3} \left(\frac{2a}{L} \right)^2 \right) \quad (51)$$

For parabola tendon (figure 2.7d):

$$\Delta = \frac{L^2}{8E_c I} \left(M_e + \frac{5}{6} M_c \right) \quad (52)$$

where M_e is the primary moment at end, $P_j e_{end}$, and M_c is the primary moment at mid span $P_j e_c$. Uncracked gross section properties are often used in calculating camber. For deflection at service loads, cracked section properties, i.e., moment of inertia I_{cr} , should be used at the post-cracking service load stage. It should be noted that long term effect of creep

and shrinkage shall be considered in the final camber calculations. In general, final camber may be assumed 3 times as great as immediate camber. (Chen and Duan, 2000)

2.4.8. Anchorage Zones

In a pre-tensioned member, prestressing tendons transfer the compression load to the surrounding concrete over a length L_t gradually. In a post-tensioned member, prestressing tendons transfer the compression directly to the end of the member through bearing plates and anchors. The anchorage zone, based on the principle of St. Venant, is geometrically defined as the volume of concrete through which the prestressing force at the anchorage device spreads transversely to a more linear stress distribution across the entire cross section at some distance from the anchorage device (AASHTO LRFD, 1994). For design purposes, the anchorage zone can be divided into general and local zones (AASHTO LRFD, 1994). The region of tensile stresses is the general zone. The region of high compressive stresses (immediately ahead of the anchorage device) is the local zone. For the design of the general zone, a “strut-and-tie model,” a refined elastic stress analysis or approximate methods may be used to determine the stresses, while the resistance to bursting forces is provided by reinforcing spirals, closed hoops, or anchored transverse ties. For the design of the local zone, bearing pressure is a major concern. For detailed requirements, see (AASHTO LRFD, 1994). (Chen and Duan, 2000)

3. NUMERICAL APPLICATION

3.1. Assumptions of the Numerical Application:

The structure was idealized using the following assumptions:

- 1- The skew slab-and-girder bridge consists of a reinforced concrete slab which is supported on four prestressed concrete I-girders.
- 2- All materials are elastic and homogenous.
- 3- The slab and the I-girders have a constant thickness.
- 4- The supporting girders are equally spaced.
- 5- I-girders are simply supported at the piers.
- 6- Diaphragms are provided with equal spacing from the span between the I-girders.
- 7- The connection between the piers and foundations was fixed.
- 8- The method of analysis was finite elements by Midas Civil.
- 9- All the values in the diagrams were taken and drawn according to center of the I-girder section.

3.2. Model Bridge Description

In this part from the research the shape of models will be described that will be analyzed by Midas Civil. In this research five models with five different skewness angles of span 0°, 21°, 37.6°, 57°, 66.6° degrees respectively. Every model has one simply supported span, pre-tension prestressed concrete, and I-girder section. The length of this span is 24 m. There is a slab over these girders with 0.2 m thickness. The superstructure of the bridge was carried by two pier caps over two piers of at the ends of the span. The height of every pier is 6 m. There are diaphragms connecting between the I-girders with section dimension of 0.6 m for thickness and 0.15 m for width. There is one diaphragm for every 3 m from the span of the bridge. The total number of the diaphragms in the bridge is 7. The all height of the section of the superstructure including deck must be not less than $0.045 L = 1.08$ m, where L is the length of the span according to AASHTO LRFD table 2.5.2.6.3-1, and because of that the I-

girder section type III AASHTO LRFD was chosen but with a height was equal to 1 m. Totally the height of the superstructure including deck was equal to 1.2 m.

All the models have four I-girder and their type were fully prestressed concrete (internal pre-tension) in the longitudinal direction. The distance between the centers of girders is 2.6 m.

In every I-girder there was a steel which consists 22 strands with a 12.7 mm diameter and every strand consists a 7 wires with type of steel (A416-270 low) that is low relaxation according to ASTM. Steel tensile strength was $f_{pu}=1863$ Mpa, and yield strength was $f_{py}=1676$ Mpa according to AASHTO LRFD table 5.4.4.1-1. The other magnitudes that not mentioned here were used as the program that gives them by default.

The connection points between the piers and the foundations of the bridge considered as a fixed supports. The connection points between the superstructure and pier caps considered as a hinge supports. The superstructure based on and contact with pier caps in four points for each pier cap and in these points there are bearings between the superstructure and pier caps at the ends of girders. The piers section is circular with a 1.2 m diameter.

The modeling was used in orthogonal grillage shape for 1 m length for every part in the girders. The type of concrete that used was C40 ($f'_c = 40$ MPa) in all the components of the bridge. All the other dimensions will be explained in the next part.

3.3. Dimensions of the Bridge Components

Five models were analyzed to study the effects of skewness angle on the behavior of the girders. Every model has a different skewness angle and all the dimensions will be explained for all of them.

3.3.1. First Model (Angle 0°)

All dimensions of the first model are shown below.

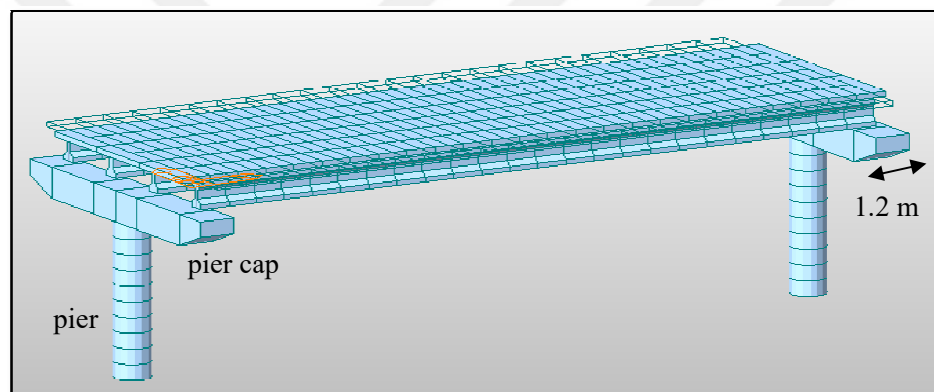


Figure 3.3.1.1. Elevation of first model (angle 0°)

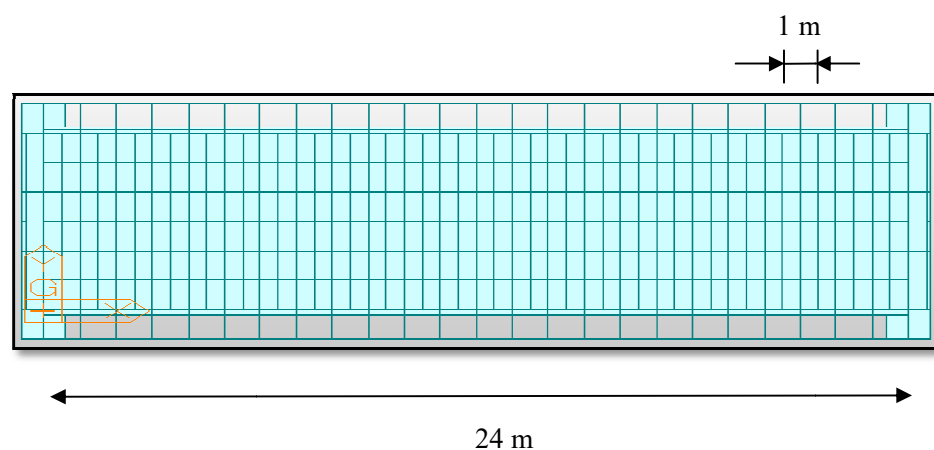


Figure 3.3.1.2. Plan of first model (angle 0°)

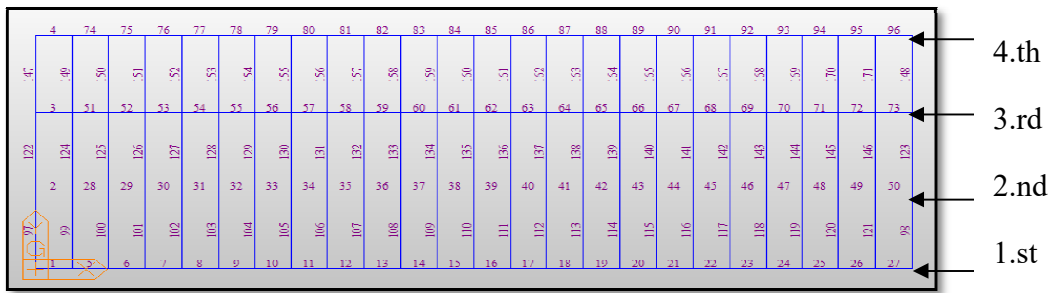


Figure 3.3.1.3. Number of elements for first model (angle 0°)

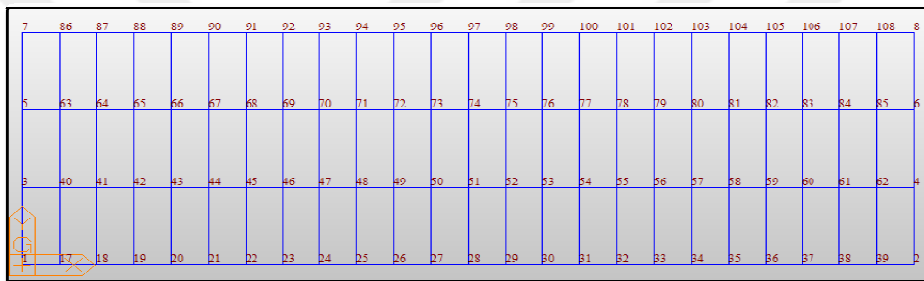


Figure 3.3.1.4. Number of nodes for first model (angle 0°)

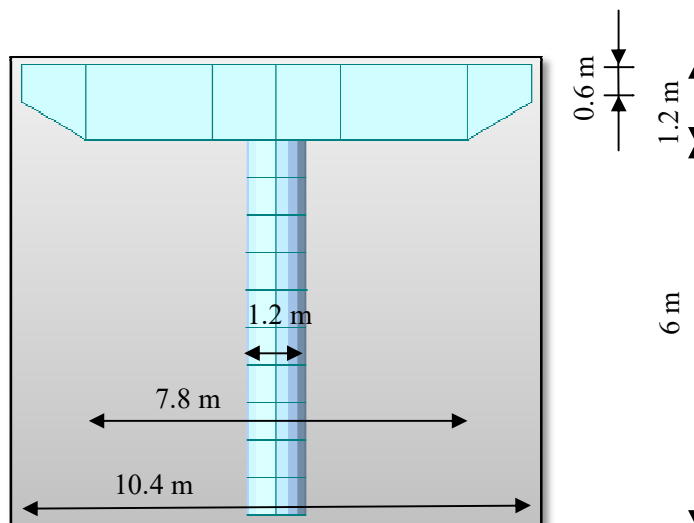


Figure 3.3.1.5. Dimensions of pier and pier cap for first model (angle 0°)

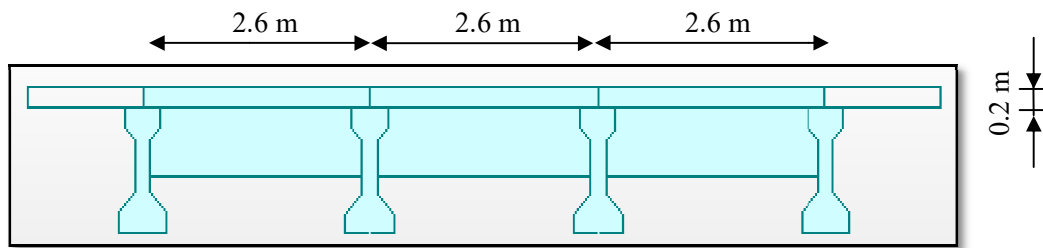


Figure 3.3.1.6. Dimensions of slab for first model (angle 0°)

$$HL1 = 0.1778 \text{ m}$$

$$HL2 = 0.1143 \text{ m}$$

$$HL3 = 0.3396 \text{ m}$$

$$HL4 = 0.1905 \text{ m}$$

$$HL5 = 0.1778 \text{ m}$$

$$HR1 = 0.1778 \text{ m}$$

$$HR2 = 0.1143 \text{ m}$$

$$HR3 = 0.3396 \text{ m}$$

$$HR4 = 0.1905 \text{ m}$$

$$HR5 = 0.1778 \text{ m}$$

$$BL1 = 0.0889 \text{ m}$$

$$BL2 = 0.2032 \text{ m}$$

$$BL4 = 0.2794 \text{ m}$$

$$BR1 = 0.0889 \text{ m}$$

$$BR2 = 0.2032 \text{ m}$$

$$BR4 = 0.2794 \text{ m}$$

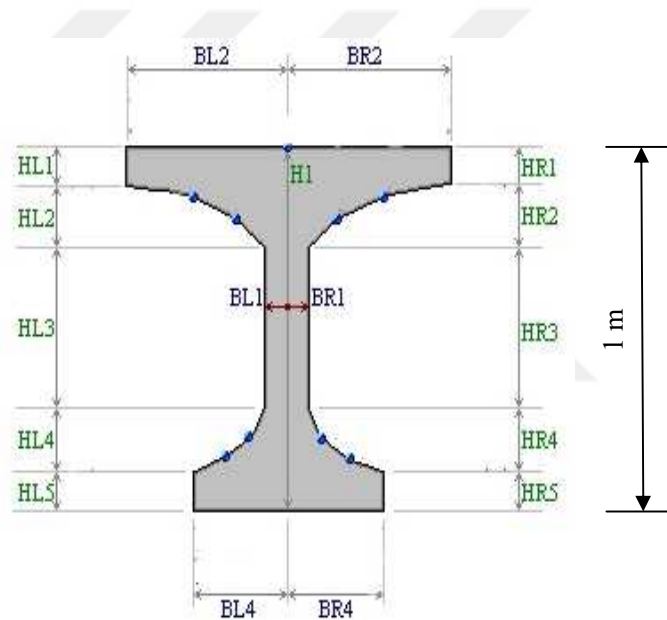


Figure 3.3.1.7. Dimensions of I-girder according to AASHTO LRFD (type III) for all models

3.3.2. Second Model (Angle 21°)

All dimensions of the second model are shown below.

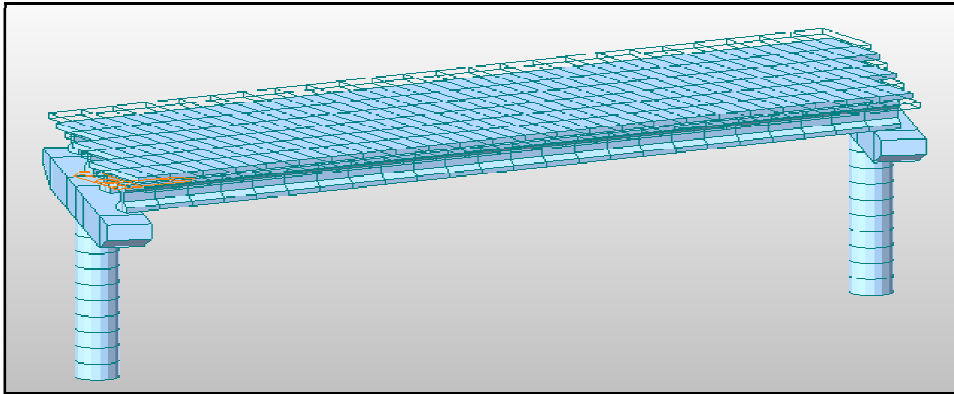


Figure 3.3.2.1. Elevation of second model (angle 21°)

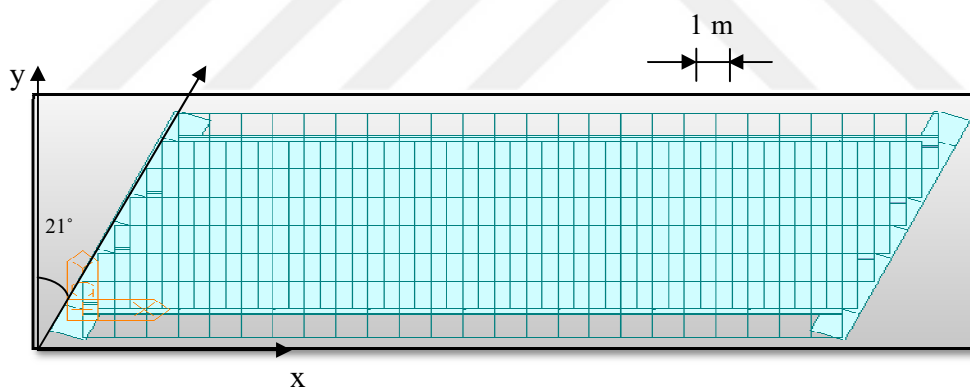


Figure 3.3.2.2. Plan of second model (angle 21°)

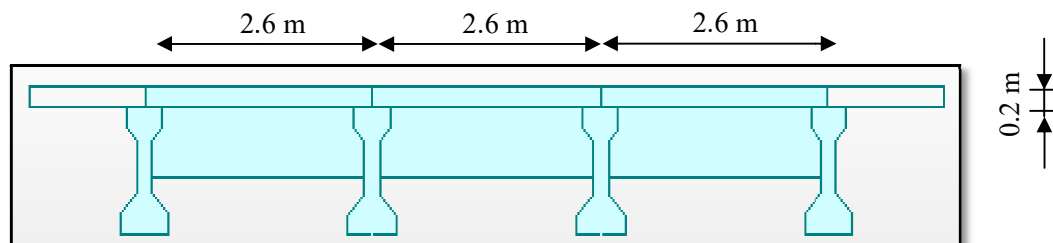


Figure 3.3.2.3. Dimensions of slab for second model (angle 21°)

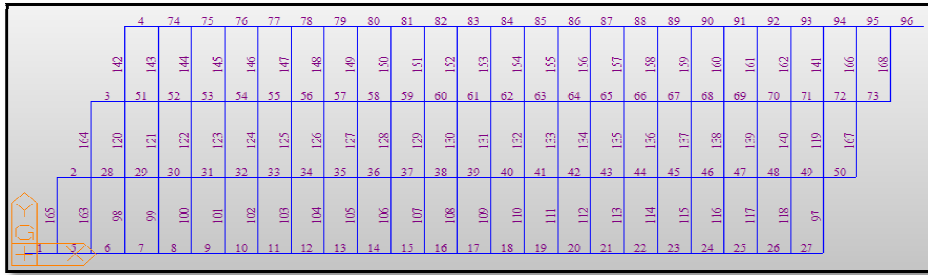


Figure 3.3.2.4. Number of elements for second model (angle 21°)

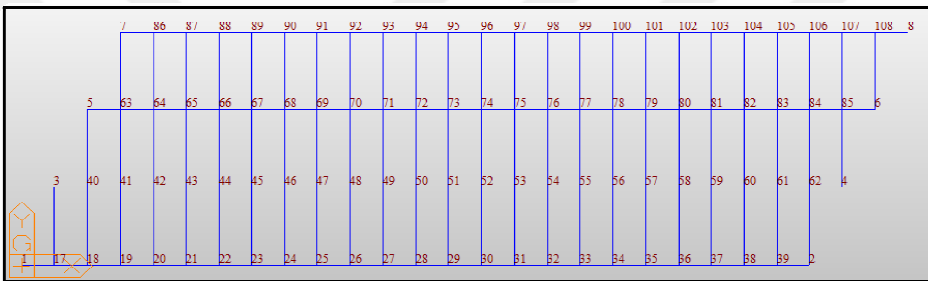


Figure 3.3.2.5. Number of nodes for second model (angle 21°)

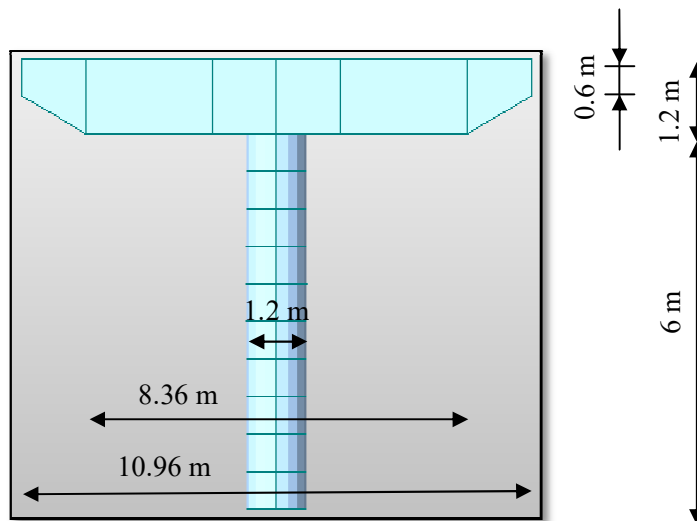


Figure 3.3.2.6. Dimensions of pier and pier cap for second model (angle 21°)

3.3.3. Third Model (Angle 37.6°)

All dimensions of the second model as shown below.

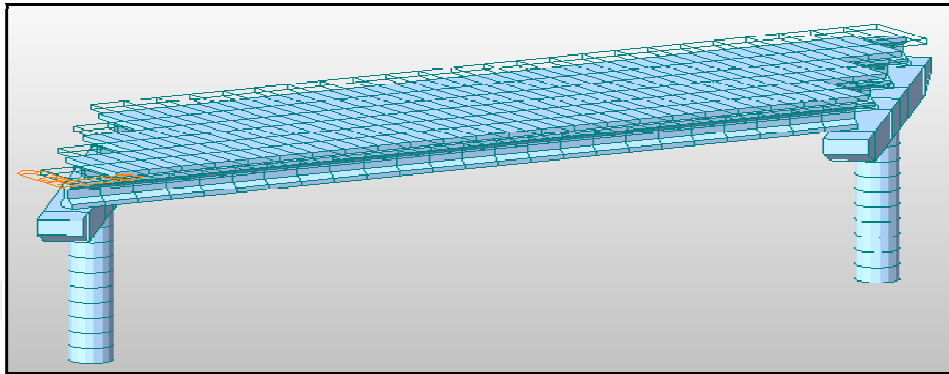


Figure 3.3.3.1. Elevation of third model (angle 37.6°)

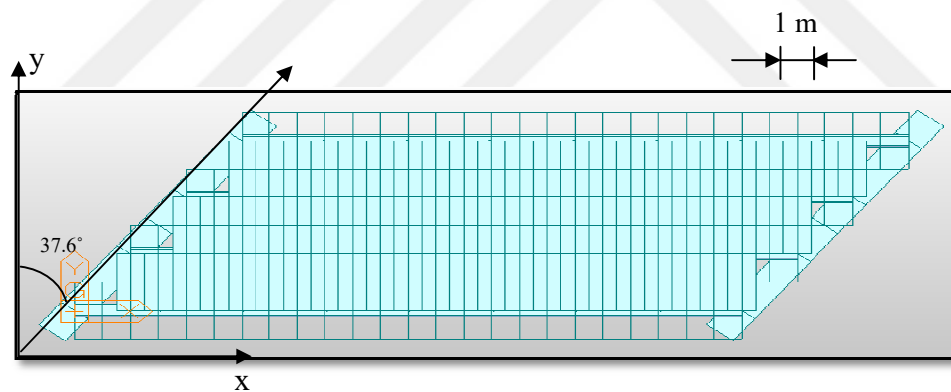


Figure 3.3.3.2. Plan of third model (angle 37.6°)

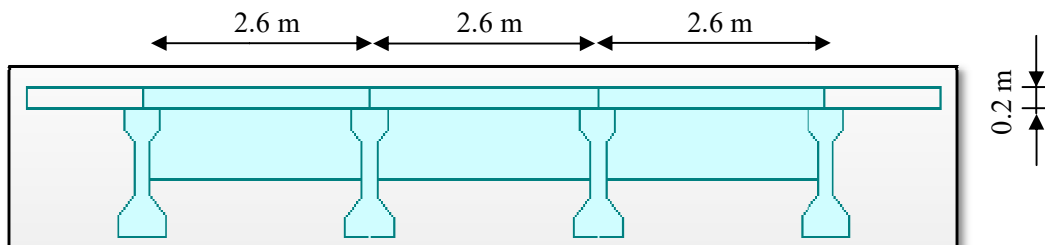


Figure 3.3.3.3. Dimensions of slab for third model (angle 37.6°)

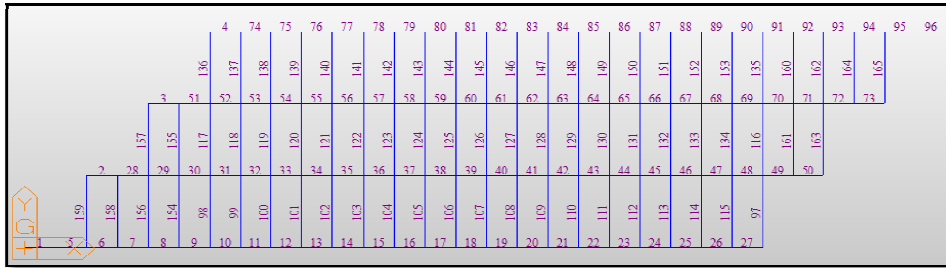


Figure 3.3.3.4. Number of elements for third model (angle 37.6°)

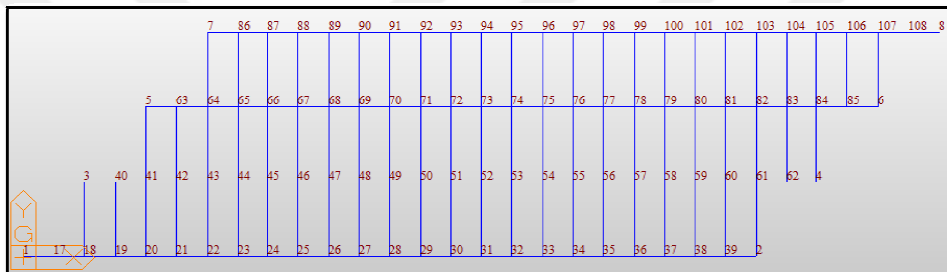


Figure 3.3.3.5. Number of nodes for third model (angle 37.6°)

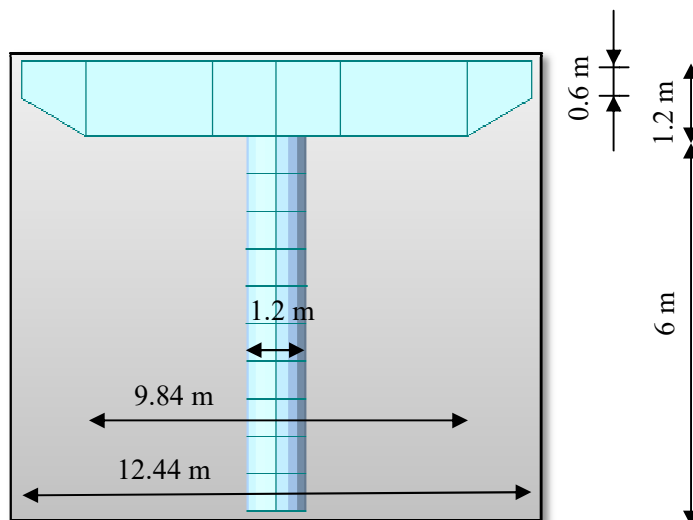


Figure 3.3.3.6. Dimensions of pier and pier cap for third model (angle 37.6°)

3.3.4. Fourth Model (Angle 57°)

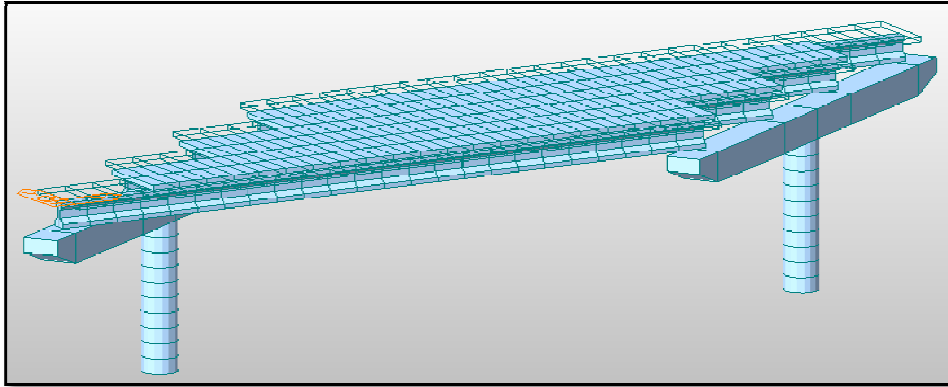


Figure 3.3.4.1. Elevation of fourth model (angle 57°)

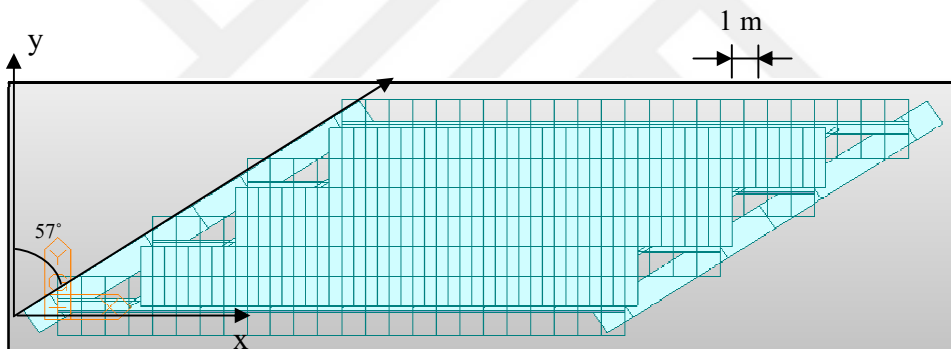


Figure 3.3.4.2. Plan of fourth model (angle 57°)

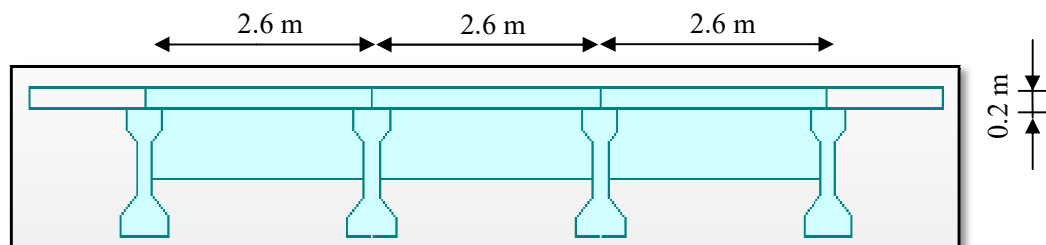


Figure 3.3.4.3. Dimensions of slab for fourth model (angle 57°)

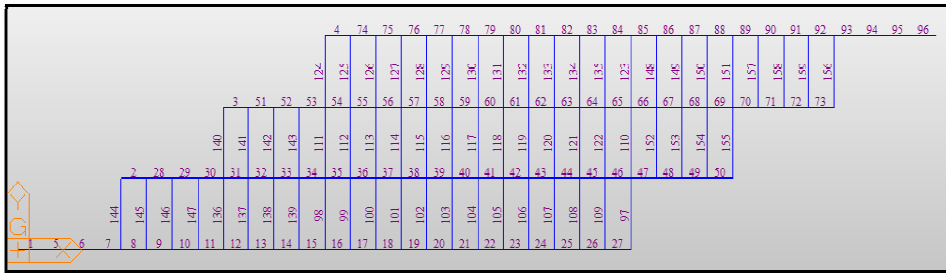


Figure 3.3.4.4. Number of elements for fourth model (angle 57°)



Figure 3.3.4.5. Number of nodes for fourth model (angle 57°)

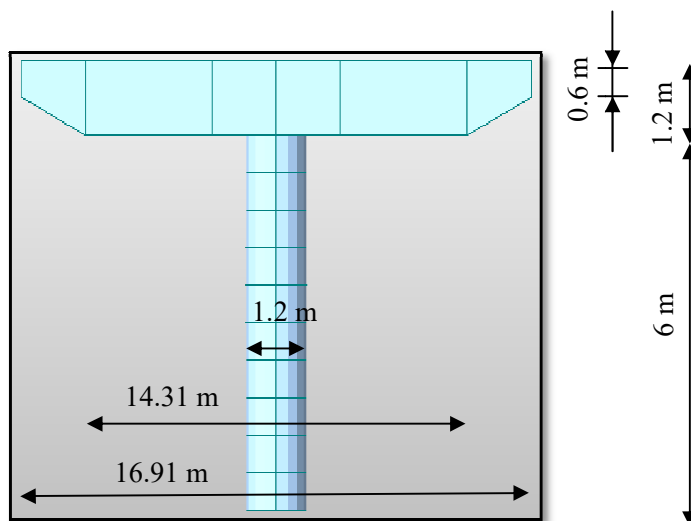


Figure 3.3.4.6. Dimensions of pier and pier cap for fourth model (angle 57°)

3.3.5. Fifth Model (Angle 66.6°)

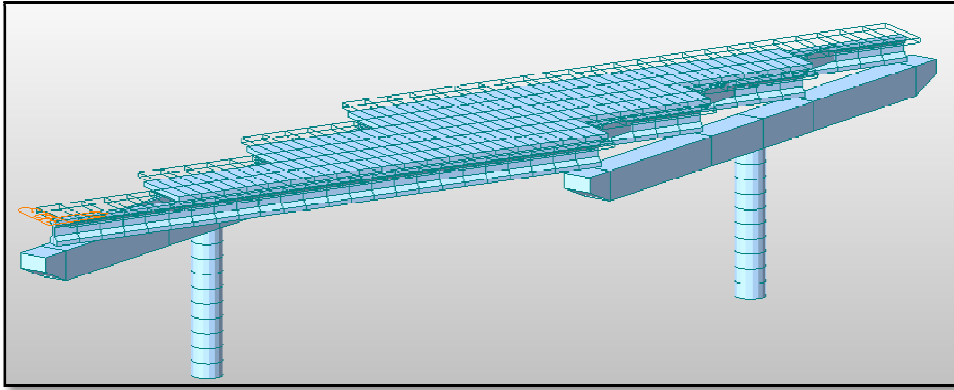


Figure 3.3.5.1. Elevation of fifth model (angle 66.6°)

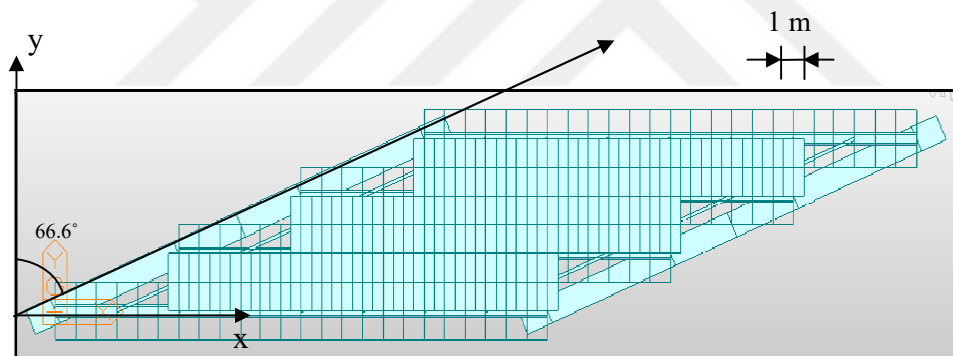


Figure 3.3.5.2. Plan of fifth model (angle 66.6°)

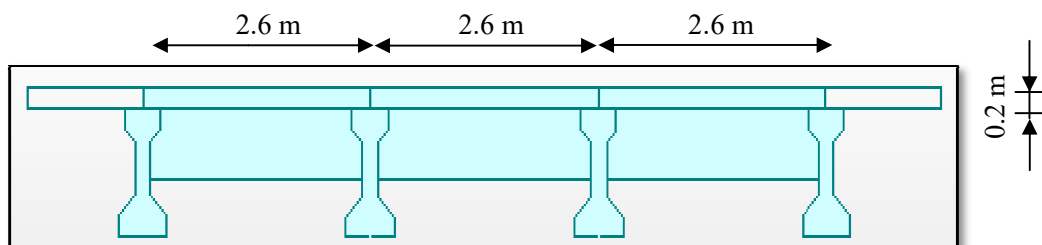


Figure 3.3.5.3. Dimensions of slab for fifth model (angle 66.6°)

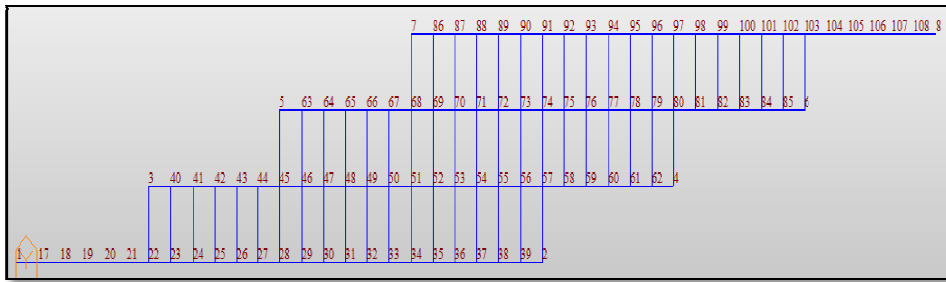


Figure 3.3.5.4. Number of elements for fifth model (angle 66.6°)

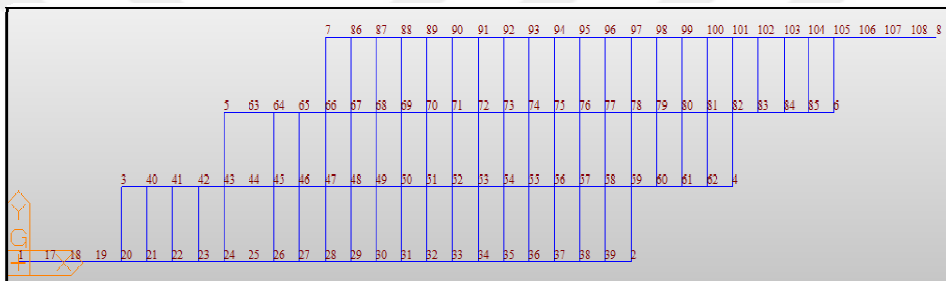


Figure 3.3.5.5. Number of nodes for fifth model (angle 66.6°)

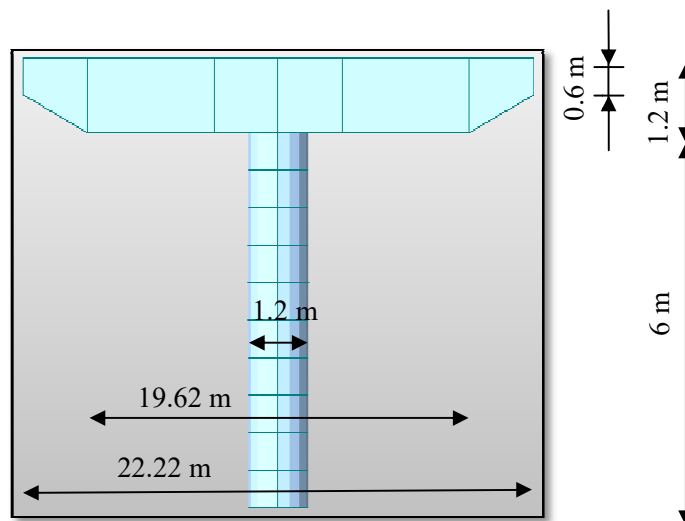


Figure 3.3.5.6. Dimensions of pier and pier cap for fifth model (angle 66.6°)

3.4. Strands Properties

The strands type that was used in all the models is internal pre-tension. Every I-girder consists twenty two strands with a 12.7 mm diameter for every one. Every strand consists 7 wires. The material of strands is steel A416-270 low relaxation. The ultimate strength of the steel f_{pu} was 1863 N/mm² and the yield strength of the steel f_{py} was 1676 N/mm². Applied prestressing was as a stress and it was equal to 1400 N/mm². The strands profile was input to program as 3-D coordinates. The coordinates of one strand in the first I-girder were given in table 3.4 :

Table 3.4. Strand profile 3-D coordinates

X(m)	Y (m)	Z (m)
0.00	0.00	-0.80
12.00	0.00	-0.80
24.00	0.00	-0.80

3.5. Applied Loads

Loads was applied under two main types :

A- Dead loads: Dead loads were self weight of bridge, wet concrete load, scaffolding load, wearing course load, and barrier load. Wet concrete load was considered equal to -80 kN/m, scaffolding load was considered equal to -23 kN/m, wearing course load was considered equal to -30 kN/m, and barrier load was considered equal to -30 kN/m too.

System temperature load also was applied with 30°F and the gradient temperature load was applied with these heights from the top of I-section

For $H1=0$ m , $H2=0.4$ m,
 $T1=50^{\circ}\text{F}$, $T2=30^{\circ}\text{F}$
 and for $H1=0.4$ m , $H2=1$ m,
 $T1=30^{\circ}\text{F}$, $T2=40^{\circ}\text{F}$

B- Live loads: The moving loads here was defined due to AASHTO LRFD code. Two traffic lane was defined. HL-93TRK type vehicular load was used with dynamic load allowance equal to 33%.

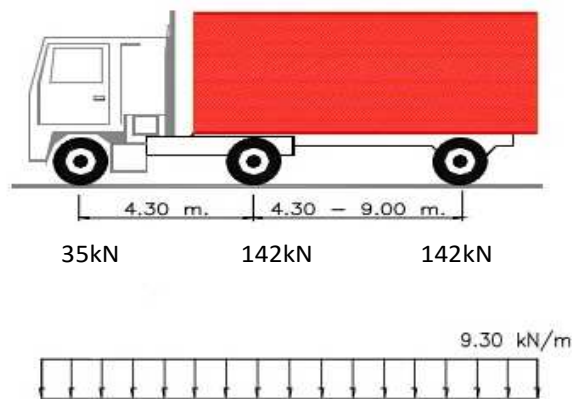


Figure 3.5. Moving load HL-93 vehicle and lane loading

3.6. Model Analysis Type Selection

Midas Civil program was used to analyze this type from bridges. This program uses finite element analysis method to analyze and design all components of bridges. When these five models was modulated with it, orthogonal grillage method was used to draw them.

3.7. Construction Stages

By this program also it could be input the stages of construction. This feature gives the ability to calculate (moment, shear forces,.....etc) at any stage that is wanted. These calculations definitely are different if is wanted to compare it with the final calculations because some of loads which was applied in construction stages, like scaffolding loads, will not be applied after finishing of construction, vice versa. In this research three stages was definded but the results that were used to draw diagrams were the results from the final stage after finishing construction and running the bridge which the program adding it by it self after running the analysis, the name of this stage is Post CS.

3.8. Analysis of Models

After finishing all steps from drawing to applying the loads on the models, now the analysis must be run to find the results. The analysis procedure takes about one minute or more due to the properties of computer. After procedure analysis finished, the commands window at down of screen must be seen and the last lines must be read to know if there are any error messages. If there are any errors, it must be read from the file which was made by the program after analysis processing to know what are these errors to correct it and run analysis again. In these models the analysis process done without errors and without any warnings too. Because of that the results was taken to draw the diagrams for every model and to discuss the shape of them.

3.9. Results and Diagrams

3.9.1. The Moment of I-girders

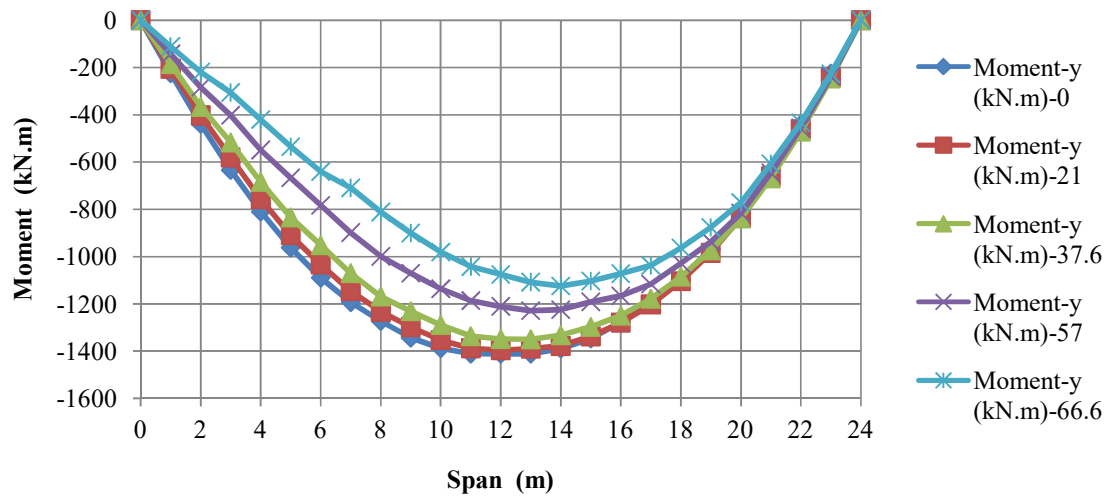


Figure 3.9.1.1. Moment diagram of the first I-girder

From figure 3.9.1.1 it can be noticed from figure that the moment generally decreased by increasing the skewness angle of span from 0° to 66.6° but the decreasing in the value of moment was more and more in the first, second and third part of the span, if it was divided to four parts equally, when the skewness angle exceeded 37.6° . The changing in moment was very slightly until the angle exceeded 37.6° and after that the changing became bigger especially in the first half of the span. The ratio of changing in moment was nearly 15% according to the values of moment when the skewness angle was 0° if these values were taken as a reference.

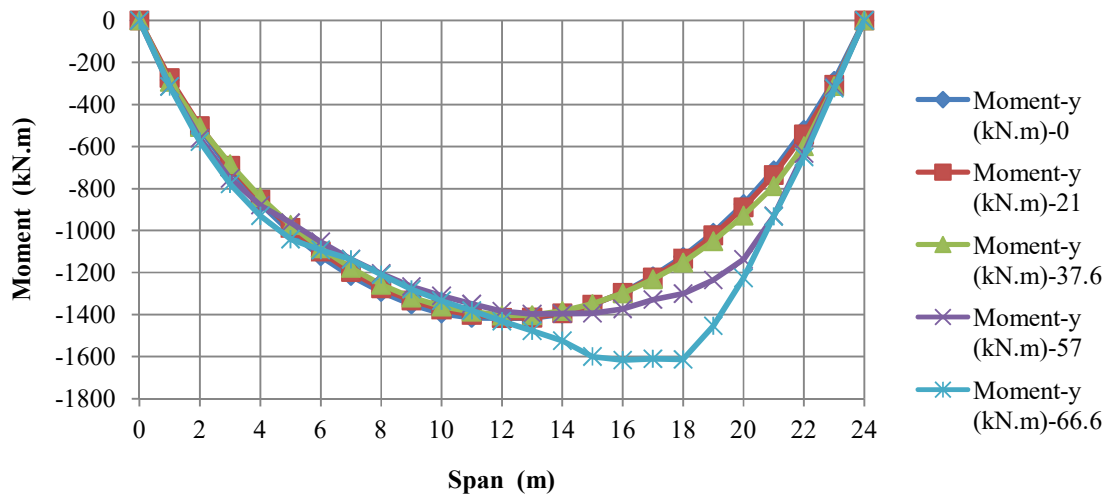


Figure 3.9.1.2. Moment diagram of the second I-girder

In figure 3.9.1.2, it can be noticed that the changing in values of the moment was very slightly until the skewness angle 37.6° but when the skewness angle became 57° there was a suddenly and rapidly huge increasing in moment just in the second half of the span. That changing was more huge and bigger when the skewness angle became 66.6° . The increasing ratio was nearly 25% if the values of moment for 0° was taken as a reference. The symmetric in shape of moment also finished when the skewness angle became more than 37.6° .

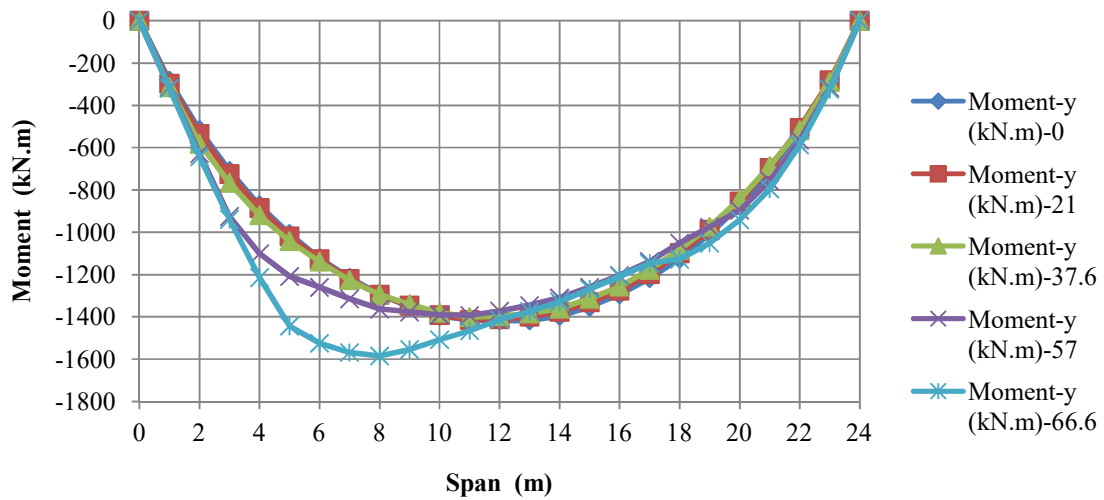


Figure 3.9.1.3. Moment diagram of the third I-girder

In figure 3.9.1.3, it was clear that the shape of moment diagram generally exactly like the shape of moment diagram of second I-girder but inversely as the span started from the end point of span. The changing in values of moment was also slightly as the second I-girder. The huge rapidly changing in values of moment here happened also but in the first half part of span with the same ratio and with the same skewness angle as second I-girder.

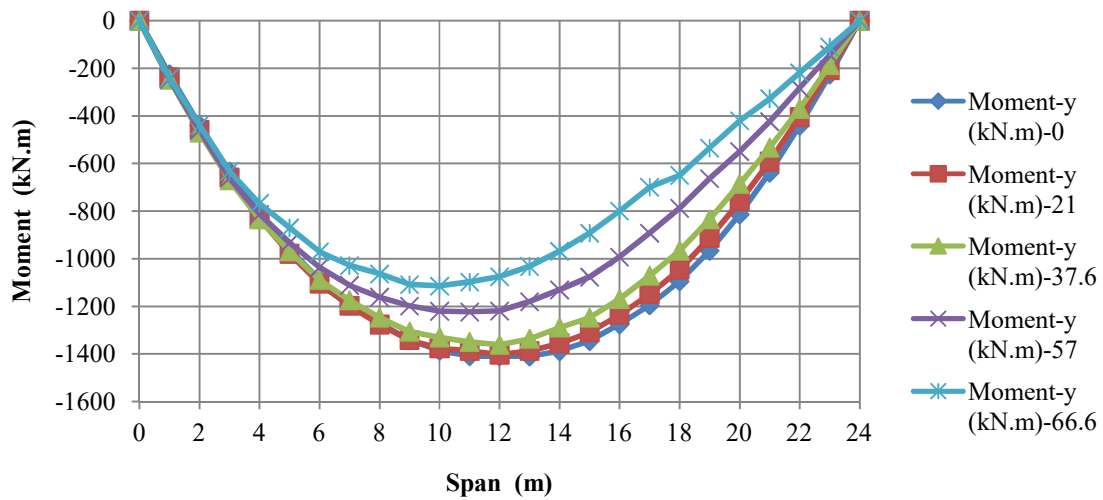


Figure 3.9.1.4. Moment diagram of the fourth I-girder

In figure 3.9.1.4, it was also clear that the behavior of the moment here as the behavior of the first I-girder in the bridge but inversely. The ratio of decreasing in the moment here same as the ratio of decreasing in the moment in the first I-girder too. The difference here just was that the decreasing happened in the second, third and fourth quarter parts of the span if the span was divided to four parts equally.

All the shapes of the moment diagrams became unsymmetrical when the skewness angle became more than 37.6° . The diagrams gives the designers the main idea about the behavior of the superstructure of the bridge and from above diagrams it was clear that when the superstructure of the bridge consists from four I-girders, the behavior of the first and fourth I-girders will be the same but inversely. Also the behavior of second and third I-girders will be the same but inversely too.

3.9.2. The Shear Forces of I-girders

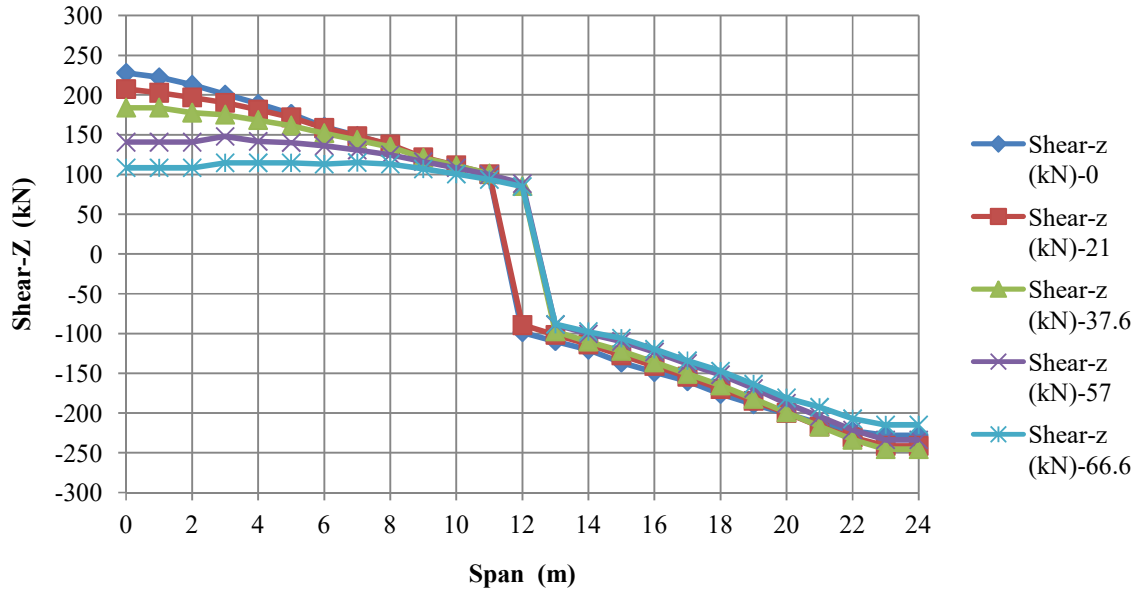


Figure 3.9.2.1. Shear force diagram of the first I-girder

In figure 3.9.2.1, it can be noticed that the shape of shear forces diagram was nearly symmetric just when the skewness angle was 0, 21° and 37.6° but after that the shape lost the symmetrical. At the first half of span, the shear forces was decreasing by the increasing in skewness angle of the span. If the curve of shear forces for skewness angle of 0° was taken as a reference, the ratio of the difference nearly was 50% between the reference and the values of shear forces for skewness angle of 66.6° at the first half of the span but these difference according to reference was very slightly in the second half from span. The point of zero shear force was nearly at the middle point of the span until the skewness angle increased and became more than 21°.

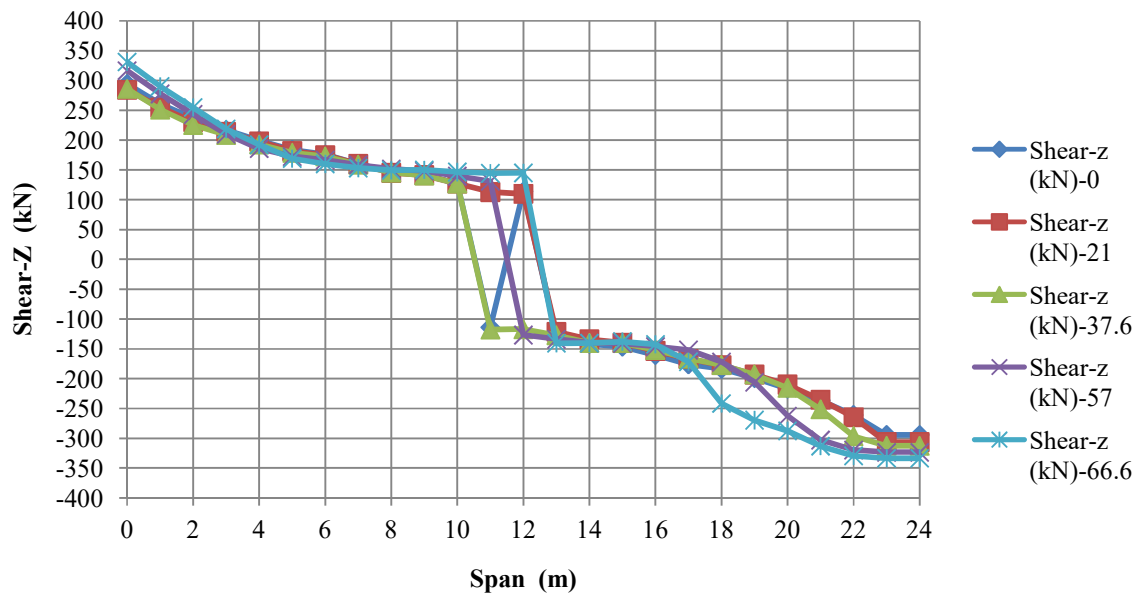


Figure 3.9.2.2. Shear force diagram of the second I-girder

In figure 3.9.2.2, it was seen that the shape of curve was unsymmetric. By increasing the skewness angle starting from 0° , the values of shear forces in the first half of span were changing slightly sometimes with increasing and sometimes with decreasing. But in the other half of the span the shape of the curves was very different if it was compared with the shape of curves in the first half of the span. Generally, in the second half of the span shear forces increased by increasing the skewed angle and when the skewness angle increased more than 37.6° , this increasing take irregular shape with a nearly ratio of 15% if the values of shear forces for 0° was taken as a reference. The point of zero shear forces also changed by changing in skewness angle but it was very near to the middle point of the span when the skewness angle was more than 37.6° .

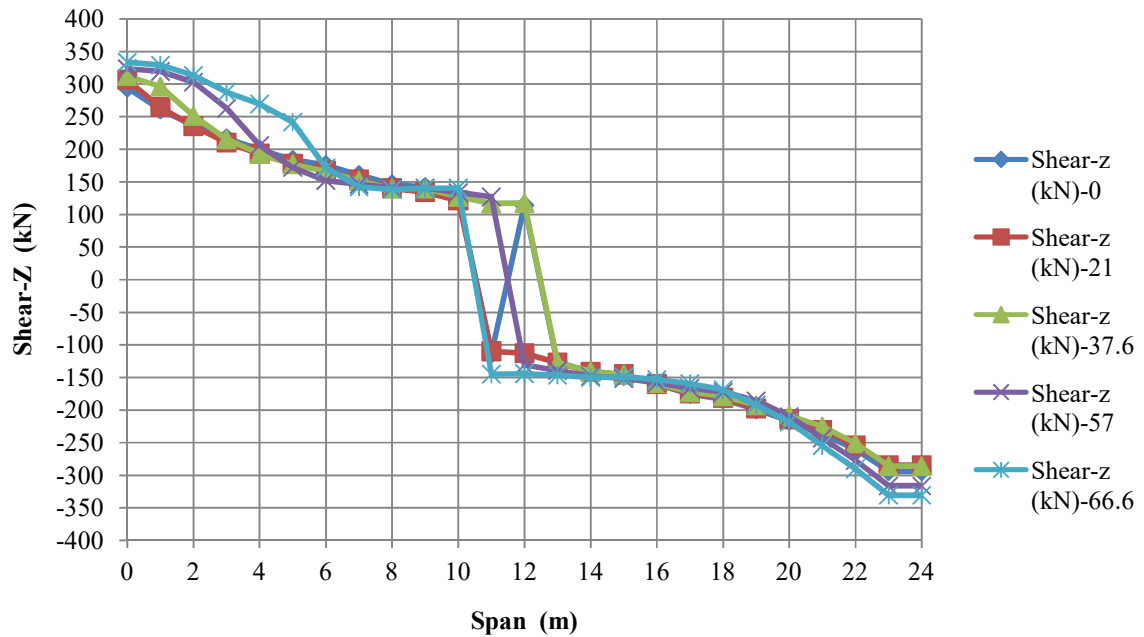


Figure 3.9.2.3. Shear force diagram of the third I-girder

In figure 3.9.2.3, it was clear generally that the shape of the curves of shear forces the same with that was in the second I-girder but inversely. All the notes which were taken about the second I-girder can be applied here too but by considerate that the first of the span there, is the end of the span here. Zero point of the shear forces here was very near to the middle of the span when the skewness angle became more than 37.6°.

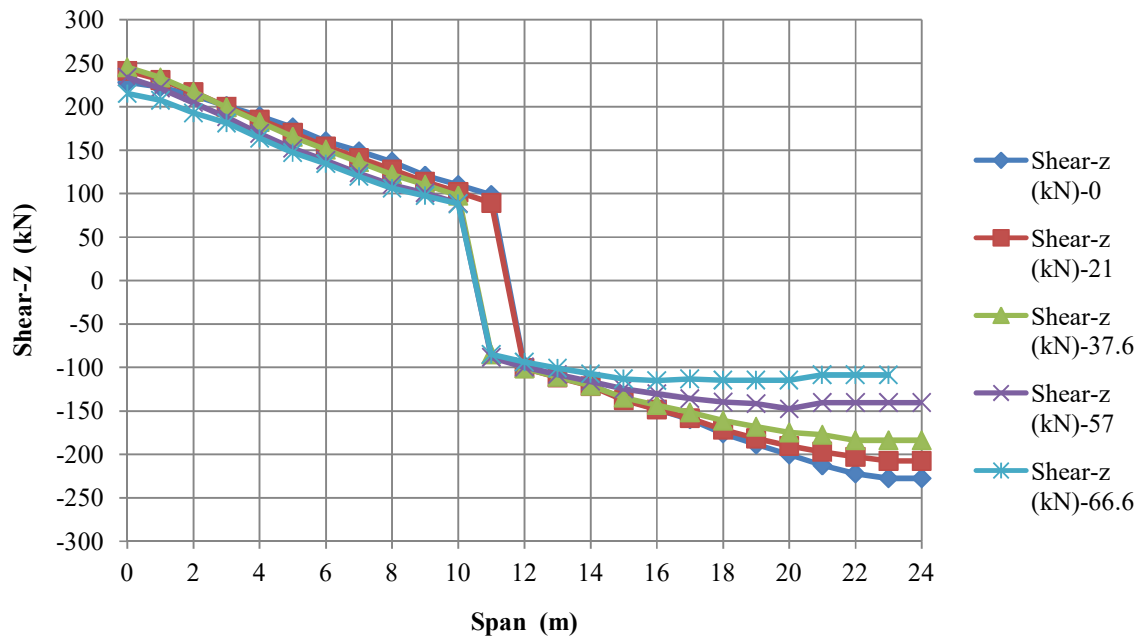


Figure 3.9.2.4. Shear force diagram of the fourth I-girder

In figure 3.9.2.4, the shape of shear forces curves also was like the shape of curves for first I-girder but inversely too. Here the zero shear force point was very near to the middle point of the span when the skewness angle was from 0° to 21° . Generally it can be said that the changes in the shape of curves for shear forces reflected in the shape of curves for moment in the same member.

3.9.3. The Torsion of I-girders

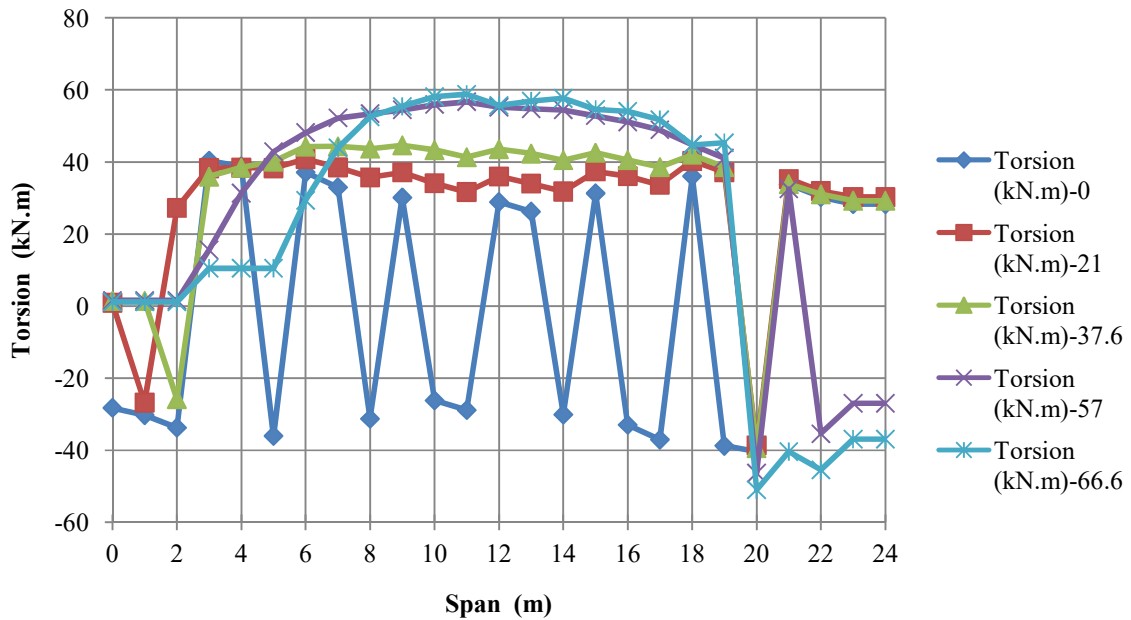


Figure 3.9.3.1. Torsion diagram of the first I-girder

In figure 3.9.3.1, the shape of curves can be seen clearly that were not symmetric. When the skewness angle started by 0° , the curve took a zigzag shape. Some of the values were positive and some of them were negative signs. But when the skewness angle increased to 21° , the torsion curve changed to be started from zero in the starting point of the span to negative side of the horizontal axis of span and after that changed to positive side. At the end of the span the torsion sign also changed to negative sign and finally to zero at the end of span. By increasing the skewness angle to 37.6° , the shape of curve stayed as like was in 21° but there was a shifting happened in first of the span. When the skewness angle increased to be 57° , the shape of curve changed to be in positive side and more curvedly in the first three quarter of the span and almost the values of the torsion increased. After that, the torsion decreased in the first quarter from span and increased in the other parts when the skewness angle became 66.6° . From above notes it was clear that by increasing in the skewness angle, the torsion values going to be just in positive side of the horizontal axis of the diagram.

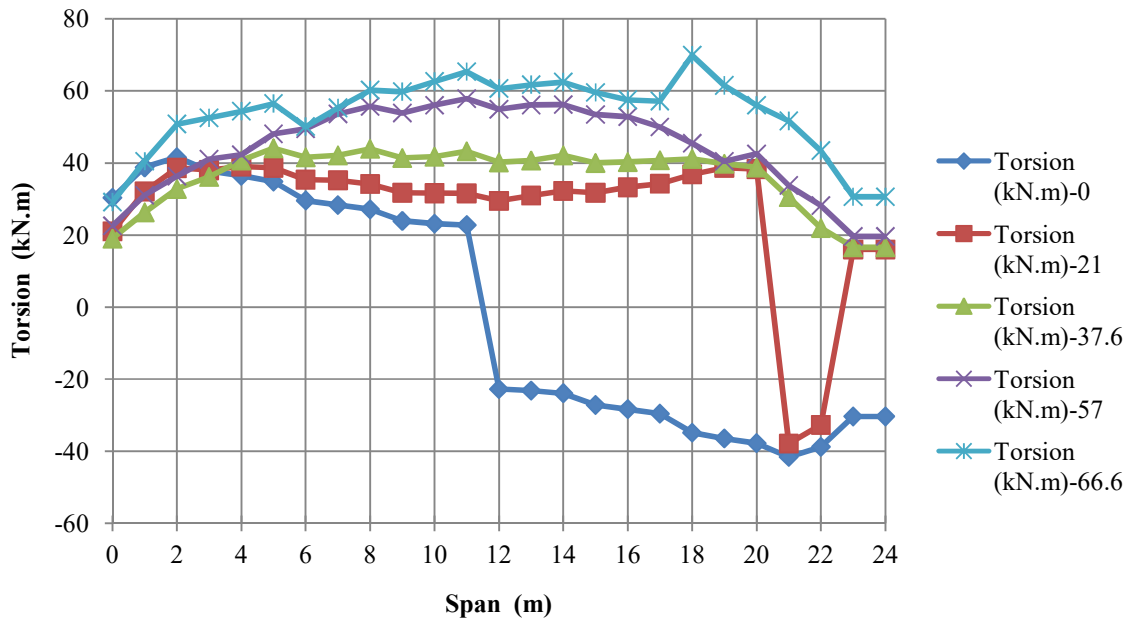


Figure 3.9.3.2. Torsion diagram of the second I-girder

In figure 3.9.3.2, the shape of diagram was symmetric when the span was straight with 0° skewness angle, but by increasing the skewness angle this symmetrical was lost. In the skewness angle of 21° the most values of torsion became with positive sign and the values increased also but just between 4m to 20m from the span. After that with complete the increasing in the skewness angle until 37.6°, all the values of the torsion became positive and the values increased also but just nearly between 6m to 18m from the span and the shape of the curve became nearly symmetric. Then when the skewness angle was changed to be 57°, the curve kept the symmetric in shape and increasing in value too. Finally, when the skewness angle became 66.6°, the curve lost the symmetrical in shape but almost of the values of torsion increased too.

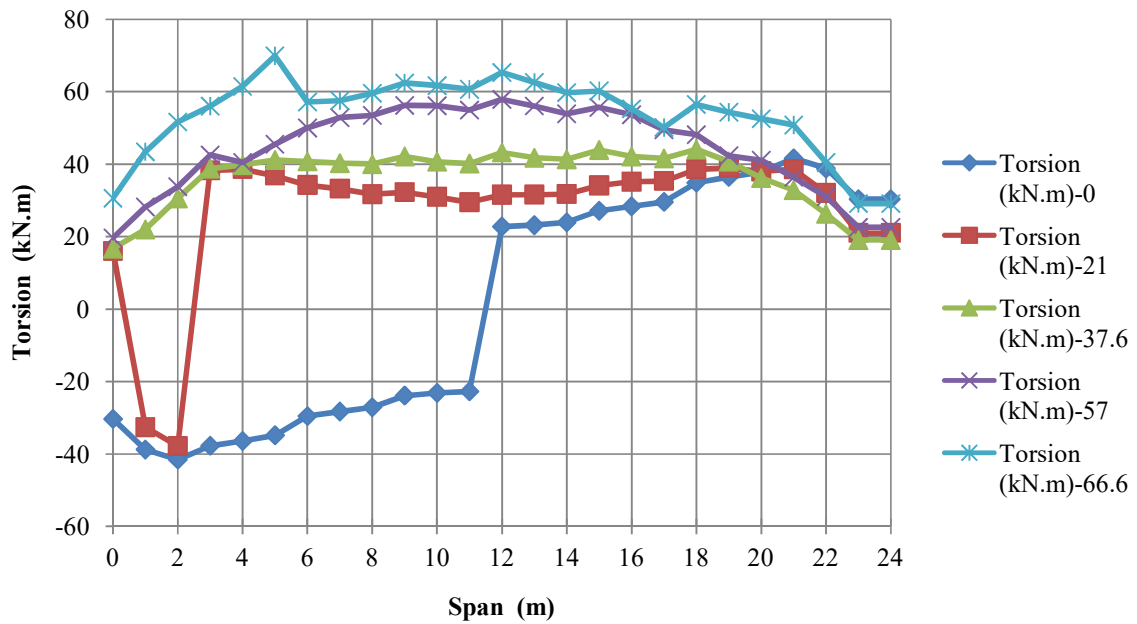


Figure 3.9.3.3. Torsion diagram of the third I-girder

In figure 3.9.3.3, the shape of the curve was like the curve in second I-girder but inversely according to span too. All the notes which were taken above could be applied here inversely too. That means the behavior of second and third I-girders similar to each others but inversely for torsion.

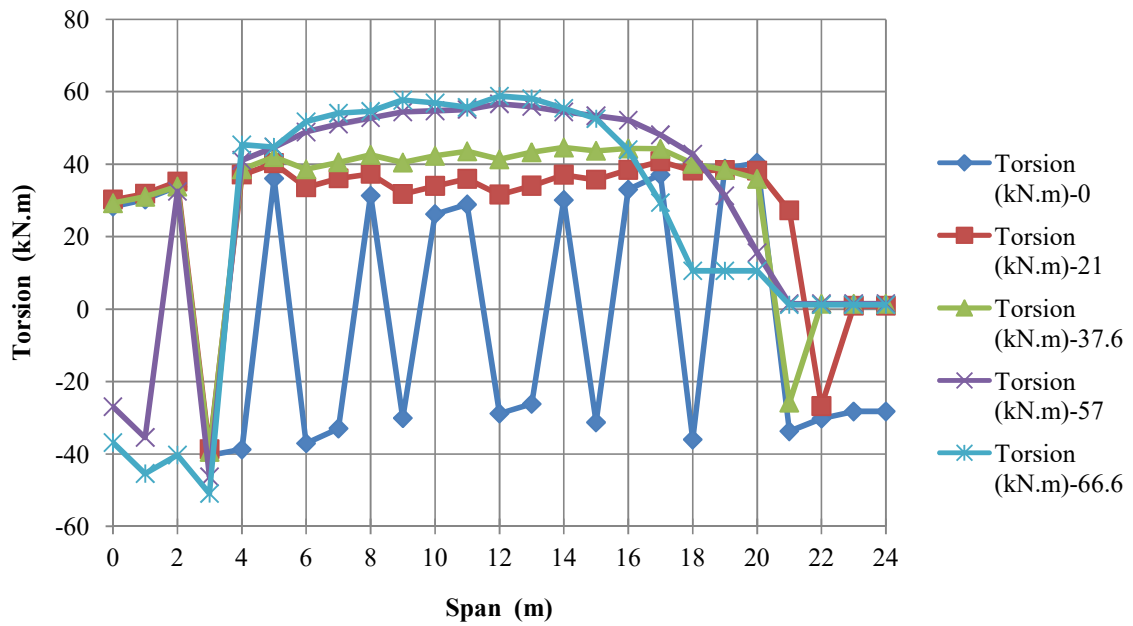


Figure 3.9.3.4. Torsion diagram of the fourth I-girder

In figure 3.9.3.4, the shape of the curve was like the curve in first I-girder but inversely according to span. That means external girders behaves the same behavior and it can be easy to guess the behavior one of them from the other.

3.9.4. The Axial Forces in I-girders

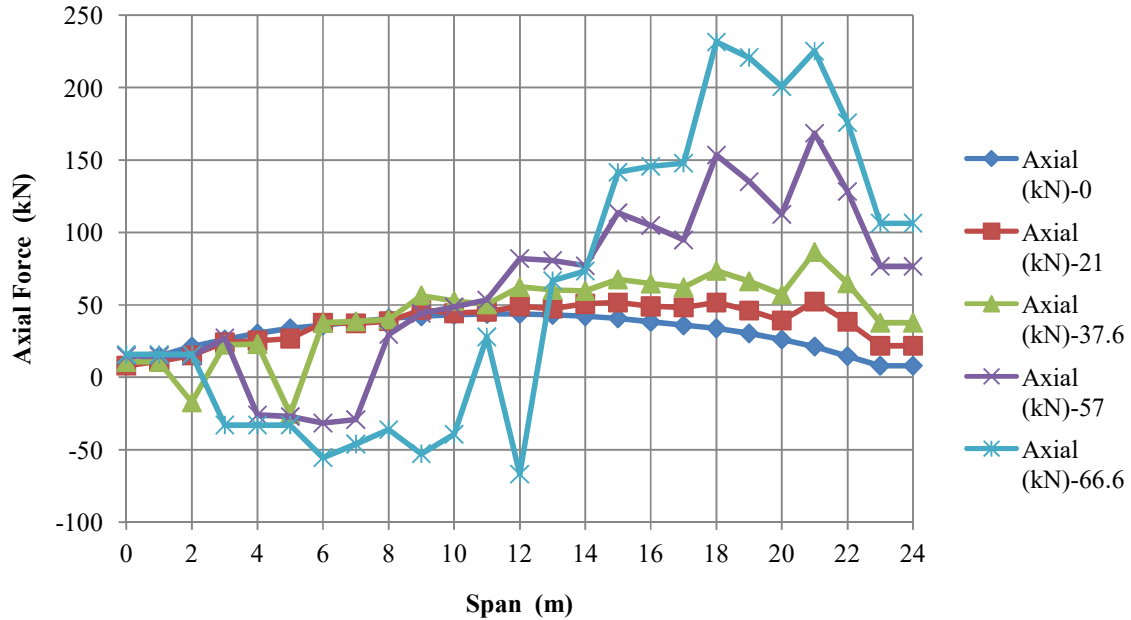


Figure 3.9.4.1. Axial forces diagram of the first I-girder

In figure 3.9.4.1, when the skewness angle was 0° , all the values of the curve were in positive sign and the shape of the curve was symmetric too. But when the skewness angle was increased to 21° , the shape of the curve started to change and be not symmetric but in the same time stayed in positive sign too. After that the shape of the curve changed to be up and down the horizontal axis of the diagram with positive and negative signs when the skewness angle was changed to be 37.6° . generally, the differences between the values were very slightly for skewness angle of 0° , 21° , 37.6° . After that when the skewness angle became 57° , the values of the axial forces increased generally and especially in the second and third quarter of the span. Finally, when the skewness angle became 66.6° , in general the axial forces increased not less than ratio of 15% comparing with values of axial forces for skewness angle 57° .

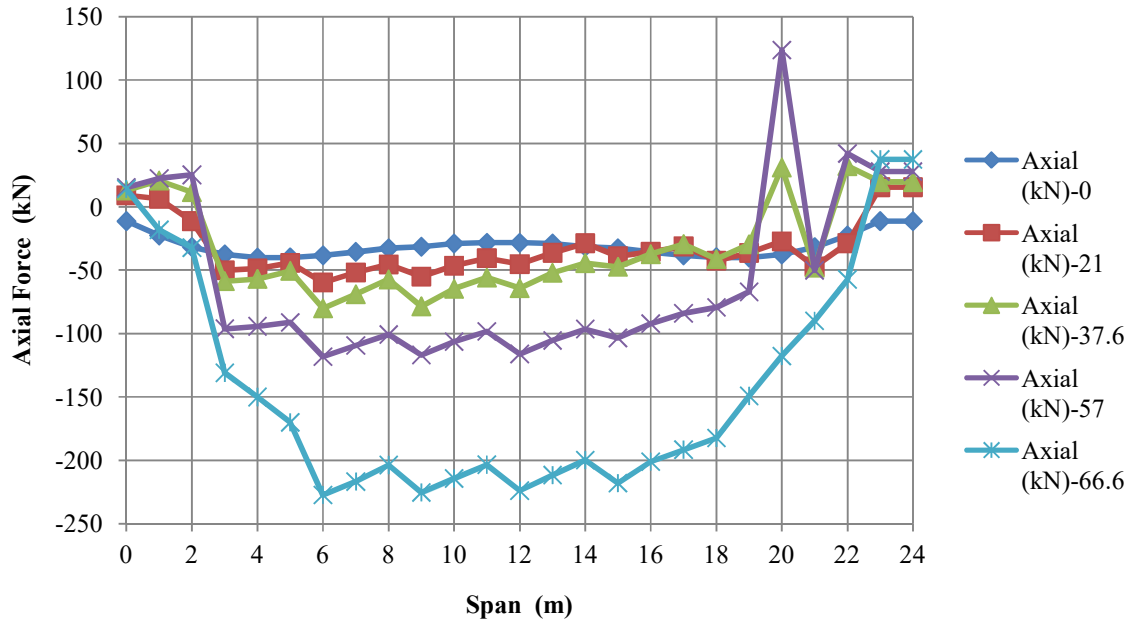


Figure 3.9.4.2. Axial forces diagram of the second I-girder

In figure 3.9.4.2, the behavior of the girder was as like the behavior of the first girder just in symmetrical of the curves but not as the shape. All the values of axial forces were positive and the shape of curves was symmetric when the skewness angle was 0° . But after that, when the skewness angle was changed to be 21° , the symmetrical in shape started to finish and some values of axial forces changed to be in negative sign in some places from the span. For skewness angle 37.6° , the symmetrical in shape of the curve completely finished and there was an increasing in the values of axial forces comparing with the values of skewness angle 21° with nearly ratio of 20%. After that when the skewness angle had been 57° , the same thing happened also and in general the shape of the curve stayed as was for 37.6° but the values increased more and more. Finally when the skewness angle became 66.6° , the axial forces increased with ratio more than 100% in the middle part of the span if the axial forces values of 57° was taken as a reference.

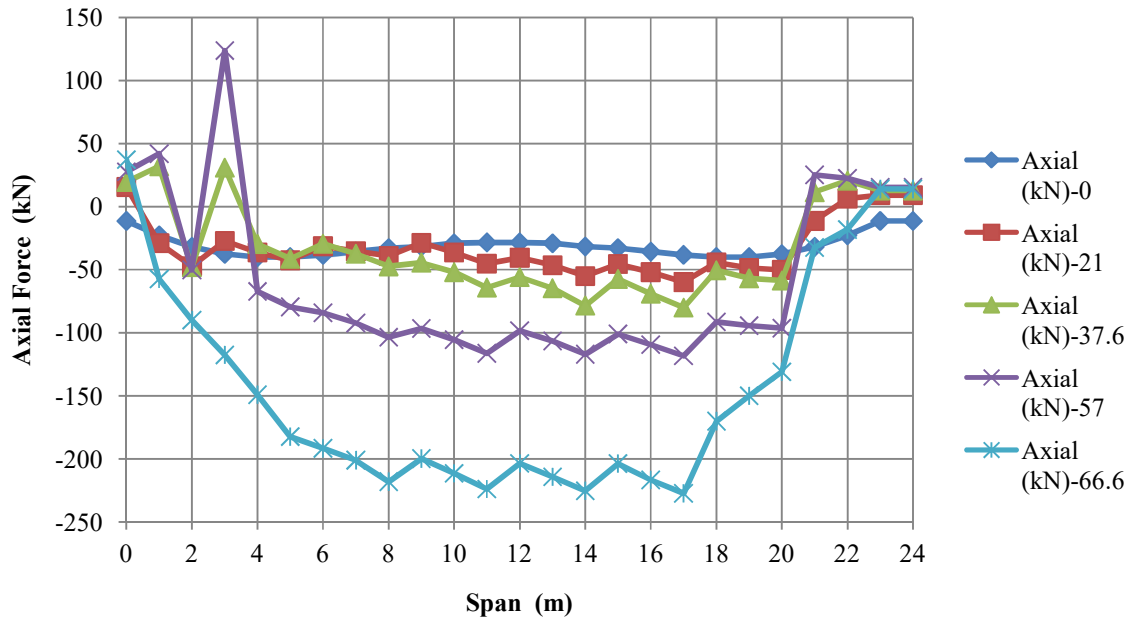


Figure 3.9.4.3. Axial forces diagram of the third I-girder

In figure 3.9.4.3, it was clear also the similarity in the shape and behavior of this I-girder with the second i girder but inversely. All the notes which were taken about the second I-girder can be applied here also but inversely according to the span.

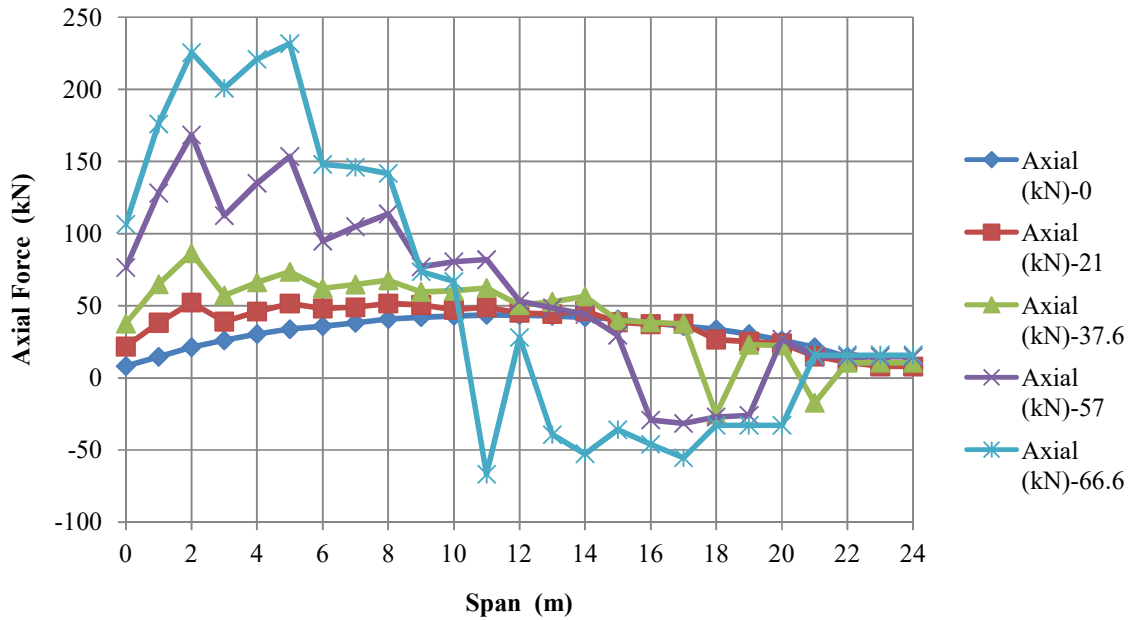


Figure 3.9.4.4. Axial forces diagram of the fourth I-girder

In figure 3.9.4.4, the behavior and shape of curves were the same as like as the first I-girder but inversely according to the span.

3.9.5. The Displacement of I-girders

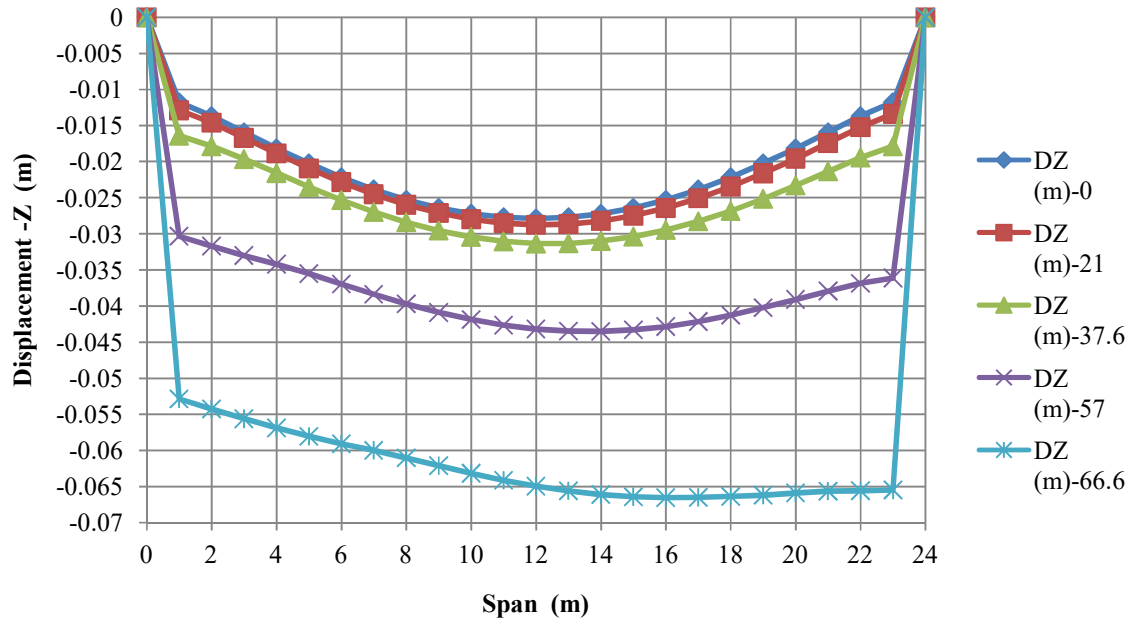


Figure 3.9.5.1. Displacement diagram of the first I-girder

In figure 3.9.5.1, when the skewness angle of the span was 0° , the shape of the curve was symmetric and the maximum value of the displacement was at the middle of the span. After that, when the skewness angle increased more to be 21° , the displacement also increased but slightly and the shape of the curve kept the symmetrical in shape also the same thing happened with the skewness angle of 37.6° and also the maximum displacement point stayed at the middle of the span too. But after the skewness angle became 57° , the shape of the curve lost the symmetrical and the maximum displacement point started to move toward and being in the second half of the span and also the displacement increased with ratio 90% if the displacement of 37.6° was taken as a reference. Then with skewness angle of 66.6° , the displacement increased with 80% ratio if the displacement of 57° was taken as a reference. Also the maximum displacement point moved towards the second half from the span. Generally, it was clear that the displacement, when the skewness angle became more than 37.6° , increased with big ratio and the maximum displacement happening in the second half of the span not in the middle of it.

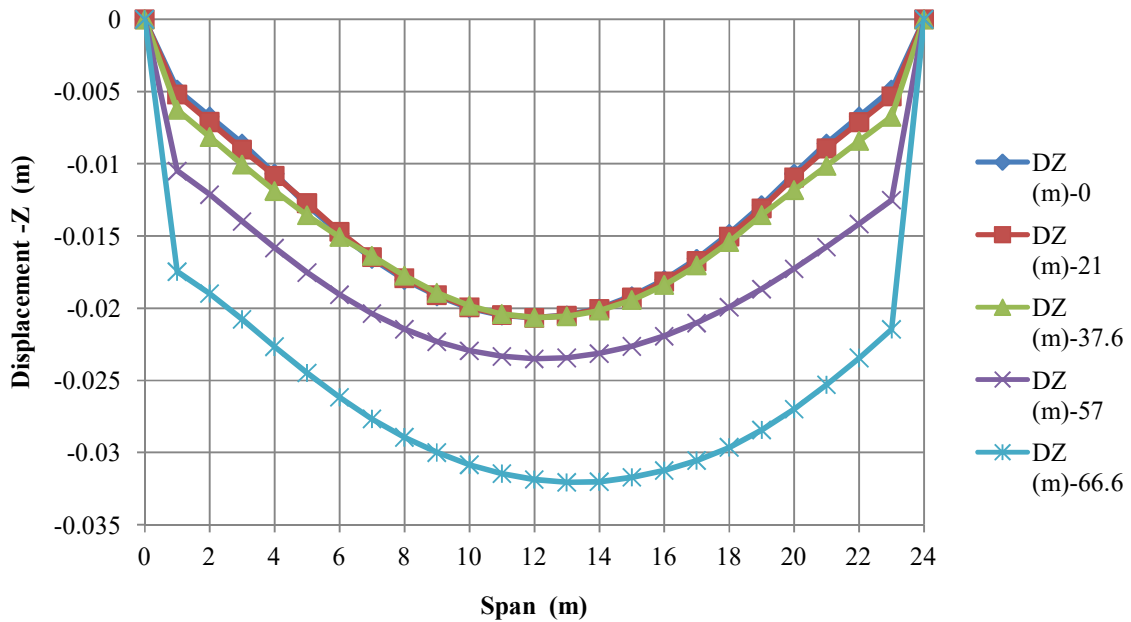


Figure 3.9.5.2. Displacement diagram of the second I-girder

In figure 3.9.5.2, for skewness angle 0°, 21°, and 37.6°, the displacement stayed at the same range and in some places from the span stayed with the same values or very near to each other. But when the skewness angle became 57°, the displacement increased everywhere in the span and the symmetric in shape of curve finished too. The maximum value of the displacement, which was at the middle of the span before, moved toward the second half of the span and moved more when the skewness angle became 66.6°. The increasing ratio in displacement was with ratio of 20% for angle 57° and 70% for angle 66.6° if the displacement value for angle 37.6° was taken as a reference.

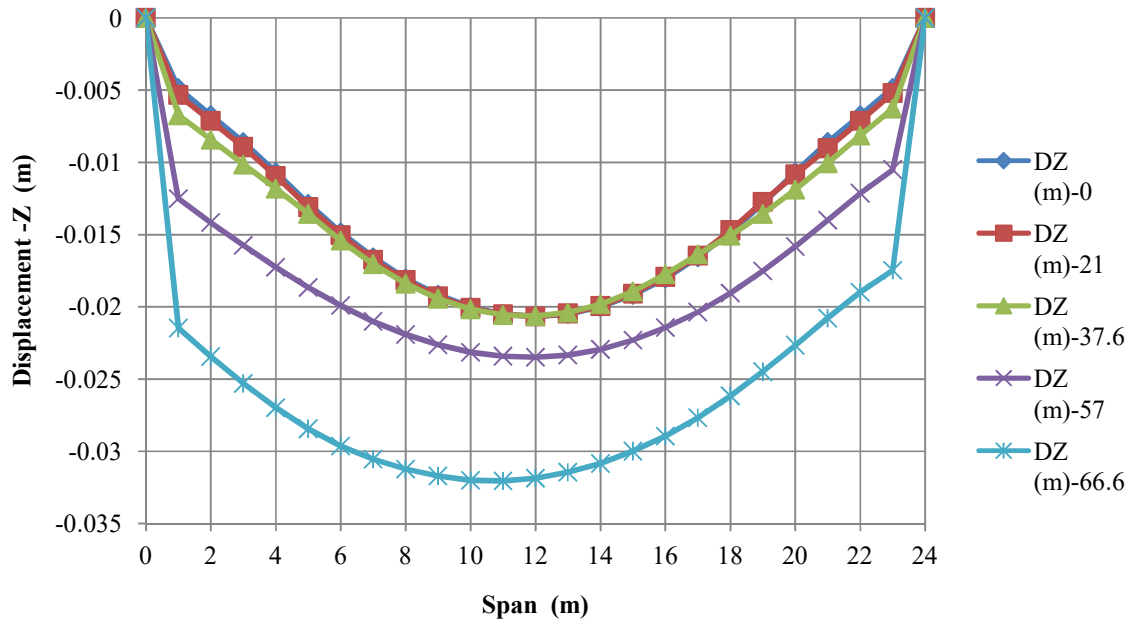


Figure 3.9.5.3. Displacement diagram of the third I-girder

In figure 3.9.5.3, the whole diagram was like the second diagram of the second I-girder but inversely according to span. So, the all notes which were written above can be applied here too.

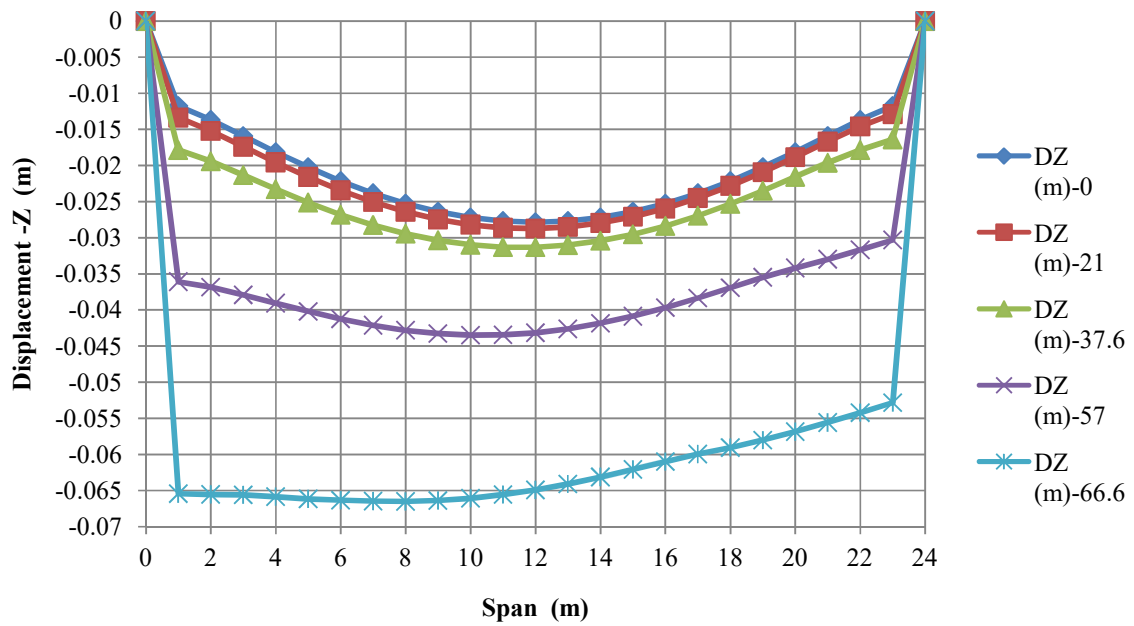


Figure 3.9.5.4. Displacement diagram of the fourth I-girder

In figure 3.9.5.4, all the diagram was like the first diagram of the first I-girder but inversely according to span. So, the all notes which were written above right for this I-girder and can be applied here too.

3.9.6. The Losses in Strands of I-girders

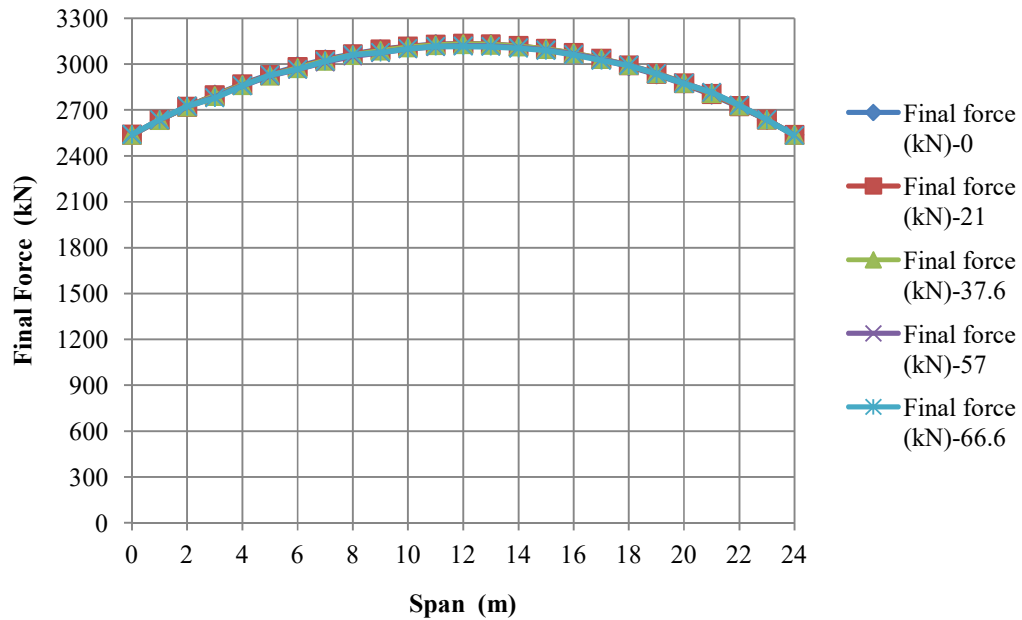


Figure 3.9.6.1. Diagram of final forces in strands after losses in the first I-girder

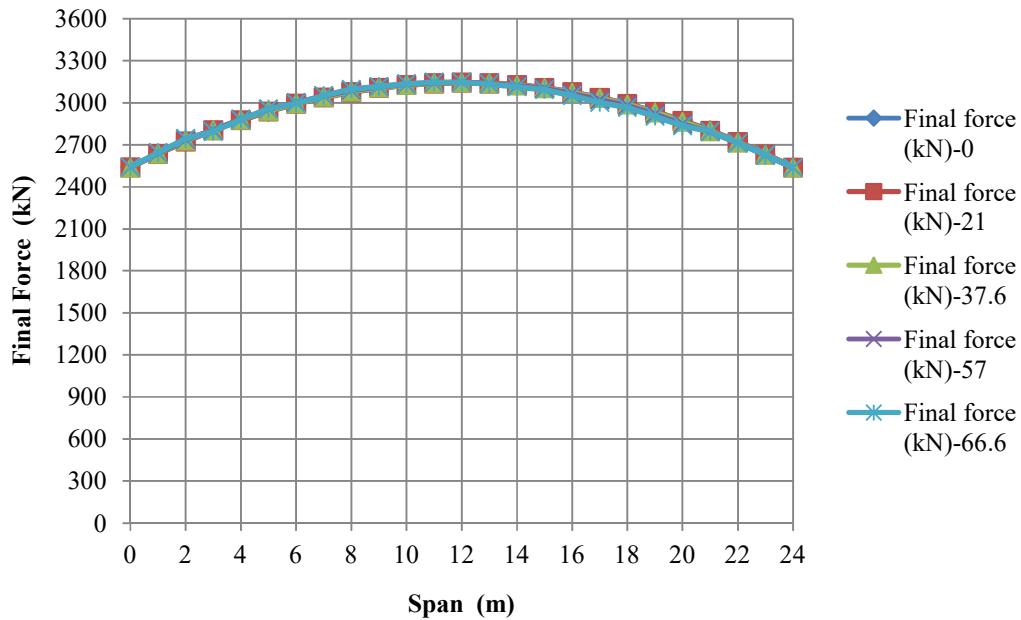


Figure 3.9.6.2. Diagram of final forces in strands after losses in the second I-girder

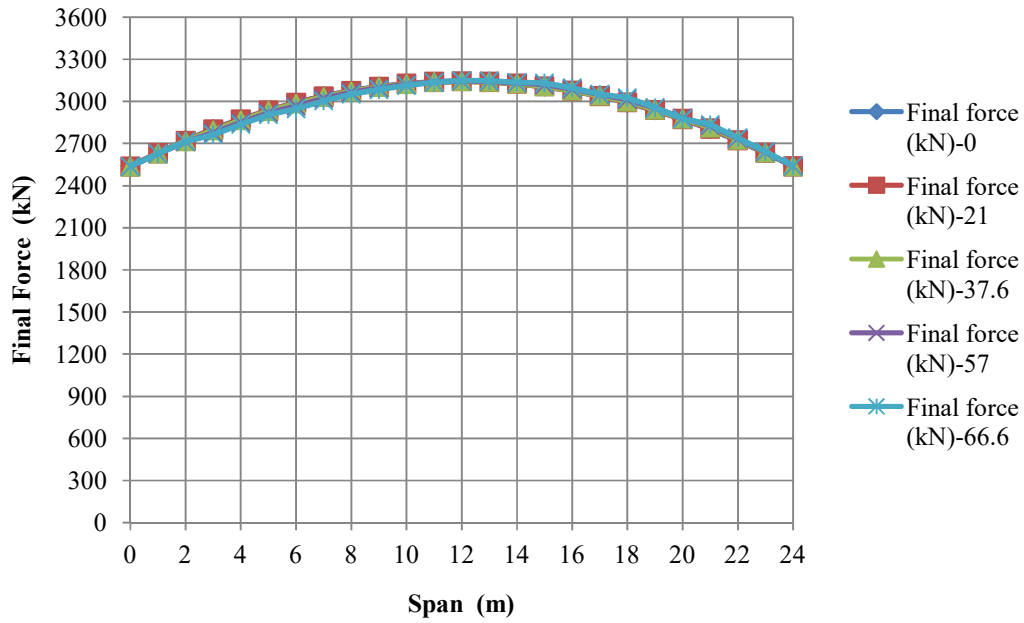


Figure 3.9.6.3. Diagram of final forces in strands after losses in the third I-girder

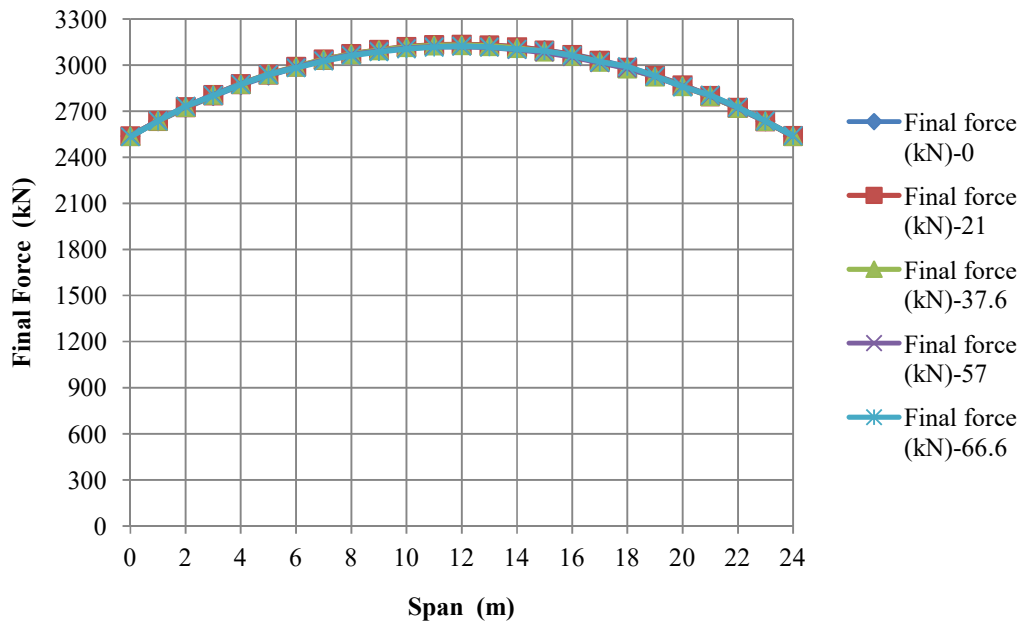


Figure 3.9.6.4. Diagram of final forces in strands after losses in the fourth I-girder

The all diagrams showed clearly that there was no effect of changing in skewness angle of span on the losses in strands forces. The differences between the first, second, third, and fourth I-girders in final forces were very very small and the values were very close to each other for all skewness angles 0°, 21°, 37.6°, 57°, and 66.6°. So, it can be concluded that generally there is no effect on the losses in pretension prestressed members by increasing the skewness angle of span.



3.9.7. The Axial Stresses in I-girders

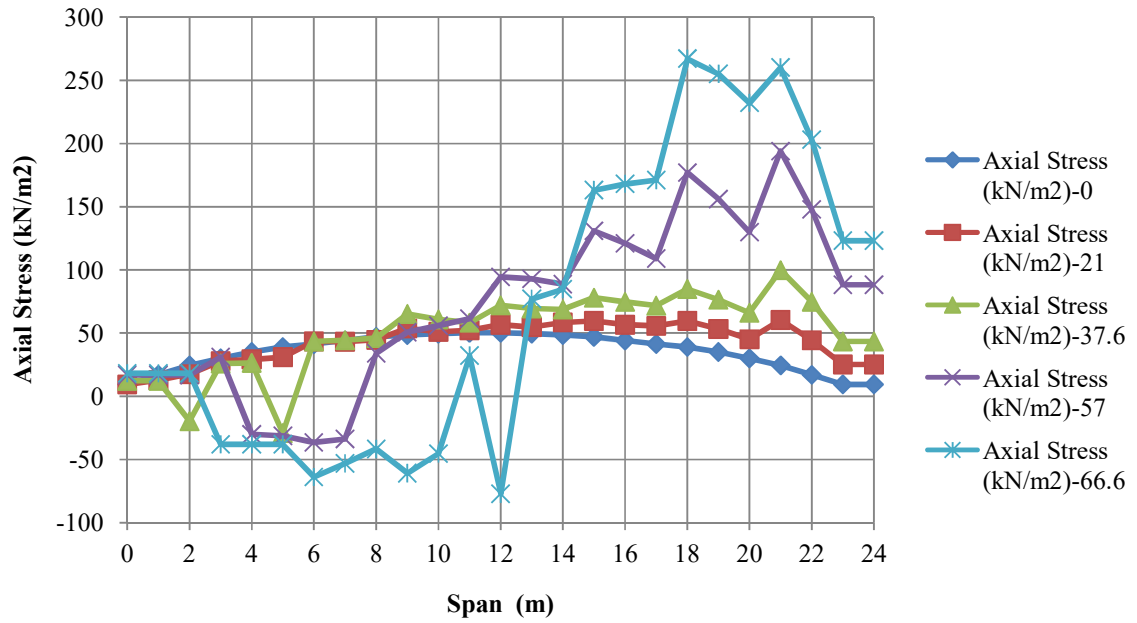


Figure 3.9.7.1. Axial stresses diagram of the first I-girder

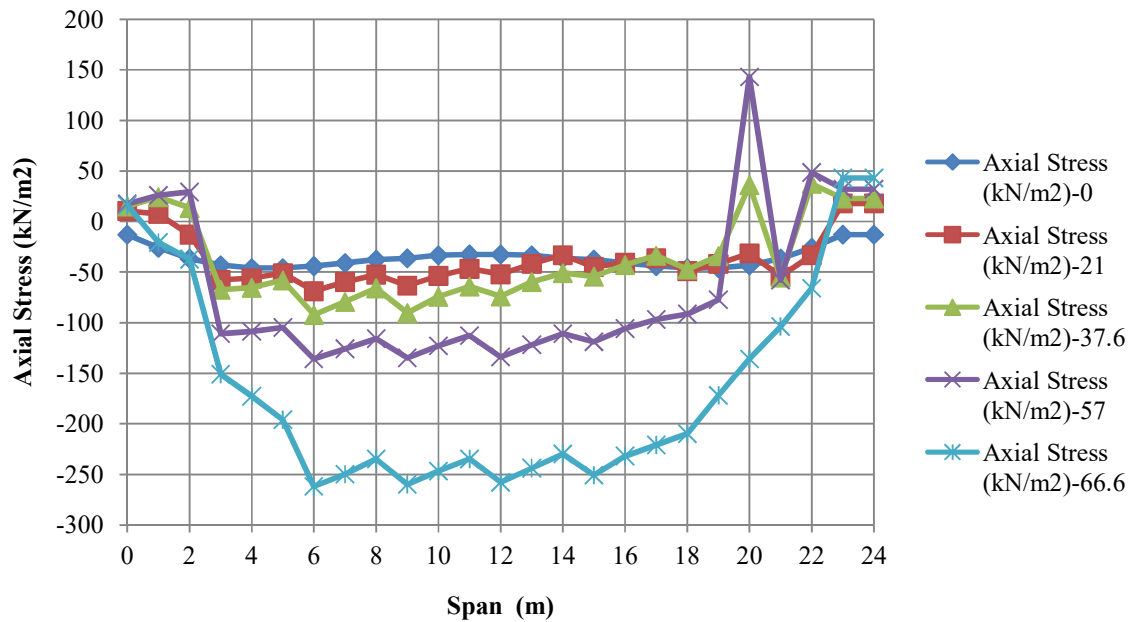


Figure 3.9.7.2. Axial stresses diagram of the second I-girder

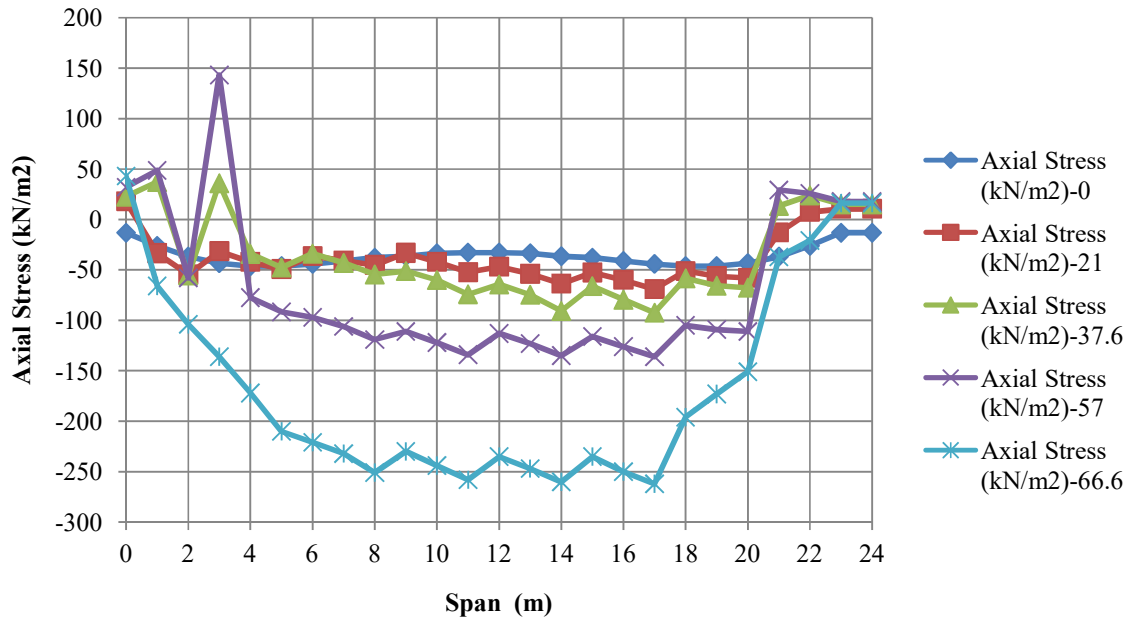


Figure 3.9.7.3. Axial stresses diagram of the third I-girder

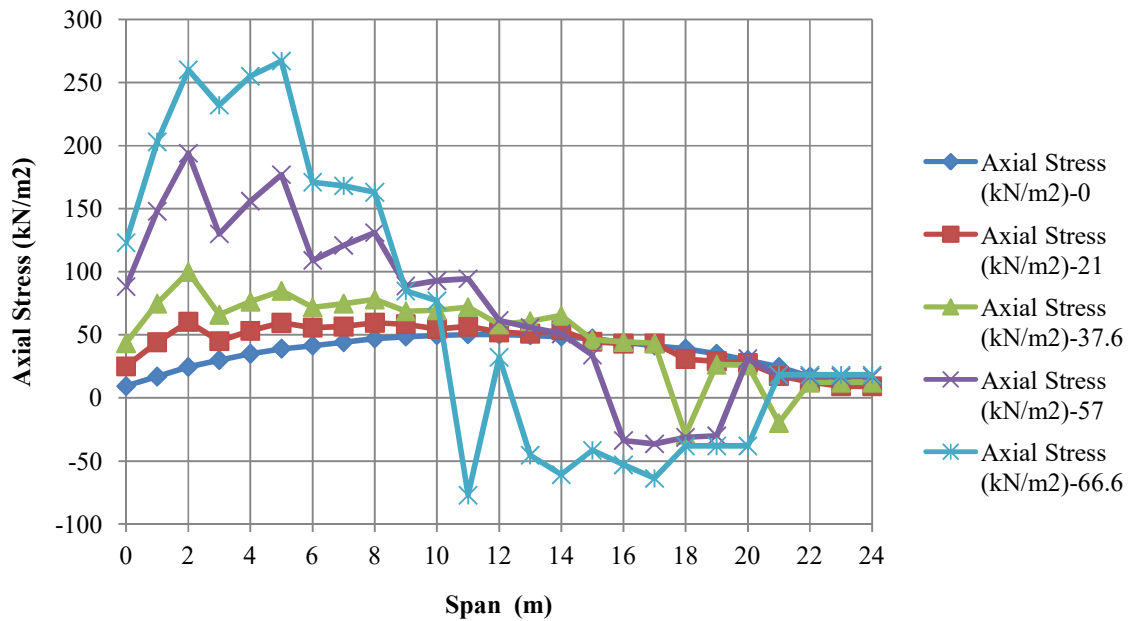


Figure 3.9.7.4. Axial stresses diagram of the fourth I-girder

As it can be seen and shown above, the all diagrams of axial stresses were the same and exactly the diagrams of axial forces in the I-girders because the all models and the all I-girders had the same section and all of these girders section was constant along the span. So, the diagrams were the same in shape but different in values and all the notes about the changing in values and ratios, which was taken before in axial forces diagrams, is the same exactly here for axial stresses too.

The results of analysis for all models in tables was given in the last part in appendix.



4. CONCLUSION AND RECOMMENDATIONS

Finally at the end of this thesis about the effects of skewness in span on the response of simply supported prestressed concrete bridges with I-girder section, for first and second I-girders it can be conclude that :

For bending moment, generally, the bending moment decreasing by increasing in skewness angle for external I-girders and because of that the designers can design these girders to resist these type from moment as they design a straight one and that will give the bridge more safety against bending moment and it was recommended. But for internal I-girders, the bending moment stayed in the same range with slightly changing until skewness angle of 37.6° . After increasing the skewness angle more than this angle, the bending moment increased rapidly with big ratio in some places of the span. Because of that, for internal I-girders, it must be designed according to the analysis results for every place or part from the span. In general the behavior of bending moment stayed similarly until 37.6° but after that a lot of changes happened and because of that, it was recommended to make more researches about it for many near and close to each other skewness angles.

For shear forces as it's known that the moment is the result of shear forces and that means the shear forces also will be effected if the skewness angle becomes more than 37.6° as was the moment and that what happened. Generally, the shear forces stayed at the same range and similar shape until the skewness angle of 37.6° . But after that when the skewness angle became 57° and 66.6° , for external I-girders, the values of shear forces changed slightly and in general and it was decreasing in the most places of the span but for internal I-girders the situation was not almost constant as the external I-girders. So, it was recommended in designing every I-girder must be studied alone and for more understanding the behavior of the shear forces, it must be making more researches about it especially the internal ones.

For torsion it was clear from the results of external I-girders that by increasing in skewness angle the torsion changed slowly to be in positive sign and one side of the horizontal axis in the diagram in the most of the places of the span especially in the middle part of it. But for internal I-girders the same thing happened for all places in the span when skewness angle being 37.6° and more. In general it can be said that by increasing the skewness angle the values of torsion were increasing in the middle part of the span. So, it was recommended to

concentrate in the design and in the next researches about the outside parts of the girders and making more studies for many and very close and near to each other skewness angles less than 37.6° to understand the behavior of it exactly.

For axial forces and stresses it can be concluded that by increasing the skewness angle more than 37.6° , for constant I-girder section along the span, the axial forces and stresses in general will be increased too. The values of the axial forces and stresses in external I-girders, by this increasing in skewness angle to 37.6° , 57° and 66.6° , will be changed to be in positive and negative signs (tension and compression) not like as the values of it before 21° which were just in one sign. The same thing can be said for internal I-girders but the values started to change to negative and positive sign with 21° , 37.6° , 57° , and 66.6° and but the most of these value were in negative especially in the middle part of the span. So, it was clear that there were a changes happened and started with skewness angle of 21° and maybe if another angle was used less than 21° this changes will be happen also. Because of that it was recommended to make more researches about which is the critical skewness angle that the sign of the values will be change in it.

For displacement it can be concluded that by increasing in skewness angle of the span, the displacement will increase also but the ratio of this increasing will be very big if the skewness angle being more than 37.6° . This increasing with big ratio in displacement will not be symmetric and it will be in the second half of the span more than the other and according to that, the maximum displacement point will not be in the middle of the span also and it will be in the second half from the span. So, it's very important for designers before designing to draw the all diagrams of all internal and external I-girders separately and it is recommended to study the displacement for skewness angle more than 66.6° to know what will be the behavior of girders with bigger angles.

For losses in strands it is clear that there is no any effect of the skewness in span on the final forces in strands and that means the losses did not effected by changing in skewness angle of the span.

Finally, from results and diagrams it was clear, when the girders numbers were from 1 to 4, that the behavior of external I-girders 1 and 4 was the same behavior but inversely according to span and also the same thing was noticed for internal I-girders 2 and 3 too. Because of that, it was recommended that, for the same situation of four I-girders properties,

section and under the same loading, to study just one from external I-girders and one from internal I-girder and it is recommended to study the middle I-girder also if the number of girders were five to know how this I-girder will behave. Although there are a lot of researches were written about skewed span bridges but it is recommended also to make more researches about the same subject but by taking more near and close skewness angles to each other and bigger than 66.6° with different number and properties of I-girders. to know how the behavior will be for every situation.



5. REFERENCES

- AASHTO, AASHTO LRFD Bridge Design Specifications, 1st edition., American Association of State Highway and Transportation Officials, Washington, D.C., 1994.
- Ameerutheen M., and Aravindan S., February 2014, Study of Stresses on Composite Girder Bridge Over Square and Skew Span, International Journal of Civil Engineering and Technology, 5, 2, 88-96.
- Abozaid L.A., Hassan A., Abouelezz A.Y., and Abdel-Hafez L.M., 2014, Nonlinear Behaviour of a Skew Slab Bridge under Traffic Loads, World Applied Sciences Journal, 30, 11, 1479-1493.
- Bakhit B., 1988, Analysis of Some Skew Bridges as Right Bridges, Journal Structural Engineering, 114, 10.
- Chen W. F., Duan L., 2000, Bridge Engineering Handbook, by CRC Press LLC, United States of America.
- Collins M. P., and Mitchell D., 1991, Prestressed Concrete Structures, Prentice-Hall, Englewood Cliffs, NJ.
- CEB-FIP, 1993, Model Code for Concrete Structures. (MC-90). Comité Euro-international du Béton (CEB)-Fédération Internationale de la précontrainte (FIP) (1990). Thomas Telford, London, U.K.
- Dhar A., Mazumder M., Chowdhury M., and Karmakar S., December 2013, Effect of Skew Angle on Longitudinal Girder (Support Shear, Moment, Torsion) and Deck Slab of an IRC Skew Bridge, The Indian Concrete Journal, 46-52.
- Deshmuk N. and Waghe Dr. U., April 2015, Analysis and Design of Skew Bridges, International Journal of Science and Research, 4, 4. 399-402.
- Deepak C. and Sabeena M. V., May-2015, Effect of Skew Angle on Uplift and Deflection of RCC Skew Slab, International Journal of Research in Engineering and Technology, 4, 5, 105-111.
- Ebeido T. and Kennedy J., 1996a, Girder moment in continuous skew composite bridge, Journal of Bridge Engineering, 1, 1, 37-45.
- Ebeido T. and Kennedy J., 1996b, Shear and Reaction Distribution in Continuous Skew Composite Bridges, Journal of Bridge Engineering, 1, 4, 155-165.
- Eubunsky I. A. and Rubinsky A., A Preliminary Investigation of The Use of Fiberglass for Prestressed Concrete, Mag. Concrete Res., 71, 1954.

- Fu G. , Zhuang Y. and Feng J. , March-April 2011, Behavior Of Reinforced Concrete Bridge Decks on Skewed Steel Superstructure under Truck Wheel Loads, *Journal of Bridge Engineering*, 16, 2, 219-225.
- FHWA, 1990, *Standard Plans for Highway Bridges, Vol. I, Concrete Superstructures*, U.S. Department of Transportation, FHWA, Washington, D.C.
- Helba, A. and Kennedy J., 1994, Parametric Study on The Collapse Loads of Skew Composite Bridge, *Journal Structural Engineering.*, 120, 5, 1415–1433.
- Huo X. and Zhang Q., January-February 2008, Effect of Skewness on The Distribution of Live Load Reaction at Piers of Skewed Continuous Bridges, *Journal of Bridge Engineering*, 13, 1, 110-114.
- Huang H., Shenton H. and Chajes M. , 2004, Load Distribution For a Highly Skewed Bridge, *Journal of Bridge Engineering*, 9, 6.
- Harba I., August 2011, Effect of Skew Angle on Behavior of Simply Supported RC T-Beam Bridge Decks, *ARPJ Journal of Engineering and Applied Sciences*, 6, 8.
- He X., Sheng X., Scanlon A., Linzell D. and YU X., 2012, Skewed concrete box girder bridge static and dynamic testing and analysis, *Journal of Engineering Stru.*, 39, 38-49.
- Iyer S.I. and Anigol M., 1991, Testing and Evaluating Fiberglass, Graphite, and Steel Prestressing Cables for Pretensioned Beams, in *Advanced Composite Materials in Civil Engineering Structures*, Iyer, S. I. and Sen, R., Eds., ASCE, New York, 44.
- Khaleel, M. and Itani R., 1990, Live-load Moment For Continuous Skew Bridge, *Journal Structural Engineering*, 116, 9, 2361–2373.
- Kalantari A. and Amjadian M., 2010, An approximate Method for Dynamic Analysis of Skewed Highway Bridges with Continuous Rigid Deck, *Engineering Structures*, 32, 9, 2850–2860.
- Kaliyaperumal G., Imam B. and Righiniotis T., 2011, Advanced Dynamic Finite Element Analysis of a Skew Steel Railway Bridge, *Journal of Engineering Structures*, 33, 1, 181–190.
- Khatri V., Maiti P., Singh P. and Kar A., May-June 2012, Analysis of Skew Bridges Using Computational Methods, *International Journal Of Computational Engineering*, 2, 3, 628-636.
- Kar A., Khatri V., Maiti P. and Singh P., 2012, Study on Effect of Skew Angle in Skew Bridges, *International Journal of Engineering Research and Development*, 2, 12, 13-18.
- Kankam A. and Dagher H., 1995, Nonlinear FE Analysis of RC Skewed Slab Bridges, *Journal Structural Engineering*, 12, 19, 1338-1345.

- Kim P. and Meier U., 1991, CFRP Cables for Large Structures, in *Advanced Composite Materials in Civil Engineering Structures*, Iyer, S. I. and Sen, R., Eds., ASCE, New York, 233–244.
- Lin T. Y. and Burns N. H., 1981, *Design of Prestressed Concrete Structure*, 3rd edition., John Wiley & Sons, New York.
- Menassa C., Mabsout M., Tarhini K. and Frederick G., March-April 2007, Influence of Skew Angle on Reinforced Concrete Slab Bridges. *Journal of Bridge Engineering*, 12, 2, 205-214.
- Mirzabozorg H. and Khaloo A., 2003, Load Distribution Factors in Simply Supported Skew Bridges. *Journal of Bridge Engineering*, 8, 4.
- Miessler H. J. and Wolff R., 1991, Experience with Fiber Composite Materials and Monitoring with Optical Fiber Sensors, in *Advanced Composite Materials in Civil Engineering Structures*, Iyer, S. I. and Sen, R., Eds., ASCE, New York, 167–182.
- Nouri G. and Ahmadi Z., July-August 2012, Influence of Skew Angle on Continuous Composite Girder Bridge, *Journal of Bridge Engineering*, 17, 4, 617–623.
- Nawy E. G., 1996, *Prestressed Concrete: A Fundamental Approach*, 2nd edition., Prentice-Hall, Englewood Cliffs, NJ.
- PCI, 1985, *PCI Design Handbook – Precast and Prestressed Concrete*, 3rd edition., Prestressed Concrete Institute, Chicago, IL.
- PTI, 1981, *Post-Tensioning Manual*, 3rd ed., Post-Tensioning Institute, Phoenix, AZ.
- Qaqish M., 2006, Effect of Skew Angle on Distribution of Bending Moments in Bridge Slabs, *Journal of Applied Sciences*, 6, 2, 366-372.
- Saber A., Roberts F., Alaywan W. and Toups J., March-April 2007, Effectiveness of Continuity Diaphragm for Skewed Continuous Prestressed Concrete Girder Bridges, *PCI Journal*, 108-114.
- Sindhu B.V., Ashwin K.N., Dattatreya J. K. and Dinesh S.V., 2013, Effect Of Skew Angle On Static Behaviour Of Reinforced Concrete Slab Bridge Decks, *International Journal of Research in Engineering and Technology*, 2, 1, 50-58.
- Theoret P., Massicotte B. and Conciatori D., March-April 2012, Analysis and Design of Straight and Skewed Slab Bridges, *Journal Of Bridge Engineering*, 17, 2, 289-301.
- Vayas I., Adamakos T. and Iliopoulos A., June 2011, Three Dimensional Modeling for Steel-Concrete Composite Bridges Using Systems of Bar Elements - Modeling of Skewed Bridges, *International Journal of Steel Structures*, 11, 2, 157-169.

Wines J. C. and Hoff G. C., 1966, Laboratory Investigation of Plastic-Glass Fiber Reinforcement for Reinforced and Prestressed Concrete, Report 1, U.S. Army Corps of Engineers, Waterway Experimental Station, Vicksburg, MI.

Wines J. C., Dietz R. J. and Hawly J. L., 1966, Laboratory Investigation of Plastic-Glass Fiber Reinforcement for Reinforced and Prestressed Concrete, Report 2, U.S. Army Corps of Engineers, Waterway Experimental Station, Vicksburg, MI.

URL-1, www.en.midasuser.com/product/civil_overview.asp, 20.05.2016.

URL-2, www.aboutcivil.org/bridges.html, 20.05.2016.



6. APPENDIX

Table 6.1. Bending moment in longitudinal direction of the bridge in the first I-girder for all models

Element	Moment-y (kN.m)-0	Moment-y (kN.m)-21	Moment-y (kN.m)-37.6	Moment-y (kN.m)-57	Moment-y (kN.m)-66.6	Span (m)
1	0	0	0	0	0	0
5	-224.39	-205.49	-185.68	-142.45	-110.58	1
6	-438.32	-402.49	-366.37	-283.01	-219.12	2
7	-633.44	-580.17	-516.76	-401.37	-305.76	3
8	-809.29	-755.81	-684.29	-548.52	-420.41	4
9	-961.76	-909.58	-834.15	-666.57	-535.06	5
10	-1088.91	-1032.89	-951.66	-782.11	-640.34	6
11	-1191.64	-1144.37	-1069.4	-898.03	-708.77	7
12	-1272.53	-1232.58	-1168.2	-998.83	-811.17	8
13	-1342.36	-1297.51	-1231.32	-1069.73	-900.4	9
14	-1386.89	-1353.6	-1288.66	-1135.54	-980.41	10
15	-1409.64	-1387.12	-1336.06	-1186.12	-1042.92	11
16	-1410.46	-1395.31	-1348.02	-1210.14	-1075.85	12
17	-1410.79	-1388.96	-1349.36	-1227.74	-1107.94	13
18	-1388.9	-1377.52	-1332.23	-1223.94	-1124.05	14
19	-1345.74	-1337.3	-1297.13	-1191.09	-1103.11	15
20	-1275.9	-1278.97	-1249.48	-1166	-1072.16	16
21	-1196.05	-1202.57	-1178.32	-1116.2	-1037.51	17
22	-1094.78	-1103.84	-1084.92	-1027.83	-963.82	18
23	-966.65	-983.79	-973.23	-936.65	-876.77	19
24	-814.01	-835.86	-837.95	-815.51	-771.06	20
25	-638.54	-659.75	-668.37	-645.75	-607.3	21
26	-441.41	-461.91	-471.58	-456.4	-433.55	22
27	-226.13	-239.57	-245.79	-238.62	-226.76	23
27	0	0	0	0	0	24

Table 6.2. Torsion moment of the bridge in the first I-girder for all models

Element	Torsion (kN.m)-0	Torsion (kN.m)-21	Torsion (kN.m)-37.6	Torsion (kN.m)-57	Torsion (kN.m)-66.6	Span (m)
1	-28.27	0.88	1.47	1.55	1.14	0
5	-30.25	-26.79	1.47	1.55	1.14	1
6	-33.76	27.22	-25.8	1.55	1.14	2
7	40.38	38.24	35.95	15.56	10.51	3
8	38.78	38.36	38.44	31.33	10.51	4
9	-36.05	38.24	40.13	42.86	10.51	5
10	37.09	40.78	44.27	48.12	29.36	6
11	32.98	38.44	44.34	52.17	43.94	7
12	-31.3	35.7	43.71	53.37	52.54	8
13	30.12	37.05	44.62	54.42	55.43	9
14	-26.22	34.04	43.29	55.91	58.06	10
15	-28.87	31.61	41.34	56.67	58.78	11
16	28.87	35.93	43.59	55.16	55.66	12
17	26.22	33.99	42.34	54.75	56.86	13
18	-30.12	31.75	40.51	54.45	57.62	14
19	31.3	37.36	42.56	52.79	54.55	15
20	-32.98	36.05	40.53	51.11	54.04	16
21	-37.09	33.61	38.61	48.9	51.71	17
22	36.05	40.23	42	44.72	44.71	18
23	-38.78	37.07	38.58	41.06	45.32	19
24	-40.38	-38.65	-39.41	-46.29	-50.97	20
25	33.76	35.23	33.86	32.48	-40.33	21
26	30.25	31.87	31.03	-35.42	-45.44	22
27	28.27	30.2	29.24	-26.97	-36.9	23
27	28.27	30.2	29.24	-26.97	-36.9	24

Table 6.3. Shear forces in z-direction of the bridge in the first I-girder for all models

Element	Shear-z (kN)-0	Shear-z (kN)-21	Shear-z (kN)-37.6	Shear-z (kN)-57	Shear-z (kN)-66.6	Span (m)
1	227.82	207.55	184.07	140.57	108.55	0
5	222.34	203.04	184.07	140.57	108.55	1
6	212.82	197.09	177.7	140.57	108.55	2
7	200.65	190.37	175.15	147.8	114.65	3
8	188.87	181.67	168.38	141.72	114.65	4
9	176.2	171.88	161.48	140.07	114.65	5
10	160.07	158.44	151.96	135.94	113.14	6
11	148.57	148.42	143.44	130.5	115.07	7
12	136.54	137.72	134.83	124.81	113.13	8
13	120.46	121.59	121.17	116.2	107.15	9
14	109.72	111.42	111.15	108.19	100.74	10
15	98.36	100.7	101.33	99.67	93.81	11
16	-98.36	-89.26	85.34	88.51	85.01	12
17	-109.72	-101.59	-97.36	-88.75	-88.21	13
18	-120.46	-113.59	-109.99	-100.63	-97.49	14
19	-136.54	-127.43	-121.78	-110.08	-105.99	15
20	-148.57	-140.8	-136.14	-123.38	-119.53	16
21	-160.07	-154.04	-150.49	-138.04	-134.15	17
22	-176.2	-169.82	-165.19	-151.8	-146.97	18
23	-188.87	-184.84	-182.02	-169.05	-163.45	19
24	-200.65	-199.77	-198.98	-187.81	-181	20
25	-212.82	-216.79	-216.92	-204.43	-192.5	21
26	-222.34	-230.61	-233.37	-221.18	-207.17	22
27	-227.82	-241.1	-245.34	-233.73	-214.81	23
27	-227.82	-241.1	-245.34	-233.73	-214.81	24

Table 6.4. Axial forces of the bridge in the first I-girder for all models

Element	Axial (kN)-0	Axial (kN)-21	Axial (kN)-37.6	Axial (kN)-57	Axial (kN)-66.6	Span (m)
1	8.1	8.02	10.59	14.62	15.75	0
5	14.63	11	10.59	14.62	15.75	1
6	21.24	15.03	-17.25	14.62	15.75	2
7	26	24.03	22.43	26.95	-32.96	3
8	30.33	25.26	22.91	-26.05	-32.96	4
9	33.8	26.66	-25.33	-27.07	-32.96	5
10	35.85	37.56	37.57	-31.59	-55.33	6
11	38.19	37.24	38.53	-29.23	-46.06	7
12	40.71	38.66	39.84	29.57	-36.03	8
13	42.04	46.43	56.43	44.08	-52.72	9
14	42.95	44.2	52.68	48.54	-39.34	10
15	43.6	45.19	50.43	53.26	27.93	11
16	43.6	48.98	62.29	81.89	-66.79	12
17	42.95	47.29	60.25	80.54	66.79	13
18	42.04	50.66	59.59	76.94	73.44	14
19	40.71	51.65	67.65	113.62	141.58	15
20	38.19	48.96	64.77	104.79	145.76	16
21	35.85	48.17	62.15	94.75	147.87	17
22	33.8	51.6	73.48	153.37	231.49	18
23	30.33	46.04	66.19	134.98	220.8	19
24	26	39.13	57.19	112.4	200.69	20
25	21.24	52.23	86.47	168.36	225.2	21
26	14.63	38.31	64.86	128.12	175.78	22
27	8.1	21.73	37.63	76.5	106.41	23
27	8.1	21.73	37.63	76.5	106.41	24

Table 6.5. Axial stresses of the bridge in the first I-girder for all models

Elem	Axial Stress (kN/m ²)-0	Axial Stress (kN/m ²)-21	Axial Stress (kN/m ²)-37.6	Axial Stress (kN/m ²)-57	Axial Stress (kN/m ²)-66.6	Span (m)
1	9.35	9.25	12.2	16.9	18.2	0
5	16.9	12.7	12.2	16.9	18.2	1
6	24.5	17.3	-19.9	16.9	18.2	2
7	30	27.7	25.9	31.1	-38	3
8	35	29.1	26.4	-30.1	-38	4
9	39	30.8	-29.2	-31.2	-38	5
10	41.4	43.3	43.3	-36.4	-63.8	6
11	44.1	43	44.4	-33.7	-53.1	7
12	47	44.6	46	34.1	-41.6	8
13	48.5	53.6	65.1	50.9	-60.8	9
14	49.6	51	60.8	56	-45.4	10
15	50.3	52.1	58.2	61.4	32.2	11
16	50.3	56.5	71.9	94.5	-77.1	12
17	49.6	54.6	69.5	92.9	77	13
18	48.5	58.4	68.7	88.8	84.7	14
19	47	59.6	78	131	163	15
20	44.1	56.5	74.7	121	168	16
21	41.4	55.6	71.7	109	171	17
22	39	59.5	84.8	177	267	18
23	35	53.1	76.4	156	255	19
24	30	45.1	66	130	232	20
25	24.5	60.3	99.8	194	260	21
26	16.9	44.2	74.8	148	203	22
27	9.35	25.1	43.4	88.3	123	23
27	9.35	25.1	43.4	88.3	123	24

Table 6.6. Displacement in z-direction of the bridge in the first I-girder for all models

Node	DZ (m)-0	DZ (m)-21	DZ (m)-37.6	DZ (m)-57	DZ (m)-66.6	Span (m)
1	0	0	0	0	0	0
17	-0.011768	-0.012884	-0.016384	-0.030316	-0.052855	1
18	-0.013693	-0.01458	-0.017871	-0.031689	-0.054248	2
19	-0.015929	-0.016705	-0.019629	-0.032993	-0.05559	3
20	-0.018153	-0.018865	-0.021578	-0.034198	-0.056858	4
21	-0.020251	-0.020932	-0.023508	-0.035488	-0.058026	5
22	-0.022172	-0.022831	-0.025321	-0.036928	-0.059068	6
23	-0.023852	-0.024527	-0.026957	-0.038361	-0.059982	7
24	-0.025287	-0.025974	-0.028379	-0.039689	-0.061	8
25	-0.026398	-0.027129	-0.029549	-0.04088	-0.062088	9
26	-0.027217	-0.027987	-0.030436	-0.041868	-0.063147	10
27	-0.02771	-0.028527	-0.031036	-0.042631	-0.064117	11
28	-0.027869	-0.02875	-0.031328	-0.043172	-0.064934	12
29	-0.02771	-0.02865	-0.031314	-0.043453	-0.065588	13
30	-0.027217	-0.028219	-0.030994	-0.043491	-0.066088	14
31	-0.026398	-0.027484	-0.030374	-0.043276	-0.066394	15
32	-0.025287	-0.02643	-0.029461	-0.042824	-0.066528	16
33	-0.023852	-0.025085	-0.028266	-0.04214	-0.066506	17
34	-0.022172	-0.023468	-0.026819	-0.041261	-0.066368	18
35	-0.020251	-0.021612	-0.025143	-0.040207	-0.066165	19
36	-0.018153	-0.019577	-0.023295	-0.039069	-0.06586	20
37	-0.015929	-0.017417	-0.021346	-0.037915	-0.065616	21
38	-0.013693	-0.015242	-0.019429	-0.036842	-0.065564	22
39	-0.011768	-0.013388	-0.017885	-0.036094	-0.065462	23
2	0	0	0	0	0	24

Table 6.7. Final forces in pre-tentioned steel of the bridge in the first I-girder for all models

Elem	Part	Final force (kN)-0	Final force (kN)-21	Final force (kN)-37.6	Final force (kN)-57	Final force (kN)-66.6	Span (m)
1	I	2537.675	2538.193	2538.354	2539.042	2540.275	0
5	I	2634.515	2634.668	2634.532	2634.983	2637.324	1
6	I	2721.705	2720.723	2721.276	2722.166	2725.616	2
7	I	2799.532	2795.396	2791.117	2783.818	2779.179	3
8	I	2870.55	2866.525	2862.838	2860.417	2858.379	4
9	I	2932.515	2928.328	2924.758	2924.825	2928.862	5
10	I	2985.569	2980.918	2974.777	2965.333	2966.019	6
11	I	3031.275	3027.091	3021.676	3014.005	3019.258	7
12	I	3068.197	3064.343	3059.505	3052.888	3060.615	8
13	I	3096.404	3093.441	3088.313	3076.208	3076.421	9
14	I	3117.348	3114.931	3110.474	3099.708	3100.935	10
15	I	3129.619	3127.714	3123.933	3114.369	3115.722	11
16	I	3133.234	3132.973	3130.395	3120.265	3116.623	12
17	I	3129.643	3129.816	3127.638	3118.355	3114.469	13
18	I	3117.397	3118.054	3116.402	3107.977	3103.755	14
19	I	3096.463	3099.128	3099.735	3094.472	3089.403	15
20	I	3068.304	3071.073	3071.608	3066.22	3061.106	16
21	I	3031.414	3034.418	3035.103	3029.819	3024.751	17
22	I	2985.713	2990.67	2994.222	2994.811	2992.15	18
23	I	2932.73	2937.129	2939.901	2939.375	2936.583	19
24	I	2870.806	2874.858	2877.134	2875.877	2872.968	20
25	I	2799.79	2804.943	2809.923	2815.407	2815.941	21
26	I	2722.037	2725.14	2728.128	2731.202	2731.07	22
27	I	2634.873	2636.176	2637.42	2638.318	2637.458	23
27	J	2537.675	2537.373	2536.906	2535.555	2533.639	24

Table 6.8. Bending moment in longitudinal direction of the bridge in the first I-girder for all models

Element	Moment-y (kN.m)-0	Moment-y (kN.m)-21	Moment-y (kN.m)-37.6	Moment-y (kN.m)-57	Moment-y (kN.m)-66.6	Span (m)
2	0	0	0	0	0	0
28	-282.52	-273.78	-291.57	-313.02	-314.62	1
29	-516.03	-503.02	-506.8	-560.1	-576.63	2
30	-709.6	-692.73	-683.74	-751.6	-778.33	3
31	-871.65	-852.54	-840.42	-879.09	-929.57	4
32	-1007.94	-987.1	-972.64	-962.51	-1040.74	5
33	-1122.37	-1099.56	-1084.1	-1052.54	-1091.96	6
34	-1216.04	-1195.45	-1177.07	-1136.26	-1137.54	7
35	-1293.02	-1274.58	-1257.03	-1204.74	-1209.59	8
36	-1352.12	-1332.69	-1318.16	-1266.19	-1279.13	9
37	-1395.21	-1374.91	-1361.05	-1310.75	-1333.62	10
38	-1416.33	-1400.34	-1385.24	-1348.99	-1380.31	11
39	-1417.2	-1415.3	-1403.71	-1383.21	-1431.18	12
40	-1417.2	-1414.37	-1402.56	-1396.53	-1476.32	13
41	-1396	-1392.97	-1382.25	-1395.59	-1524.2	14
42	-1353.11	-1351.87	-1349.46	-1394.07	-1599.15	15
43	-1294.08	-1295.67	-1298.36	-1373.34	-1615.85	16
44	-1217.6	-1223.67	-1231.1	-1328.84	-1610.12	17
45	-1124.24	-1133.27	-1151.99	-1300.29	-1613.27	18
46	-1009.73	-1022.48	-1049.63	-1234.72	-1453.4	19
47	-873.87	-889.47	-928.28	-1137.02	-1225.44	20
48	-713.09	-734.61	-787.83	-930.56	-932.04	21
49	-520.01	-542.58	-598.03	-633.13	-649.17	22
50	-287.2	-307.3	-312.09	-316.02	-323.4	23
50	0	0	0	0	0	24

Table 6.9. Torsion moment of the bridge in the first I-girder for all models

Element	Torsion (kN.m)-0	Torsion (kN.m)-21	Torsion (kN.m)-37.6	Torsion (kN.m)-57	Torsion (kN.m)-66.6	Span (m)
2	30.34	21.01	19.01	22.59	29.16	0
28	38.79	32.07	26.31	31.03	40.46	1
29	41.58	38.61	32.84	36.32	50.82	2
30	37.76	37.99	36.17	41.05	52.52	3
31	36.45	38.97	40.73	42.31	54.34	4
32	34.85	38.66	44.11	48.1	56.49	5
33	29.58	35.36	41.6	49.45	50.1	6
34	28.32	35.16	42.13	53.64	55.28	7
35	27.14	34.12	43.96	55.67	60.22	8
36	23.91	31.74	41.39	53.89	59.77	9
37	23.16	31.59	41.76	56.06	62.62	10
38	22.76	31.54	43.26	57.84	65.31	11
39	-22.76	29.48	40.19	54.92	60.67	12
40	-23.16	30.97	40.7	56.09	61.7	13
41	-23.91	32.25	42.15	56.21	62.45	14
42	-27.14	31.72	40.04	53.47	59.56	15
43	-28.32	33.23	40.28	52.81	57.53	16
44	-29.58	34.24	40.78	49.98	57.16	17
45	-34.85	36.82	41.2	45.49	69.89	18
46	-36.45	38.65	39.8	40.47	61.47	19
47	-37.76	38.3	38.8	42.52	56.01	20
48	-41.58	-37.82	30.55	33.76	51.65	21
49	-38.79	-32.63	21.98	28.17	43.42	22
50	-30.34	16.02	16.63	19.65	30.61	23
50	-30.34	16.02	16.63	19.65	30.61	24

Table 6.10. Shear forces in z-direction of the bridge in the first I-girder for all models

Element	Shear-z (kN)-0	Shear-z (kN)-21	Shear-z (kN)-37.6	Shear-z (kN)-57	Shear-z (kN)-66.6	Span (m)
2	294.27	284.53	285.91	316.32	330.96	0
28	260.95	254.64	251.22	277.55	290.13	1
29	236.3	230.5	225.36	243	254.82	2
30	216.95	214.23	208.56	209.9	218.81	3
31	199.23	197.7	192.89	185.94	192.33	4
32	183.68	181.49	178.83	172.58	169.15	5
33	175.68	174.85	172.76	166.65	160.05	6
34	160.24	160.27	159.04	158.58	153.15	7
35	146.34	145.26	145.63	151.85	149.56	8
36	141.85	141.36	140.85	148.12	150.24	9
37	127.09	127.46	127.43	139.72	146.36	10
38	-113.91	112.98	-117.61	131	144.35	11
39	113.91	109.91	-116.85	-126.68	145.13	12
40	-127.09	-121.27	-126.82	-133.67	-140.51	13
41	-141.85	-134.15	-139.77	-140.03	-140.33	14
42	-146.34	-139.92	-139.85	-140.94	-137.83	15
43	-160.24	-153.36	-151.58	-145.94	-142.32	16
44	-175.68	-167.07	-166.07	-151.75	-171.36	17
45	-183.68	-177.35	-176.81	-171.84	-241.66	18
46	-199.23	-192.88	-192.77	-205.74	-269.44	19
47	-216.95	-210.07	-215.29	-262.3	-287.65	20
48	-236.3	-235.29	-251.1	-302.67	-313.17	21
49	-260.95	-264.76	-296.12	-319.29	-329.28	22
50	-294.27	-306.35	-312.38	-323.19	-333.38	23
50	-294.27	-306.35	-312.38	-323.19	-333.38	24

Table 6.11. Axial forces of the bridge in the first I-girder for all models

Element	Axial (kN)-0	Axial (kN)-21	Axial (kN)-37.6	Axial (kN)-57	Axial (kN)-66.6	Span (m)
2	-11.37	9.07	12.85	15.24	13.97	0
28	-22.62	6.48	20.7	22.38	-18.14	1
29	-31.87	-11.22	11.55	25.22	-32.28	2
30	-37.56	-50.11	-58.54	-96.28	-130.94	3
31	-40	-48.72	-56.84	-94.34	-149.98	4
32	-39.93	-44.26	-50.45	-91.32	-170.09	5
33	-38.26	-59.76	-80.01	-118.26	-227.22	6
34	-35.6	-51.86	-68.93	-109.49	-216.64	7
35	-32.77	-45.47	-57.24	-100.9	-203.65	8
36	-31.51	-55.04	-78.48	-116.91	-225.27	9
37	-28.97	-46.54	-64.62	-106.52	-214.23	10
38	-28.37	-40.52	-55.81	-98.3	-203.51	11
39	-28.37	-45.23	-64.11	-116.2	-223.84	12
40	-28.97	-36.28	-51.96	-105.52	-211.53	13
41	-31.51	-28.69	-44.32	-96.54	-199.75	14
42	-32.77	-39.02	-47.26	-103.49	-217.99	15
43	-35.6	-35.41	-37.32	-92.21	-200.95	16
44	-38.26	-31.38	-29.39	-84.1	-191.53	17
45	-39.93	-42.53	-41.23	-79.41	-182.27	18
46	-40	-36.35	-29.6	-67.14	-149.07	19
47	-37.56	-27.22	31.01	123.64	-117.62	20
48	-31.87	-47.18	-47.93	-50.15	-89.89	21
49	-22.62	-28.84	32.13	42.03	-57.21	22
50	-11.37	15.51	19.56	27.71	37.29	23
50	-11.37	15.51	19.56	27.71	37.29	24

Table 6.12. Axial stresses of the bridge in the first I-girder for all models

Element	Axial Stress (kN/m ²)-0	Axial Stress (kN/m ²)-21	Axial Stress (kN/m ²)-37.6	Axial Stress (kN/m ²)-57	Axial Stress (kN/m ²)-66.6	Span (m)
2	-13.1	10.5	14.8	17.6	16.1	0
28	-26.1	7.47	23.9	25.8	-20.9	1
29	-36.8	-12.9	13.3	29.1	-37.2	2
30	-43.3	-57.8	-67.5	-111	-151	3
31	-46.1	-56.2	-65.6	-109	-173	4
32	-46.1	-51.1	-58.2	-105	-196	5
33	-44.1	-68.9	-92.3	-136	-262	6
34	-41.1	-59.8	-79.5	-126	-250	7
35	-37.8	-52.5	-66	-116	-235	8
36	-36.4	-63.5	-90.5	-135	-260	9
37	-33.4	-53.7	-74.5	-123	-247	10
38	-32.7	-46.7	-64.4	-113	-235	11
39	-32.7	-52.2	-74	-134	-258	12
40	-33.4	-41.9	-59.9	-122	-244	13
41	-36.4	-33.1	-51.1	-111	-230	14
42	-37.8	-45	-54.5	-119	-251	15
43	-41.1	-40.8	-43.1	-106	-232	16
44	-44.1	-36.2	-33.9	-97	-221	17
45	-46.1	-49.1	-47.6	-91.6	-210	18
46	-46.1	-41.9	-34.1	-77.5	-172	19
47	-43.3	-31.4	35.8	143	-136	20
48	-36.8	-54.4	-55.3	-57.9	-104	21
49	-26.1	-33.3	37.1	48.5	-66	22
50	-13.1	17.9	22.6	32	43	23
50	-13.1	17.9	22.6	32	43	24

Table 6.13. Displacement in z-direction of the bridge in the first I-girder for all models

Node	DZ (m)-0	DZ (m)-21	DZ (m)-37.6	DZ (m)-57	DZ (m)-66.6	Span (m)
3	0	0	0	0	0	0
40	-0.004851	-0.0052	-0.006268	-0.0105	-0.017471	1
41	-0.006723	-0.007107	-0.008144	-0.012138	-0.01899	2
42	-0.008595	-0.009016	-0.010061	-0.014001	-0.02078	3
43	-0.010682	-0.010835	-0.011886	-0.015831	-0.022661	4
44	-0.012863	-0.012718	-0.013566	-0.017527	-0.024487	5
45	-0.014838	-0.014704	-0.015073	-0.019057	-0.026169	6
46	-0.01657	-0.016456	-0.016374	-0.020368	-0.027668	7
47	-0.018038	-0.017921	-0.01775	-0.021451	-0.028942	8
48	-0.019169	-0.019088	-0.018942	-0.022316	-0.029994	9
49	-0.020003	-0.019935	-0.019828	-0.022945	-0.030837	10
50	-0.0205	-0.020461	-0.020403	-0.02334	-0.031454	11
51	-0.020658	-0.020658	-0.020651	-0.023504	-0.031859	12
52	-0.0205	-0.020521	-0.020569	-0.02343	-0.032054	13
53	-0.020003	-0.020061	-0.020166	-0.023146	-0.032013	14
54	-0.019169	-0.019268	-0.019441	-0.022635	-0.031705	15
55	-0.018038	-0.018151	-0.018399	-0.021927	-0.031237	16
56	-0.01657	-0.016729	-0.017045	-0.021021	-0.030554	17
57	-0.014838	-0.015027	-0.01542	-0.01992	-0.029632	18
58	-0.012863	-0.013087	-0.013555	-0.018669	-0.02844	19
59	-0.010682	-0.010943	-0.011817	-0.017273	-0.026984	20
60	-0.008595	-0.008935	-0.010145	-0.015757	-0.025299	21
61	-0.006723	-0.007122	-0.008419	-0.014166	-0.023441	22
62	-0.004851	-0.005328	-0.006738	-0.012511	-0.021467	23
4	0	0	0	0	0	24

Table 6.14. Final forces in pre-tentioned steel of the bridge in the first I-girder for all models.

Element	Part	Final force (kN)-0	Final force (kN)-21	Final force (kN)-37.6	Final force (kN)-57	Final force (kN)-66.6	Span (m)
2	I	2538.352	2538.476	2538.69	2539.347	2540.438	0
28	I	2633.397	2635.023	2636.81	2640.821	2644.175	1
29	I	2721.595	2724.562	2729.152	2737.533	2743.911	2
30	I	2802.695	2804.291	2805.665	2803.482	2794.471	3
31	I	2873.082	2874.918	2877.916	2883.074	2878.711	4
32	I	2936.131	2938.041	2942.264	2953.865	2956.874	5
33	I	2991.728	2992.971	2995.345	3000.192	2996.198	6
34	I	3037.239	3038.315	3040.96	3049.075	3051.563	7
35	I	3075.217	3076.026	3078.641	3089.005	3096.775	8
36	I	3105.613	3106.216	3107.811	3113.674	3114.958	9
37	I	3125.893	3126.262	3127.436	3132.719	3135.77	10
38	I	3138.57	3138.628	3139.161	3143.074	3146.803	11
39	I	3143.636	3143.957	3144.412	3146.552	3146.022	12
40	I	3138.546	3138.463	3138.023	3137.111	3133.797	13
41	I	3125.844	3125.29	3123.768	3119.294	3112.398	14
42	I	3105.554	3105.479	3104.646	3101.177	3092.576	15
43	I	3075.111	3074.324	3072.19	3064.23	3050.268	16
44	I	3037.1	3035.561	3031.999	3019.414	3000.776	17
45	I	2991.583	2990.461	2988.138	2979.201	2965.734	18
46	I	2935.915	2933.989	2930.294	2917.045	2903.014	19
47	I	2872.826	2870.148	2865.159	2848.716	2835.102	20
48	I	2802.436	2799.873	2797.086	2792.841	2794.053	21
49	I	2721.263	2718.929	2716.002	2712.533	2712.276	22
50	I	2633.039	2631.291	2629.699	2627.147	2626.033	23
50	J	2538.352	2537.892	2537.784	2537.486	2536.937	24

Table 6.15. Bending moment in longitudinal direction of the bridge in the first I-girder for all models

Element	Moment-y (kN.m)-0	Moment-y (kN.m)-21	Moment-y (kN.m)-37.6	Moment-y (kN.m)-57	Moment-y (kN.m)-66.6	Span (m)
3	0	0	0	0	0	0
51	-282.52	-297.59	-313.96	-314.67	-320.06	1
52	-516.03	-534.63	-581.08	-628.61	-643.33	2
53	-709.6	-724.23	-766.22	-925.2	-939.3	3
54	-871.65	-885.18	-918.71	-1101.61	-1214.73	4
55	-1007.94	-1019.27	-1042.63	-1208.49	-1443.7	5
56	-1122.37	-1126.3	-1138.59	-1260.74	-1525.14	6
57	-1216.04	-1221.56	-1227.06	-1315.4	-1569.44	7
58	-1293.02	-1293.93	-1295.25	-1363.62	-1585.33	8
59	-1352.12	-1346.84	-1340.27	-1376.72	-1554.43	9
60	-1395.21	-1391.82	-1380.42	-1390.63	-1509.11	10
61	-1416.33	-1413.46	-1401.19	-1392.78	-1465.69	11
62	-1417.2	-1410.82	-1396.72	-1373.1	-1414.68	12
63	-1417.2	-1399.42	-1384.58	-1346.13	-1374.59	13
64	-1396	-1375.82	-1361.53	-1310.14	-1329.03	14
65	-1353.11	-1330.68	-1314.18	-1260.75	-1268.25	15
66	-1294.08	-1275.38	-1257.5	-1204.66	-1209.08	16
67	-1217.6	-1196.5	-1177.69	-1137.3	-1146.96	17
68	-1124.24	-1098.68	-1082.13	-1051.06	-1127.75	18
69	-1009.73	-988.76	-974.43	-976	-1051.72	19
70	-873.87	-854.7	-843.29	-897.12	-941.21	20
71	-713.09	-694.52	-686.58	-757.44	-796.02	21
72	-520.01	-506.87	-517.85	-564.94	-587.83	22
73	-287.2	-280.91	-289.8	-316.19	-323.94	23
73	0	0	0	0	0	24

Table 6.16. Torsion moment of the bridge in the first I-girder for all models

Element	Torsion (kN.m)-0	Torsion (kN.m)-21	Torsion (kN.m)-37.6	Torsion (kN.m)-57	Torsion (kN.m)-66.6	Span (m)
3	-30.34	16.02	16.63	19.65	30.61	0
51	-38.79	-32.63	21.98	28.17	43.42	1
52	-41.58	-37.82	30.55	33.76	51.65	2
53	-37.76	38.3	38.8	42.52	56.01	3
54	-36.45	38.65	39.8	40.47	61.47	4
55	-34.85	36.82	41.2	45.49	69.89	5
56	-29.58	34.24	40.78	49.98	57.16	6
57	-28.32	33.23	40.28	52.81	57.53	7
58	-27.14	31.72	40.04	53.47	59.56	8
59	-23.91	32.25	42.15	56.21	62.45	9
60	-23.16	30.97	40.7	56.09	61.7	10
61	-22.76	29.48	40.19	54.92	60.67	11
62	22.76	31.54	43.26	57.84	65.31	12
63	23.16	31.59	41.76	56.06	62.62	13
64	23.91	31.74	41.39	53.89	59.77	14
65	27.14	34.12	43.96	55.67	60.22	15
66	28.32	35.16	42.13	53.64	55.28	16
67	29.58	35.36	41.6	49.45	50.1	17
68	34.85	38.66	44.11	48.1	56.49	18
69	36.45	38.97	40.73	42.31	54.34	19
70	37.76	37.99	36.17	41.05	52.52	20
71	41.58	38.61	32.84	36.32	50.82	21
72	38.79	32.07	26.31	31.03	40.46	22
73	30.34	21.01	19.01	22.59	29.16	23
73	30.34	21.01	19.01	22.59	29.16	24

Table 6.17. Shear forces in z-direction of the bridge in the first I-girder for all models

Element	Shear-z (kN)-0	Shear-z (kN)-21	Shear-z (kN)-37.6	Shear-z (kN)-57	Shear-z (kN)-66.6	Span (m)
3	294.27	306.35	312.38	323.19	333.38	0
51	260.95	264.76	296.12	319.29	329.28	1
52	236.3	235.29	251.1	302.67	313.17	2
53	216.95	210.07	215.29	262.3	287.65	3
54	199.23	192.88	192.77	205.74	269.44	4
55	183.68	177.35	176.81	171.84	241.66	5
56	175.68	167.07	166.07	151.75	171.36	6
57	160.24	153.36	151.58	145.94	142.32	7
58	146.34	139.92	139.85	140.94	137.83	8
59	141.85	134.15	139.77	140.03	140.33	9
60	127.09	121.27	126.82	133.67	140.51	10
61	-113.91	-109.91	116.85	126.68	-145.13	11
62	113.91	-112.98	117.61	-131	-144.35	12
63	-127.09	-127.46	-127.43	-139.72	-146.36	13
64	-141.85	-141.36	-140.85	-148.12	-150.24	14
65	-146.34	-145.26	-145.63	-151.85	-149.56	15
66	-160.24	-160.27	-159.04	-158.58	-153.15	16
67	-175.68	-174.85	-172.76	-166.65	-160.05	17
68	-183.68	-181.49	-178.83	-172.58	-169.15	18
69	-199.23	-197.7	-192.89	-185.94	-192.33	19
70	-216.95	-214.23	-208.56	-209.9	-218.81	20
71	-236.3	-230.5	-225.36	-243	-254.82	21
72	-260.95	-254.64	-251.22	-277.55	-290.13	22
73	-294.27	-284.53	-285.91	-316.32	-330.96	23
73	-294.27	-284.53	-285.91	-316.32	-330.96	24

Table 6.18. Axial forces of the bridge in the first I-girder for all models

Element	Axial (kN)-0	Axial (kN)-21	Axial (kN)-37.6	Axial (kN)-57	Axial (kN)-66.6	Span (m)
3	-11.37	15.51	19.56	27.71	37.29	0
51	-22.62	-28.84	32.13	42.03	-57.21	1
52	-31.87	-47.18	-47.93	-50.15	-89.89	2
53	-37.56	-27.22	31.01	123.64	-117.62	3
54	-40	-36.35	-29.6	-67.14	-149.07	4
55	-39.93	-42.53	-41.23	-79.41	-182.27	5
56	-38.26	-31.38	-29.39	-84.1	-191.53	6
57	-35.6	-35.41	-37.32	-92.21	-200.95	7
58	-32.77	-39.02	-47.26	-103.49	-217.99	8
59	-31.51	-28.69	-44.32	-96.54	-199.75	9
60	-28.97	-36.28	-51.96	-105.52	-211.53	10
61	-28.37	-45.23	-64.11	-116.2	-223.84	11
62	-28.37	-40.52	-55.81	-98.3	-203.51	12
63	-28.97	-46.54	-64.62	-106.52	-214.23	13
64	-31.51	-55.04	-78.48	-116.91	-225.27	14
65	-32.77	-45.47	-57.24	-100.9	-203.65	15
66	-35.6	-51.86	-68.93	-109.49	-216.64	16
67	-38.26	-59.76	-80.01	-118.26	-227.22	17
68	-39.93	-44.26	-50.45	-91.32	-170.09	18
69	-40	-48.72	-56.84	-94.34	-149.98	19
70	-37.56	-50.11	-58.54	-96.28	-130.94	20
71	-31.87	-11.22	11.55	25.22	-32.28	21
72	-22.62	6.48	20.7	22.38	-18.14	22
73	-11.37	9.07	12.85	15.24	13.97	23
73	-11.37	9.07	12.85	15.24	13.97	24

Table 6.19. Axial stresses of the bridge in the first I-girder for all models

Elem	Axial Stress (kN/m ²)-0	Axial Stress (kN/m ²)-21	Axial Stress (kN/m ²)-37.6	Axial Stress (kN/m ²)-57	Axial Stress (kN/m ²)-66.6	Span (m)
3	-13.1	17.9	22.6	32	43	0
51	-26.1	-33.3	37.1	48.5	-66	1
52	-36.8	-54.4	-55.3	-57.9	-104	2
53	-43.3	-31.4	35.8	143	-136	3
54	-46.1	-41.9	-34.1	-77.5	-172	4
55	-46.1	-49.1	-47.6	-91.6	-210	5
56	-44.1	-36.2	-33.9	-97	-221	6
57	-41.1	-40.8	-43.1	-106	-232	7
58	-37.8	-45	-54.5	-119	-251	8
59	-36.4	-33.1	-51.1	-111	-230	9
60	-33.4	-41.9	-59.9	-122	-244	10
61	-32.7	-52.2	-74	-134	-258	11
62	-32.7	-46.7	-64.4	-113	-235	12
63	-33.4	-53.7	-74.5	-123	-247	13
64	-36.4	-63.5	-90.5	-135	-260	14
65	-37.8	-52.5	-66	-116	-235	15
66	-41.1	-59.8	-79.5	-126	-250	16
67	-44.1	-68.9	-92.3	-136	-262	17
68	-46.1	-51.1	-58.2	-105	-196	18
69	-46.1	-56.2	-65.6	-109	-173	19
70	-43.3	-57.8	-67.5	-111	-151	20
71	-36.8	-12.9	13.3	29.1	-37.2	21
72	-26.1	7.47	23.9	25.8	-20.9	22
73	-13.1	10.5	14.8	17.6	16.1	23
73	-13.1	10.5	14.8	17.6	16.1	24

Table 6.20. Displacement in z-direction of the bridge in the first I-girder for all models

Node	DZ (m)-0	DZ (m)-21	DZ (m)-37.6	DZ (m)-57	DZ (m)-66.6	Span (m)
5	0	0	0	0	0	0
63	-0.00485	-0.00533	-0.00674	-0.01251	-0.02147	1
64	-0.00672	-0.00712	-0.00842	-0.01417	-0.02344	2
65	-0.0086	-0.00894	-0.01015	-0.01576	-0.0253	3
66	-0.01068	-0.01094	-0.01182	-0.01727	-0.02698	4
67	-0.01286	-0.01309	-0.01356	-0.01867	-0.02844	5
68	-0.01484	-0.01503	-0.01542	-0.01992	-0.02963	6
69	-0.01657	-0.01673	-0.01705	-0.02102	-0.03055	7
70	-0.01804	-0.01815	-0.0184	-0.02193	-0.03124	8
71	-0.01917	-0.01927	-0.01944	-0.02264	-0.03171	9
72	-0.02	-0.02006	-0.02017	-0.02315	-0.03201	10
73	-0.0205	-0.02052	-0.02057	-0.02343	-0.03205	11
74	-0.02066	-0.02066	-0.02065	-0.0235	-0.03186	12
75	-0.0205	-0.02046	-0.0204	-0.02334	-0.03145	13
76	-0.02	-0.01994	-0.01983	-0.02295	-0.03084	14
77	-0.01917	-0.01909	-0.01894	-0.02232	-0.02999	15
78	-0.01804	-0.01792	-0.01775	-0.02145	-0.02894	16
79	-0.01657	-0.01646	-0.01637	-0.02037	-0.02767	17
80	-0.01484	-0.0147	-0.01507	-0.01906	-0.02617	18
81	-0.01286	-0.01272	-0.01357	-0.01753	-0.02449	19
82	-0.01068	-0.01084	-0.01189	-0.01583	-0.02266	20
83	-0.0086	-0.00902	-0.01006	-0.014	-0.02078	21
84	-0.00672	-0.00711	-0.00814	-0.01214	-0.01899	22
85	-0.00485	-0.0052	-0.00627	-0.0105	-0.01747	23
6	0	0	0	0	0	24

Table 6.21. Final forces in pre-tensioned steel of the bridge in the first I-girder for all models

Elem	Part	Final force (kN)-0	Final force (kN)-21	Final force (kN)-37.6	Final force (kN)-57	Final force (kN)-66.6	Span (m)
3	I	2538.3524	2537.8921	2537.7843	2537.4864	2536.9365	0
51	I	2633.3966	2631.8391	2630.0328	2628.0413	2627.634	1
52	I	2721.5947	2719.4398	2716.9701	2713.6135	2714.1009	2
53	I	2802.6949	2799.5424	2793.931	2777.5775	2764.1632	3
54	I	2873.0817	2870.5428	2865.8994	2850.6745	2837.1482	4
55	I	2936.1306	2934.3181	2930.9146	2918.6829	2905.0943	5
56	I	2991.7277	2989.5199	2984.6846	2968.3966	2948.0712	6
57	I	3037.2386	3035.7743	3032.4058	3020.4778	3003.0299	7
58	I	3075.2174	3074.483	3072.5022	3065.0549	3052.0589	8
59	I	3105.6129	3104.5743	3101.8985	3093.8329	3083.7091	9
60	I	3125.8926	3125.3641	3123.9209	3119.7321	3113.4733	10
61	I	3138.5703	3138.4959	3138.1065	3137.3941	3134.613	11
62	I	3143.6363	3143.314	3143.0136	3145.0001	3148.8116	12
63	I	3138.5457	3138.5947	3139.1229	3143.1147	3147.2335	13
64	I	3125.8436	3126.1923	3127.3417	3132.6594	3136.0374	14
65	I	3105.5543	3105.9804	3108.2634	3119.8229	3132.0218	15
66	I	3075.1108	3075.8894	3078.4378	3088.7679	3096.6655	16
67	I	3037.0996	3038.138	3040.702	3048.7354	3051.1861	17
68	I	2991.5832	2993.3687	2998.3752	3015.2915	3026.5992	18
69	I	2935.9154	2937.7812	2941.8819	2953.2245	2954.8499	19
70	I	2872.826	2874.61	2877.4585	2882.1984	2876.6789	20
71	I	2802.4363	2806.4211	2813.4033	2827.323	2836.6244	21
72	I	2721.2626	2724.1457	2728.479	2736.1267	2741.9238	22
73	I	2633.0393	2634.5487	2636.0338	2639.5056	2642.2647	23
73	J	2538.3524	2538.4757	2538.6901	2539.3466	2540.4377	24

Table 6.22. Bending moment in longitudinal direction of the bridge in the first I-girder for all models

Element	Moment-y (kN.m)-0	Moment-y (kN.m)-21	Moment-y (kN.m)-37.6	Moment-y (kN.m)-57	Moment-y (kN.m)-66.6	Span (m)
4	0	0	0	0	0	0
74	-224.39	-238.7	-247.46	-245.37	-240.1	1
75	-438.32	-459.12	-470.33	-459.15	-438.93	2
76	-633.44	-658.29	-670.77	-661.21	-632.68	3
77	-809.29	-831.55	-834.01	-812.41	-767.18	4
78	-961.76	-979.57	-969.48	-932.38	-870.14	5
79	-1088.91	-1104.67	-1089.22	-1035.82	-971.23	6
80	-1191.64	-1198.83	-1174.81	-1111.92	-1029.06	7
81	-1272.53	-1276.58	-1247.22	-1161.43	-1064.25	8
82	-1342.36	-1342.14	-1306.49	-1199.22	-1108.88	9
83	-1386.89	-1376.3	-1330.85	-1220.22	-1114.98	10
84	-1409.64	-1388.75	-1349.49	-1223.49	-1097.89	11
85	-1410.46	-1403.9	-1361.68	-1219.52	-1076.25	12
86	-1410.79	-1388.76	-1336.85	-1180.62	-1031.93	13
87	-1388.9	-1356.19	-1289.8	-1130.39	-968.78	14
88	-1345.74	-1309.19	-1247.29	-1077.17	-892.72	15
89	-1275.9	-1236.28	-1169.58	-993.09	-799.97	16
90	-1196.05	-1148.48	-1070.6	-892.5	-699.53	17
91	-1094.78	-1046	-966.67	-787.39	-649.71	18
92	-966.65	-913.22	-834.89	-663.4	-535.06	19
93	-814.01	-759.22	-685.36	-549.17	-420.41	20
94	-638.54	-591.69	-532.71	-423.58	-327.67	21
95	-441.41	-405.09	-369.75	-283.01	-219.12	22
96	-226.13	-208.53	-185.68	-142.45	-110.58	23
96	0	0	0	0	0	24

Table 6.23. Torsion moment of the bridge in the first I-girder for all models

Element	Torsion (kN.m)-0	Torsion (kN.m)-21	Torsion (kN.m)-37.6	Torsion (kN.m)-57	Torsion (kN.m)-66.6	Span (m)
4	28.27	30.2	29.24	-26.97	-36.9	0
74	30.25	31.87	31.03	-35.42	-45.44	1
75	33.76	35.23	33.86	32.48	-40.33	2
76	-40.38	-38.65	-39.41	-46.29	-50.97	3
77	-38.78	37.07	38.58	41.06	45.32	4
78	36.05	40.23	42	44.72	44.71	5
79	-37.09	33.61	38.61	48.9	51.71	6
80	-32.98	36.05	40.53	51.11	54.04	7
81	31.3	37.36	42.56	52.79	54.55	8
82	-30.12	31.75	40.51	54.45	57.62	9
83	26.22	33.99	42.34	54.75	56.86	10
84	28.87	35.93	43.59	55.16	55.66	11
85	-28.87	31.61	41.34	56.67	58.78	12
86	-26.22	34.04	43.29	55.91	58.06	13
87	30.12	37.05	44.62	54.42	55.43	14
88	-31.3	35.7	43.71	53.37	52.54	15
89	32.98	38.44	44.34	52.17	43.94	16
90	37.09	40.78	44.27	48.12	29.36	17
91	-36.05	38.24	40.13	42.86	10.51	18
92	38.78	38.36	38.44	31.33	10.51	19
93	40.38	38.24	35.95	15.56	10.51	20
94	-33.76	27.22	-25.8	1.55	1.14	21
95	-30.25	-26.79	1.47	1.55	1.14	22
96	-28.27	0.88	1.47	1.55	1.14	23
96	-28.27	0.88	1.47	1.55	1.14	24

Table 6.24. Shear forces in z-direction of the bridge in the first I-girder for all models

Element	Shear-z (kN)-0	Shear-z (kN)-21	Shear-z (kN)-37.6	Shear-z (kN)-57	Shear-z (kN)-66.6	Span (m)
4	227.82	241.1	245.34	233.73	214.81	0
74	222.34	230.61	233.37	221.18	207.17	1
75	212.82	216.79	216.92	204.44	192.5	2
76	200.65	199.77	198.98	187.81	181	3
77	188.87	184.84	182.02	169.05	163.45	4
78	176.2	169.82	165.19	151.8	146.97	5
79	160.07	154.04	150.49	138.04	134.15	6
80	148.57	140.8	136.14	123.38	119.53	7
81	136.54	127.43	121.78	110.08	105.99	8
82	120.46	113.59	109.99	100.63	97.49	9
83	109.72	101.59	97.36	88.75	88.21	10
84	98.36	89.26	-85.34	-88.51	-85.01	11
85	-98.36	-100.7	-101.33	-99.67	-93.81	12
86	-109.72	-111.42	-111.15	-108.19	-100.74	13
87	-120.46	-121.59	-121.17	-116.2	-107.15	14
88	-136.54	-137.72	-134.83	-124.81	-113.13	15
89	-148.57	-148.42	-143.44	-130.5	-115.07	16
90	-160.07	-158.44	-151.96	-135.94	-113.14	17
91	-176.2	-171.88	-161.48	-140.07	-114.65	18
92	-188.87	-181.67	-168.38	-141.72	-114.65	19
93	-200.65	-190.37	-175.15	-147.8	-114.65	20
94	-212.82	-197.09	-177.7	-140.57	-108.55	21
95	-222.34	-203.04	-184.07	-140.57	-108.55	22
96	-227.82	-207.55	-184.07	-140.57	-108.55	23
96	-227.82	-207.55	-184.07	-140.57	-108.55	24

Table 6.25. Axial forces of the bridge in the first I-girder for all models

Element	Axial (kN)-0	Axial (kN)-21	Axial (kN)-37.6	Axial (kN)-57	Axial (kN)-66.6	Span (m)
4	8.1	21.73	37.63	76.5	106.41	0
74	14.63	38.31	64.86	128.12	175.78	1
75	21.24	52.23	86.47	168.36	225.2	2
76	26	39.13	57.19	112.4	200.69	3
77	30.33	46.04	66.19	134.98	220.8	4
78	33.8	51.6	73.48	153.37	231.49	5
79	35.85	48.17	62.15	94.75	147.87	6
80	38.19	48.96	64.77	104.79	145.76	7
81	40.71	51.65	67.65	113.62	141.58	8
82	42.04	50.66	59.59	76.94	73.44	9
83	42.95	47.29	60.25	80.54	66.79	10
84	43.6	48.98	62.29	81.89	-66.79	11
85	43.6	45.19	50.43	53.26	27.93	12
86	42.95	44.2	52.68	48.54	-39.34	13
87	42.04	46.43	56.43	44.08	-52.72	14
88	40.71	38.66	39.84	29.57	-36.03	15
89	38.19	37.24	38.53	-29.23	-46.06	16
90	35.85	37.56	37.57	-31.59	-55.33	17
91	33.8	26.66	-25.33	-27.07	-32.96	18
92	30.33	25.26	22.91	-26.05	-32.96	19
93	26	24.03	22.43	26.95	-32.96	20
94	21.24	15.03	-17.25	14.62	15.75	21
95	14.63	11	10.59	14.62	15.75	22
96	8.1	8.02	10.59	14.62	15.75	23
96	8.1	8.02	10.59	14.62	15.75	24

Table 6.26. Axial stresses of the bridge in the first I-girder for all models

Elem	Axial Stress (kN/m ²)-0	Axial Stress (kN/m ²)-21	Axial Stress (kN/m ²)-37.6	Axial Stress (kN/m ²)-57	Axial Stress (kN/m ²)-66.6	Span (m)
4	9.35	25.1	43.4	88.3	123	0
74	16.9	44.2	74.8	148	203	1
75	24.5	60.3	99.8	194	260	2
76	30	45.1	66	130	232	3
77	35	53.1	76.4	156	255	4
78	39	59.5	84.8	177	267	5
79	41.4	55.6	71.7	109	171	6
80	44.1	56.5	74.7	121	168	7
81	47	59.6	78	131	163	8
82	48.5	58.4	68.7	88.8	84.7	9
83	49.6	54.6	69.5	92.9	77	10
84	50.3	56.5	71.9	94.5	-77.1	11
85	50.3	52.1	58.2	61.4	32.2	12
86	49.6	51	60.8	56	-45.4	13
87	48.5	53.6	65.1	50.9	-60.8	14
88	47	44.6	46	34.1	-41.6	15
89	44.1	43	44.4	-33.7	-53.1	16
90	41.4	43.3	43.3	-36.4	-63.8	17
91	39	30.8	-29.2	-31.2	-38	18
92	35	29.1	26.4	-30.1	-38	19
93	30	27.7	25.9	31.1	-38	20
94	24.5	17.3	-19.9	16.9	18.2	21
95	16.9	12.7	12.2	16.9	18.2	22
96	9.35	9.25	12.2	16.9	18.2	23
96	9.35	9.25	12.2	16.9	18.2	24

Table 6.27. Displacement in z-direction of the bridge in the first I-girder for all models

Node	DZ (m)-0	DZ (m)-21	DZ (m)-37.6	DZ (m)-57	DZ (m)-66.6	Span (m)
7	0	0	0	0	0	0
86	-0.011768	-0.013388	-0.017885	-0.036094	-0.065462	1
87	-0.013693	-0.015242	-0.019429	-0.036842	-0.065564	2
88	-0.015929	-0.017417	-0.021346	-0.037915	-0.065616	3
89	-0.018153	-0.019577	-0.023295	-0.039069	-0.06586	4
90	-0.020251	-0.021612	-0.025143	-0.040207	-0.066165	5
91	-0.022172	-0.023468	-0.026819	-0.041261	-0.066368	6
92	-0.023852	-0.025085	-0.028266	-0.04214	-0.066506	7
93	-0.025287	-0.02643	-0.029461	-0.042824	-0.066528	8
94	-0.026398	-0.027484	-0.030374	-0.043276	-0.066394	9
95	-0.027217	-0.028219	-0.030994	-0.043491	-0.066088	10
96	-0.02771	-0.02865	-0.031314	-0.043453	-0.065588	11
97	-0.027869	-0.02875	-0.031328	-0.043172	-0.064934	12
98	-0.02771	-0.028527	-0.031036	-0.042631	-0.064117	13
99	-0.027217	-0.027987	-0.030436	-0.041868	-0.063147	14
100	-0.026398	-0.027129	-0.029549	-0.04088	-0.062088	15
101	-0.025287	-0.025974	-0.028379	-0.039689	-0.061	16
102	-0.023852	-0.024527	-0.026957	-0.038361	-0.059982	17
103	-0.022172	-0.022831	-0.025321	-0.036928	-0.059068	18
104	-0.020251	-0.020932	-0.023508	-0.035488	-0.058026	19
105	-0.018153	-0.018865	-0.021578	-0.034198	-0.056858	20
106	-0.015929	-0.016705	-0.019629	-0.032993	-0.05559	21
107	-0.013693	-0.01458	-0.017871	-0.031689	-0.054248	22
108	-0.011768	-0.012884	-0.016384	-0.030316	-0.052855	23
8	0	0	0	0	0	24

Table 6.28. Final forces in pre-tentioned steel of the bridge in the first I-girder for all models

Elem	Part	Final force (kN)-0	Final force (kN)-21	Final force (kN)-37.6	Final force (kN)-57	Final force (kN)-66.6	Span (m)
4	I	2537.675	2537.373	2536.906	2535.555	2533.639	0
74	I	2634.515	2635.857	2637.104	2638.018	2637.281	1
75	I	2721.705	2724.926	2727.997	2731.237	2731.347	2
76	I	2799.532	2803.682	2805.857	2804.587	2801.909	3
77	I	2870.55	2874.842	2877.326	2876.456	2873.961	4
78	I	2932.515	2937.199	2940.226	2940.17	2937.845	5
79	I	2985.569	2989.315	2990.652	2986.321	2981.859	6
80	I	3031.275	3034.632	3035.647	3030.946	3026.4	7
81	I	3068.197	3071.344	3072.237	3067.472	3062.882	8
82	I	3096.404	3098.044	3097.427	3090.606	3086.602	9
83	I	3117.348	3118.415	3117.164	3109.405	3105.687	10
84	I	3129.619	3130.213	3128.448	3119.84	3116.443	11
85	I	3133.234	3132.284	3129.624	3121.866	3123.16	12
86	I	3129.643	3128.167	3124.815	3115.912	3117.745	13
87	I	3117.397	3115.407	3111.377	3101.253	3102.965	14
88	I	3096.463	3093.27	3089.327	3083.915	3093.138	15
89	I	3068.304	3064.857	3060.431	3054.394	3062.6	16
90	I	3031.414	3027.621	3022.6	3015.466	3021.164	17
91	I	2985.713	2981.508	2978.145	2979.503	2990.642	18
92	I	2932.73	2928.878	2925.643	2926.139	2928.862	19
93	I	2870.806	2867.075	2863.68	2861.587	2858.379	20
94	I	2799.79	2797.41	2797.734	2800.61	2805.169	21
95	I	2722.037	2721.234	2721.95	2722.166	2725.616	22
96	I	2634.873	2635.122	2634.532	2634.983	2637.324	23
96	J	2537.675	2538.193	2538.354	2539.042	2540.275	24

CURRICULUM VITAE

My name is Osama GHZAYEL. I was born in Yemen in 01/03/1987. I am a syrian. I have graduated with a bachelor's degree from civil engineering department in Sana'a University in Yemen at academic year (2009-2010) . My graduation project for bachelor's degree was about analysis and design of reinforcement concrete bridges. I have courses in project management by trainers from Calgary University-Canada and in programs of structural analysis and design Staad Pro, Sap2000, Sta4-Cad and programs of geometric drawing AutoCAD and program of geometric design for roads Land Development. I worked in teaching programs of Land Development and Staad Pro in faculty of engineering-Sana'a University-Yemen. I came to Turkey in 2011 and I learned Turkish language for one year in Ege University in the same year. Beside Arabic which is my original language I also have studied English language in American institute in Yemen and in KTÜ languages center in Trabzon.

